

POLITECNICO DI TORINO

MSc in Energy and Nuclear Engineering

Innovation in Energy Production

Master Thesis

Techno-economic analysis of integrated processes
for the decarbonization of a waste-to-energy plant



Supervisor

Prof. Massimo Santarelli

Co-supervisor

Giulio Buffo

Candidate

Lorenzo Baroni

Academic Year 2019/2020

Acknowledgements

Un forte ringraziamento va di sicuro a Giulio per la sua gentilezza e pazienza nel rispondere ai dubbi durante questi mesi di preparazione della tesi così come al Prof. Massimo Santarelli per la sua disponibilità e per avermi dato l'opportunità di approfondire argomenti sempre molto attuali.

Ringrazio i miei genitori, Stefania e Tiziano, per avermi sostenuto non solo economicamente e soprattutto per avermi spronato a dare sempre il meglio di me anche nei momenti più difficili e nonostante si trovassero a più di 600 km di distanza. Vi voglio bene. Ringrazio Simona per essermi stata vicina in questi ultimi importanti mesi. Ringrazio anche tutti i miei amici di Perugia, quelli che conosco da sempre, quelli che ho meglio conosciuto a Torino e quelli che se ne sono andati in giro per il mondo. Un grazie va anche agli ingegneri di Perugia e tutta la squadra del CUS PoliTO. Per ultimo, ma non meno importante, ringrazio me stesso, la mia testardaggine e il mio impegno senza i quali sicuramente ora non sarei arrivato a questo traguardo.

Infine vorrei dedicare a te, nonna, questa mia tesi. Nel tuo essere nonna apprensiva e tanto altruista mi hai insegnato sempre a rispettare e ad essere rispettati. So che da lassù mi stai guardando e sei fiera di me. Ti voglio tanto bene.

Abstract

This work aims at providing a deeper insight into different possible solutions for the decarbonization of existing power plants as support for the achievement of the goals planned by the European Commission 2030 strategy for climate and energy framework.

In particular, the study is focused on the conversion of carbon dioxide contained inside the exhausts of a waste-to-energy plant, into valuable products. Two different solutions are addressed:

- the **Power-to-gas** pathway to produce synthetic natural gas (SNG) from the captured CO₂ and the H₂ produced by electrolysis
- The **CO₂ capture** pathway for the sequestration of CO₂ and its storage in liquid form in a tank that is emptied every 48 hours.

Firstly, the results of the annual simulations from a previous study on the power-to-gas were adapted and rescaled to the two systems to obtain material and energy flows. With these results, a detailed analysis of the energy consumption is implemented to evaluate some environmental and energy parameters along with a preliminary sizing of the two systems. Secondly, a detailed economic analysis is performed to understand the feasibility of the two plants.

The results of the energy and economic analysis show that the two solutions analysed are technically feasible, thus allowing to avoid the emissions of 7740 t/y of CO₂.

The electrolysis section is the critical part of the entire power-to-gas plant with an electric consumption of 82.69 GWh_{el}/y. This is reflected in the total cost of the plant and, thus, on the levelized cost of the SNG produced of 1.77 €/Nm³ in a realistic scenario: this value is much higher than the actual price of natural gas (0.61 €/Nm³). To reduce the cost for the annual electric consumption, it is necessary to use the energy surplus coming from renewable energy sources as much as possible, so that the cost to produce SNG can reach acceptable values.

For the liquid CO₂ production plant, the fundamental part is represented by the thermal energy fed to the reboiler. Two different configurations for the waste-to-energy plant are considered for the solvent regeneration: a CHP layout and the use of an electric heater. Despite the CAPEX is lower for the full-electric configuration, the CHP pathway is preferable because it leads to a lower value of the levelized cost of the liquid CO₂ produced (83.77 €/t). This result is in line with the market values of liquid CO₂ both for the bulk conditions (i.e. for food and beverage) and for the retail market (i.e. technical gases for laboratory).

In conclusion, although these plants still have evident technological and economic limitations, the development of even more efficient processes can accelerate the route towards a faster energy transition, thus contributing to the mitigation of climate change down the line.

Contents

LIST OF TABLES	IV
LIST OF FIGURES	VI
LIST OF ACRONYMS.....	VIII
1 INTRODUCTION	1
2 TECHNOLOGICAL OVERVIEW	3
2.1 Introduction to carbon capture and storage process	3
2.1.1 The post-combustion carbon capture	4
2.1.2 Absorption processes	5
2.1.3 Chemical reactions in the absorption process	8
2.2 Electrolysis.....	10
2.2.1 Electrolytic cell.....	10
2.3 The process of CO₂ Methanation	13
2.3.1 Reactor concepts	14
2.4 Introduction to the Power-to-X route	15
2.4.1 State of the art of power-to-gas systems.....	17
3 CASE STUDY.....	20
3.1 Input data from the waste-to-energy plant	20
4 METHODS FOR ENERGY AND ENVIRONMENTAL ANALYSIS	23
4.1 Modelling of the power-to-gas plant.....	23
4.1.1 CO ₂ capture section	24
4.1.2 Electrolysis section.....	28
4.1.3 Methanation section.....	32
4.1.4 Thermal integration between the sections	35
4.2 Modelling of the liquid CO₂ production plant.....	37
4.2.1 Data and technologies considered.....	37

4.2.2 Configurations for the waste-to-energy plant	40
4.3 Energy and environmental indicators	42
5 METHODS FOR THE ECONOMIC ANALYSIS	44
5.1 CAPEX estimation	44
5.1.1 Estimation of process equipment cost	45
5.1.2 Definition of different scenarios for the estimation of the CAPEX.....	47
5.1.3 Estimation of bare erected cost (BEC).....	48
5.1.4 Estimation of the Total Overnight Capital (TOC).....	49
5.2 OPEX and cash flow analysis.....	50
5.3 Economic analysis applied to the power-to-gas	53
5.3.1 CO ₂ capture section	53
5.3.2 Electrolysis section.....	56
5.3.3 Methanation section.....	59
5.4 Economic analysis applied to the liquid CO ₂ production plant.....	62
5.4.1 Waste-to-energy in CHP configuration.....	62
5.4.2 Waste-to-energy in full-electric configuration.....	64
5.5 Economic indicators	65
6 RESULTS AND DISCUSSION	66
6.1 Power-to-gas system: energy and environmental analysis.....	66
6.1.1 CO ₂ capture section	66
6.1.2 Electrolysis section.....	69
6.1.3 Methanation section.....	71
6.2 Liquid CO ₂ production plant: energy and environmental analysis.....	74
6.2.1 Results of the simulation for the intercooling compression stage	74
6.2.2 Material and energy flow	74
6.2.3 Sizing of the system	76
6.3 Energy and environmental indicators: results and comments	77
6.4 Power-to-gas system: economic analysis.....	79
6.4.1 CO ₂ capture section	79
6.4.2 Electrolysis section.....	82
6.4.3 Methanation section.....	87

6.4.4 General overview of the results for the entire power-to-gas plant	90
6.4.5 Comparison of the LC _{SNG} with prices of other commodities	93
6.5 Liquid CO₂ production plant: economic analysis	95
6.5.1 CHP configuration: economic results.....	95
6.5.2 Full-electric configuration: economic results.....	98
6.5.3 Comparison between CHP and full-electric configuration	100
6.5.4 Final considerations on the levelized cost of liquid CO ₂	101
7 CONCLUSIONS	103

List of Tables

Table 4.1 Global heat transfer coefficients for the different heat exchangers analysed	27
Table 4.2 Operative data for the alkaline cell	28
Table 4.3 Quality parameter of SNG (HHE and Wobbe index are referred to conditions of 15°C and 1 atm while the dew point is defined at 70 barg)	32
Table 4.4 Input parameters for the model	39
Table 4.5 Data for the two coolers	41
Table 5.1 CEPCI indexes referred to 2001 and 2019.....	47
Table 5.2 Hypothesis for the estimation of the cost of the minor component expressed in percentage of $C_{bm,tot}$	48
Table 5.3 Hypothesis for evaluation of BEC	48
Table 5.4 Hypothesis for the evaluation of the TOC	49
Table 5.5 Summary of the hypothesis made for the cash flow analysis	52
Table 5.6 Hypothesis for the price of MEA and the ionic liquid (constant for all three scenarios).....	53
Table 5.7 Parameters used for the estimation of the bare module cost of the components composing the CO ₂ capture section	54
Table 5.8 Coefficients for the estimation of the C_{bm} of the water pump (operating pressure of 15 bar)	58
Table 5.9 Assumption for the evaluation of the O&M cost of pump and water tank.....	58
Table 5.10 Parameters used for the estimation of the bare module cost of the components composing the methanation section	61
Table 6.1 Material flows of the CO ₂ capture section	66
Table 6.2 Electric and thermal annual energy consumption of the CO ₂ capture section's components.....	67
Table 6.3 Footprint of the components composing the carbon capture section.....	68
Table 6.4 Dimensions of the container for the CO ₂ capture section	68
Table 6.5 Material and energy annual flows of the electrolysis section	69
Table 6.6 Material flows of the methanation section.....	71
Table 6.7 Thermal energy exchanged inside the exchangers and reactors and electric consumption of the methanation section.....	72
Table 6.8 Footprint of the components composing the methanation section.....	72
Table 6.9 Dimensions of the container for the methanation section.....	73
Table 6.10 Results from the Aspen simulation of the intercooling compression	74
Table 6.11 Material flows of the liquid CO ₂ production plant.....	75
Table 6.12 Electric and thermal annual energy consumptions for the two configurations of the waste-to-energy plant	75
Table 6.13 Dimensions of the container for the liquid CO ₂ production plant.	76
Table 6.14 Energy and environmental indicators for both the two solutions considered	77

Table 6.15 Results of the bare module cost of the main components of the CO ₂ capture section derived from the parameter A	79
Table 6.16 TOC and other main costs of the CO ₂ capture section in k€ for the three different scenarios	80
Table 6.17 Expenditures composing the annual budget of the carbon capture section	81
Table 6.18 EBITDA of the CO ₂ capture section for the three scenarios	81
Table 6.19 Levelized cost of CO ₂ for the three scenarios	82
Table 6.20 Bare module cost of the components of the electrolysis section	82
Table 6.21 TOC and other main costs of the electrolysis section for the three scenarios.....	83
Table 6.22 Expenditures composing the annual budget of the electrolysis section.....	83
Table 6.23 O&M costs of the electrolysis section	84
Table 6.24 EBITDA of the electrolysis section for the three scenarios and the 2 cases of power supply	84
Table 6.25 Levelized cost of the H ₂ produced for the two cases and the three different scenarios	86
Table 6.26 Results of the bare module cost of the main components of the methanation section derived from the parameter A	87
Table 6.27 TOC and other main costs of the methanation section in k€ for the three different scenarios	87
Table 6.28 Expenditures composing the annual budget of the methanation section	88
Table 6.29 EBITDA of the methanation section for the three scenarios	88
Table 6.30 Levelized cost of the SNG produced for the two cases and the three different scenarios	89
Table 6.31 Results of the bare module cost of the main components of the liquid CO ₂ production plant derived from the parameter A (CHP configuration).....	95
Table 6.32 TOC and other main costs of the liquid CO ₂ production plant in k€ for the three different scenarios for CHP configuration	96
Table 6.33 Expenditures composing the annual budget of the liquid CO ₂ production plant for CHP configuration.....	96
Table 6.34 EBITDA of the liquid CO ₂ production plant for the three scenarios for CHP configuration	97
Table 6.35 Levelized cost of liquid CO ₂ for the three scenarios (CHP configuration).....	97
Table 6.36 TOC and other main costs of the liquid CO ₂ production plant in k€ for the three different scenarios for full-electric configuration	98
Table 6.37 Expenditures composing the annual budget of the liquid CO ₂ production plant for full-electric configuration.....	98
Table 6.38 EBITDA of the liquid CO ₂ production plant for the three scenarios for full-electric configuration	99
Table 6.39 Levelized cost of liquid CO ₂ for the three scenarios (full-electric configuration). 99	
Table 6.40 Comparison of the main economic results of the liquid CO ₂ production plant between CHP and full-electric configuration in the realistic scenario	100
Table 6.41 Comparison between levelized cost of liquid CO ₂ (CHP configuration and realistic scenario) and market values	102

List of Figures

Figure 1.1 Energy-related CO ₂ emissions and reductions in the “Sustainable Development Scenario” developed by IEA [2]	1
Figure 2.1 Schematic representation of the three main types of CO ₂ capture [3].....	4
Figure 2.2 Scheme of post-combustion CO ₂ capture [4]	4
Figure 2.3 Chemical structure of amines [4].	6
Figure 2.4 Scheme of an amine-based PCC plant [7]	7
Figure 2.5 Schematic cross section of a PEM electrolytic cell [8].	11
Figure 2.6 Schematic representation of the different kinds of EES systems divided by forms of energy [15].	15
Figure 2.7 Schematic representation of power-to-X pathways [15].	16
Figure 2.8 Schematic representation of PtG pathway [17].	18
Figure 3.1 Annual profile of exhaust flow rate (kNm ³ /h) ejected from the line of the waste-to-energy plant	21
Figure 3.2 Annual profile of the exhaust’s macro-composition (%v).....	21
Figure 3.3 Yearly net power produced by the waste-to-energy plant vs exhaust flow rate	22
Figure 4.1 Process scheme of the power-to-gas system.....	24
Figure 4.2 Scheme of the CO ₂ capture section.....	24
Figure 4.3 Schematic representation of the electrolysis section	31
Figure 4.4 Schematization of the methanation process with 3 cooled-fixed bed reactors [29]	32
Figure 4.5 Schematic representation of the methanation section.....	33
Figure 4.6 Scheme of the thermal integration between the methanation and the CO ₂ capture section.....	36
Figure 4.7 Schematic representation of the entire liquid CO ₂ production plant	38
Figure 4.8 Phase diagram of CO ₂ [32]	38
Figure 4.9 Aspen Plus scheme of the intercooling compression section	39
Figure 5.1 Capital cost levels and their elements [33]	44
Figure 5.2 CAPEX data for PEM and alkaline electrolyzers; for the alkaline solution, data are based on a single stack of 2.13MW [39].....	56
Figure 6.1 Arrangement of the components inside the carbon capture section (dimensions in meters).....	69
Figure 6.2 Dimensions of a 2 MW _{el} unit by McPhy [46].....	70
Figure 6.3 Arrangement of the components inside the liquid CO ₂ production plant (dimensions in meters)	76
Figure 6.4 Cumulative free cash flow of the CO ₂ capture section for the three scenarios	81
Figure 6.5 CFCF of the electrolysis section for the three scenarios (CASE A).....	85
Figure 6.6 CFCF of the electrolysis section for the three scenarios (CASE B).....	85
Figure 6.7 CFCF of the methanation section for the three scenarios.....	89
Figure 6.8 Contribution of each section to the CAPEX of the entire power-to-gas plant in the three scenarios	90

Figure 6.9 Contribution of each section to the OPEX of the entire power-to-gas plant (CASE A).....	91
Figure 6.10 Contribution of each section to the OPEX of the entire power-to-gas plant (CASE B).....	91
Figure 6.11 Comparison between levelized cost of SNG and selling price of natural gas	93
Figure 6.12 Comparison between levelized cost of SNG and selling price of biomethane.....	94
Figure 6.13 CFCF for the liquid CO ₂ production plant in the three scenarios for CHP configuration	97
Figure 6.14 CFCF for the liquid CO ₂ production plant in the three scenarios for full-electric configuration	99
Figure 6.15 CFCF for the CHP and full-electric configuration for the realistic scenario.....	101

List of Acronyms

Acronym	Meaning
AEC	Alkaline Electrolytic Cell
BEC	Bare Erected Cost
BoP	Balance of Plant
CAPEX	CAPital EXpenditure
CCS	Carbon Capture and Storage
CEPCI	Chemical Engineering Plant Cost Index
CFCF	Cumulative Free Cash Flow
CHP	Combined Heat and Power
CIC	Certificati di Immissione in Consumo
EES	Electrical Energy Storage
EBITDA	Earnings Before Interest, Taxes, Depreciation and Amortization
EPCC	Engineering, Procurement and Construction Cost
FCF	Free Cash Flow
GHG	Greenhouse Gases
GSE	Gestore Servizi Energetici
HHV	Higher Heating Value
LC	Levelized Cost
LHV	Lower Heating Value
LMTD	Log Mean Temperature Difference
MEA	Mono-EthanolAmine
NETL	National Energy Technology Laboratory
O&M	Operation and Maintenance
OPEX	Operating Expense
PEMEC	Proton Exchange Membrane Electrolytic Cell
PCC	Post-Combustion Capture
PtG	Power-to-Gas
PUN	Prezzo Unico Nazionale
PZN	Prezzo Zona Nord
RES	Renewable Energy Sources
SME	Sistema di Monitoraggio in continuo delle Emissioni
SNG	Synthetic Natural Gas
SOEC	Solid Oxide Electrolytic Cell
SPECCA	Specific Primary Energy Consumption for CO ₂ Avoided
TOC	Total Overnight Capital
TPC	Total Plant Cost

1 Introduction

“Today, the European Commission has shown the way to a prosperous, modern, competitive and climate neutral economy by 2050.

We can do it, and if we succeed, others will follow.”

Miguel Arias Cañete (November 28, 2018)

It is with these words that the European Commissioner for Climate Action and Energy, Miguel Arias Cañete, concluded his speech at the European Commission in Brussels on November 28, 2018. On that day the European Union presented its long-term strategy to be climate-neutral by 2050 developing a net-zero greenhouse gas emissions economy. This goal is also at the heart of the European Green Deal and in line with the EU's commitment to global climate action under the Paris Agreement. Bearing this in mind, in order to achieve the net-zero emissions target (i.e. the difference between the CO₂ emitted and the amount of CO₂ removed), a 50% reduction in CO₂ emissions by 2030 and a further 50% by 2040 would be needed [1].

The road to achieve these goals is complex and encompasses a combination of different methodologies. *Figure 1.1* represents the contribution of each technology to the possible reduction of CO₂ emissions in the Sustainable Development Scenario drawn up by the International Energy Agency. Among these technologies, the penetration of renewable energy sources (RES) in the energy production systems is an important step that should lead to the progressive decarbonization and thus, a reduction in emission of GHG.

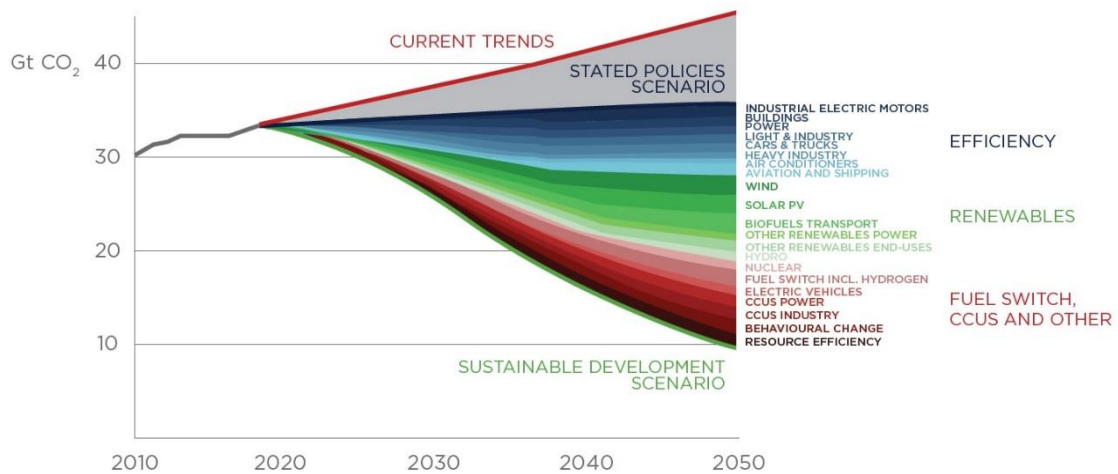


Figure 1.1 Energy-related CO₂ emissions and reductions in the “Sustainable Development Scenario” developed by IEA [2]

The great problem to be overcome is represented by the fluctuation and intermittent production of RES and the subsequent mismatch between supply and electrical demand. A possible solution to address these issues could be the increase in the storage capacity using different kinds of electrical energy storage technologies (EESs). Within these systems, a recent concept has been designed for the large-size and long-term storage of electricity exploiting chemical energy: the Power-to-X scheme.

In this perspective, this thesis studied the techno economic feasibility of the application of power-to-gas technology to a waste-to-energy plant for the conversion of the CO₂ present in the exhausts of the plant in order to produce Synthetic Natural Gas (SNG). Moreover, a second plant configuration is considered in order to only capture the CO₂ in the exhausts of the waste-to-energy plant and to produce liquid CO₂ stored in a tank that is supposed to be emptied every 48 hours. To this end, results of the annual simulations from a previous study on the power-to-gas were adapted and rescaled to the two configurations. These results were used to assess the energy performance of the two systems and the feasibility of the configurations through an economic analysis. Finally, by comparing the results obtained with the real market prices of the respective products, this study tried to understand whether the solutions adopted can be considered competitive or not, laying the foundations for further insights on this topic.

2 Technological overview

In this paragraph a general overview of the different technologies considered inside this study will be presented, introducing the literature review and the state of the art of the processes analysed.

2.1 Introduction to carbon capture and storage process

During the combustion and conversion process, energy from fossil fuel (e.g. coal, oil, or natural gas) is released also resulting in the emission of CO₂ as a by-product. Carbon capture and storage (CCS) is a typical process of advanced polygeneration plants in which CO₂ is separated from other components composing the combustion's exhaust. At the end of this process, a stream of relatively pure CO₂ is produced, which can be directly utilized (e.g. exploited to produce chemicals) or transported through a pipeline and then stored in a geological site or via chemical treatments.

Three different types of CO₂ capture processes exist (*Figure 2.1*):

- 1) Post-combustion capture – separates CO₂ from the exhausts of the combustion and then it can be captured using a solvent, for example in liquid or solid phase. This type of process is suitable for the existing infrastructure.
- 2) Pre-combustion capture – it consists of the conversion of the fuel into a gaseous mixture of H₂ and CO₂ called syngas. Then H₂ can be separated and burnt, instead, CO₂ can be compressed for storage and transport. The steps for the fuel conversion involve more complex transformations with respect to the post-combustion process; for this reason, this type of CO₂ capture process is more difficult to apply to an existing power plant.
- 3) Oxyfuel combustion – in this case, the oxygen in the air is separated from nitrogen so the combustion of the fuel uses only O₂. This results in the production of exhaust gas mainly constituted of water vapor and CO₂; for this reason, carbon dioxide can be easily separated to produce a stream of CO₂ with very high purity.

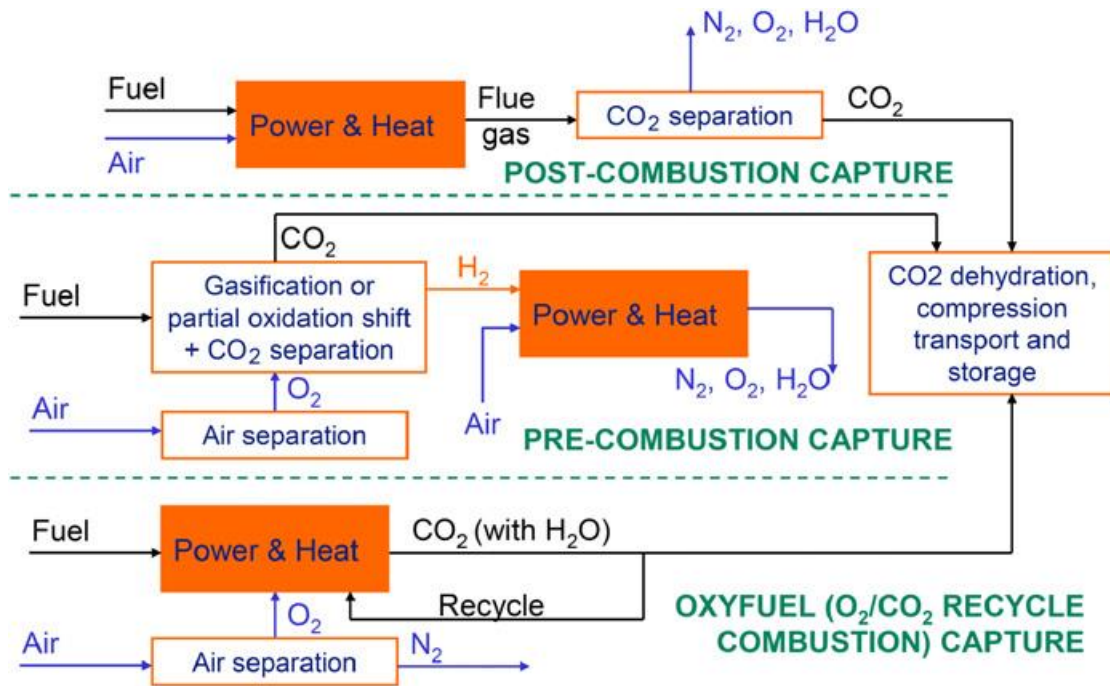


Figure 2.1 Schematic representation of the three main types of CO₂ capture [3]

In this dissertation, the attention will be focused on the post-combustion pathway, so in the following paragraph an introduction to the fundamentals of this type of process will be provided.

2.1.1 The post-combustion carbon capture

In post-combustion capture (PCC), CCS is applied to the exhaust of a combustion process, for example coming from fossil fuel-fired power stations, to reduce the emission of CO₂ in the atmosphere. To do so, the CO₂ needs to be extracted and separated from a mixture of H₂O, O₂, N₂ and other components like NO_x or SO_x. As shown in *Figure 2.2*, the entire process produces two different streams: a concentrated flow of CO₂ generally stored, and a flue gas released into the atmosphere and made up mostly of nitrogen, oxygen and water but with a very low content of CO₂.

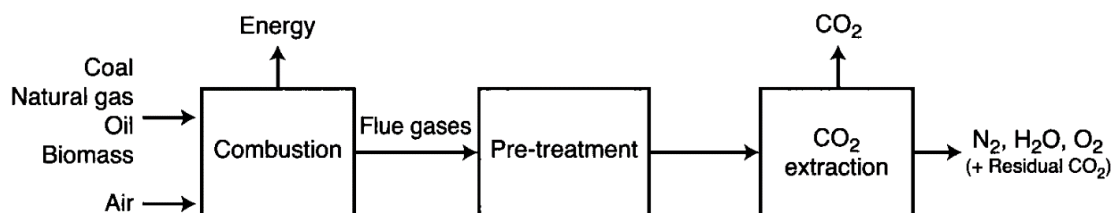


Figure 2.2 Scheme of post-combustion CO₂ capture [4]

There are several techniques suitable for the post-combustion CO₂ capture but the most used are:

- absorption in solvents
- adsorption in solids
- membrane separation
- cryogenics

Absorption processes consist of the dilution of a solute contained in a gas mixture using a solvent, in the liquid phase. The type of solvent used defines the most important characteristics of the absorption process itself: the techniques are based on physical, chemical, or mixed solvent processes.

Adsorption is the process of retention of liquid or gas molecules on a solid surface. It is used in different sectors for gas purification to remove for example acid compounds, organic solvents and water vapours. The process of separation of the CO₂ involves regenerable adsorbent, usually porous solids with high adsorbing properties such as zeolite or active carbon. The exhausts flow on a fluidized bed and the CO₂ is adsorbed by the surface of the adsorbent through Van der Waals interactions (for physical adsorption) or through covalent bonds (for the chemical one).

Finally, **membrane separation and cryogenics** are alternative processes still under development based on different technologies with respect to the first two ([5],[6]).

Amongst the technologies currently being considered, absorption by solvents is by far the most technically advanced and used method for PCC; for this reason and for the purpose of this dissertation, the attention will be focused only on this type of process.

2.1.2 Absorption processes

As introduced in the previous paragraph, the processes with which the absorption can take place vary with the type of solvent. In particular, the most important two types of CO₂ separation are the chemical and the physical one:

Physical separation is based on the absorption of the gas components by dissolution in liquid; this is possible without any kind of chemical reaction, but only exploiting the

differences in the size of gas molecules or vapor pressure, boiling point, etc. The most used physical solvents are organic liquids, such as methanol, that can be regenerated only by reducing the pressure, making all the process of absorption very cheaply. On the other hand, the absorption performance is based on the temperature between solvent and gas and also on the partial pressure of the compound that has to be separated from the gas mixture (in this case the CO_2): the lower the temperature of the absorption process and the higher the CO_2 partial pressure, the higher the performance. In this perspective, the operating conditions of PCC (low concentration of CO_2 and temperature of absorption about $50\text{ }^\circ\text{C}$) are disadvantageous for the use of physical solvents. For this reason, this type of process would be applied to pre-combustion, for instance for the treatment of syngas.

On the contrary, **chemical separation** exploits an acid-based chemical reaction in order to capture CO_2 . The most important solvents used in this type of process are the aqueous solutions containing an alkanolamine, commonly referred to simply amines (compounds containing Nitrogen). The amines make the aqueous solvent basic, allowing it to react with CO_2 that is acid; in particular, if CO_2 reacts with water it can form carbonic acid (H_2CO_3) and if this acid reacts further with bases in proton exchange reactions, it can form bicarbonate (HCO_3^-). Only bicarbonate is trapped inside the aqueous solution unlike the other gases escape. Nevertheless, the CO_2 -absorbing capacity of this aqueous amines and their absorption rate is mainly given by the great ability of CO_2 to react with the amines present in the solution; also other impurities, such as SO_x or NO_x , present in the post-combustion flue gases, can react with amines, but this second reaction can lead to a degradation of the solvents and problems for the facility.

Amines can be distinguished, depending on the number and nature of the nitrogen's substituents, in three different types that exhibit distinct reactivity with respect to CO_2 : primary, secondary and tertiary amines (*Figure 2.3*).

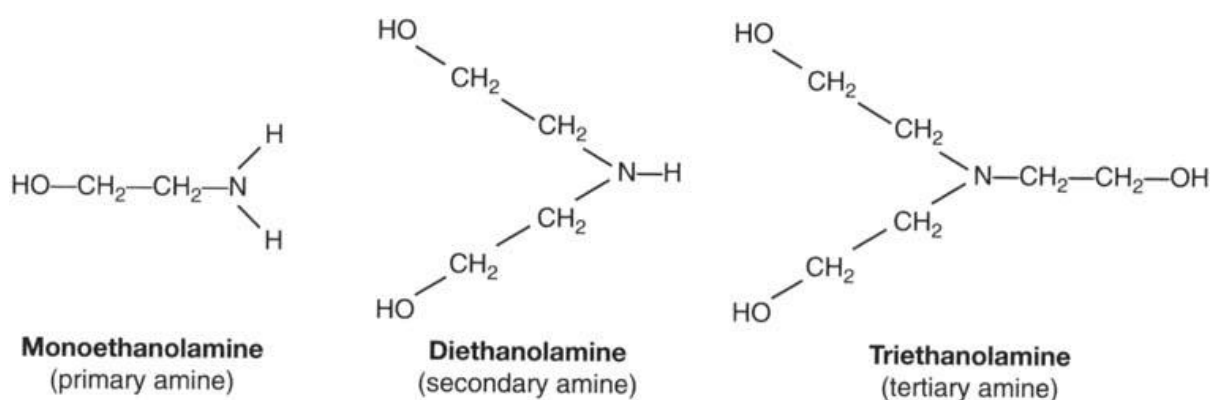


Figure 2.3 Chemical structure of amines [4].

Primary amines, such as monoethanolamine (MEA), are the most reactive with CO_2 . Although they have different disadvantages (e.g. more corrosive, the regeneration requires more energy, costly...), they are by far the most used in PCC processes.

Despite the fact that absorption can be made with different techniques according to the type of solvent used, all of them have two essential steps (*Figure 2.4*):

- The *absorption step* consisting of a counter-flow of gas to be solved with solvent in an absorber (also called absorption column or packed column because it is filled with coarsely porous packing material). The solvent is injected into the top of the absorber and, under gravity, comes into contact with the gas deriving from the bottom; in this way, the CO_2 in the gas is absorbed by the solvent. At the end of the process, the CO_2 -rich solvent is recovered at the bottom, instead, the CO_2 -free gas leaves the column from the top.
- The *step of solvent regeneration*, in which the process of desorption (extraction of CO_2 from the rich solvent) occurs in a regeneration column (called stripper). Here the solvent rich in CO_2 , coming from the absorber, flows down from the top; at the base of the stripper, steam is produced and is used to dilute the CO_2 that is released from the top. The lean solvent is then recirculated back to the absorber.

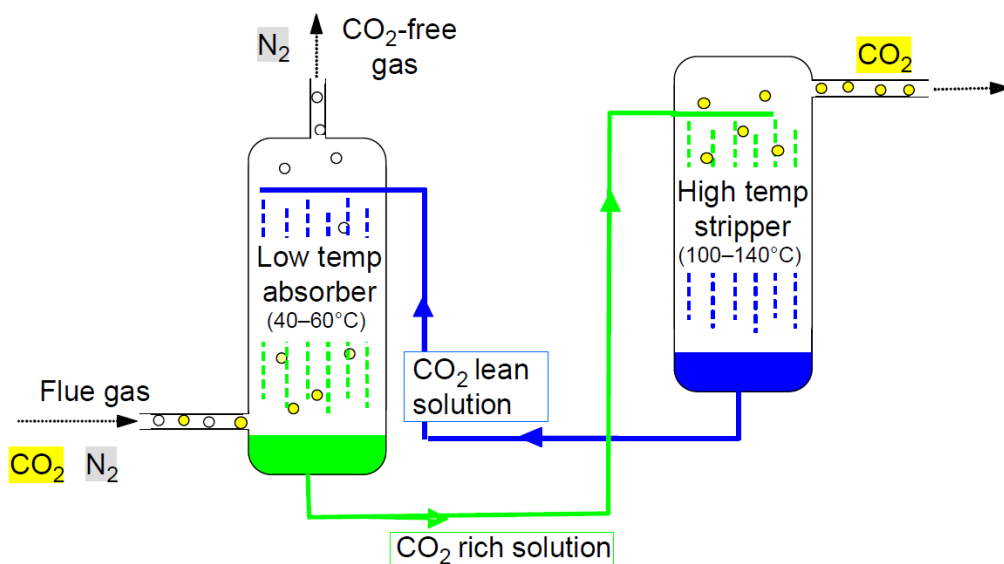


Figure 2.4 Scheme of an amine-based PCC plant [7]

2.1.3 Chemical reactions in the absorption process

In this section are shown the chemical reactions occurring when CO₂ is absorbed by an aqueous amine solution. There are 2 different types of reactions: those that are almost instantaneous and those that are relatively slow and observable. The latter are mainly 3 reactions (*Eqs.*[2-1],[2-2],[2-3]):



In particular, RNH₂ is the chemical formula of primary amine where R stands for the alkyl substituent (an alkane missing one hydrogen). Coupled with these 3 reactions there are the protonation equilibria of carbonate ([2-4],[2-5]), of the amine ([2-6]), of the hydroxide ([2-7]) and finally of the carbamate ([2-8]):



For primary amine, the overall reaction is:



Using an aqueous solution of MEA, where its concentration in the solution is generally about 30% w/w, the reaction is the following:



As for equation [2-9], each molecule of CO₂ absorbed requires two molecules of amine; this because the carbamic acid ([2-8]) deprotonates at relevant values of pH and for this reason, this proton need to be captured by a second molecule of amine. Furthermore, *eq.* [2-10] represents a balanced reaction that can be shifted in both directions. The absorption of

CO₂ occurs from left to right and during it, the CO₂ reacts with MEA at ambient temperature releasing a certain amount of energy (as a matter of fact the reaction is exothermic); on the other side, from right to left, MEA regeneration takes place at high temperature through heat input since desorption is an endothermic process.

As previously analysed, MEA is chosen for its very high reactivity with CO₂ and also because it has a low molar mass (61.1 g/mole); in this way the capacity of absorbing CO₂ is high and at the same time the flow rates of solvent can be lower. Moreover, MEA is quite simple to produce and its cost is quite limited (from 1000 to 1500 €/t [4]). However, there are important disadvantages in using this type of solvent: the most important one is its high enthalpy of reaction with CO₂ that increases the cost of all the process especially for the energy expenditure during the step of solvent regeneration. Finally, together with the high corrosivity given by the CO₂ rich solution, there is also the problem of the losses of solvent by vaporization due to its high vapor pressure (0.05 kPa at 20°C).

Although the process of CO₂ capture with a solution of MEA is considered a baseline for the assessment of these type of capture systems, in the last few years different companies have developed alternative solvents that allowed to reduce the energy costs of the capture process and in particular the solvent regeneration heat and the desorption temperature. An example of these new solvents are the ionic liquids (salts that are in the liquid state at ambient temperature) entirely composed of ions; their temperature of decomposition is higher than 160 °C (so suitable for the capture process) and the vapor pressure is very low: in this way it is difficult to have contamination of the gas which escapes from the absorber.

In the following paragraphs, the solvent considered is a blending of MEA and an ionic liquid called 1-Butylpyridinium tetrafluoroborate ([Bpy][BF₄]); even with this kind of solvent, the process followed during the absorption is as explained before.

2.2 Electrolysis

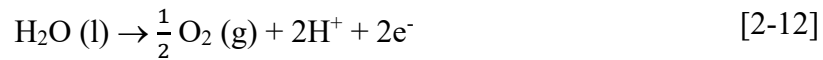
The process of electrolysis consists of a non-spontaneous chemical reaction driven by an electric current (usually DC current). It is commercially used for the separation of elements coming from different kind of sources by exploiting an open electrochemical cell working in reverse mode, called electrolyzer. Liquid water is the main molecule that can be dissociated into its elemental components according to:



In particular, in this dissertation, this process aims at producing the hydrogen needed for the reaction of methanation to generate synthetic natural gas (SNG).

2.2.1 Electrolytic cell

An electrolyzer, as in general all the fuel cells, is composed of three layers: two electrodes (electronic conductor) separated by a third thin layer of an ionic conductor, the electrolyte. The full reaction occurring in the device is defined in *eq.[2-11]*, whereas at the two electrodes two different half-reactions occur:



In particular *eq. [2-12]* occurs at the anode and *eq. [2-13]* at the cathode of a PEMEC (*Figure 2.5*). Between the two electrodes, there is the electrolyte, a thin layer with low electronic and molecule conductivity but where ions can pass through easily.

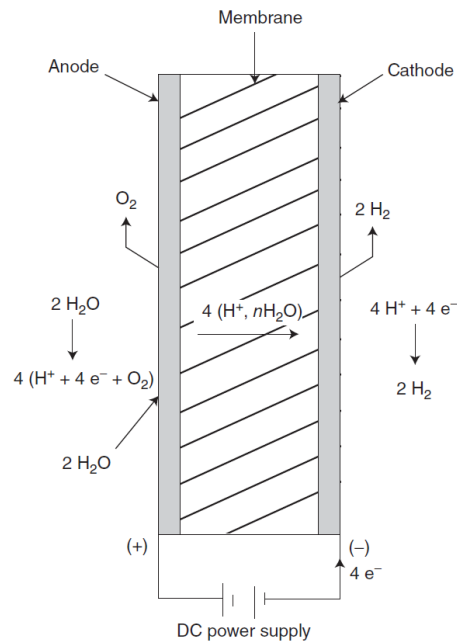
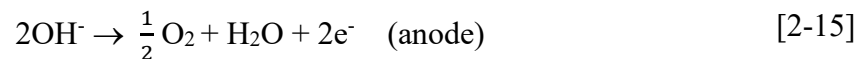
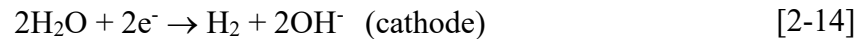


Figure 2.5 Schematic cross section of a PEM electrolytic cell [8].

Depending on the material of the electrolyte and the temperature reached in the cell, there are three different types of commercial electrolyzers:

- Proton exchange membrane electrolytic cell (PEMEC) that works at low temperature (60/80 °C), where the electrolyte is made of a hydrated polymer such as Nafion; the ions that are conducted inside the electrolyte are H^+ .
- Alkaline electrolytic cell (AEC) as for the PEMEC works at low temperature and the electrolyte is a solution of water and potassium hydroxide (KOH) or sodium hydroxide (NaOH); here the anion conducted into the electrolyte is the hydroxide (OH^-) so the two half-reactions are:



- Solid oxide electrolytic cell (SOEC) working at 800 °C with a solid electrolyte made by a ceramic material (the best one is the Ytria-stabilized Zirconia) and crossed by O^{2-} .

From a thermodynamic point of view, SOEC is better performing in respect to the other two cells for the high temperature reached and because it can perform also the CO-electrolysis

of both CO₂ and H₂O; on the contrary, this type of cell causes problems of shut-down, start-up, costs, etc that are very important to consider.

Currently, the alkaline technology is the best choice as regards the large-scale production of hydrogen; as a matter of fact, it is a very mature technology with good stability in the long term and cost-effectiveness compared to the other options. There are, however, several disadvantages to take into account: to reduce the ohmic losses, the current density is very low causing the reduction of compactness of the stack. Moreover, for safety reasons the power modulation range is restricted, and the hydrogen produced has a degree of purity lower than the one produced by PEMEC. However, PEM electrolytic cell has a dynamic behaviour with a large power modulation range, high compactness and high current density; the great disadvantages of these systems are the high investment cost (due to the use of noble metals as catalysts) and the problem of degradation that needs to be improved.

Even though all three types of electrolytic cells have different pros and cons, the cell considered in this work is the AEC.

2.3 The process of CO₂ Methanation

The process of methanation aims at producing CH₄ from H₂ and carbon oxides (CO or CO₂); when the reactions involve CO₂, its conversion is referred to as CO₂ methanation; it can be done both in the biological and catalytic reactor but in this thesis the attention will be focused only on the catalytic process as shown in this section.

The entire process of methanation is characterized by several different reactions which occur inside a reactor; the three main reactions are:



Equation [2-16] represents the CO₂ hydrogenation to methane (also known as the Sabatier reaction) that is an extremely exothermic reaction and for this reason, from the definition of Gibbs free energy and also Le Chatelier-Brown law, it is favored at high pressure and low temperature. Moreover, the Reverse Water Gas Shift reaction (*Eq. [2-18]*) converts H₂ and the remaining part of CO₂ that is not hydrogenated in the previous reaction into CO and H₂O. The produced CO reacts subsequently with 3 moles of H₂ to form CH₄ and H₂O in the so-called CO hydrogenation (*Eq. [2-17]*). Also, the latter reaction is highly exothermic (as for the CO₂ hydrogenation) and for this reason it is favored at high pressure and low temperature. Finally, the CO₂ methanation can be seen globally as an exothermic process.

All the reactions that occur inside the reactor are realized with the help of a catalyst that has a crucial role in the process of methanation. The active compound of the catalyst is generally a metal (e.g. Ru, Rh, Ni, Fe, CO...); it has to show a good compromise between activity, selectivity and cost: for all these reasons the best and most used metal is Nickel [9]. To increase the performance of the catalyst, generally, the active metal is supported to increase the surface area of the catalyst; metal oxides (e.g. Al₂O₃, SiO₂, TiO₂) are the common supports for the methanation catalyst and among them the most frequently used is the γ -modification of Al₂O₃ [10].

In addition to that, another important aspect to consider to optimize the process of methanation is the regulation of the thermodynamic; different studies in literature analyze in detail the influence of temperature and pressure in the CO₂ methanation [11]. In particular, one parameter to be considered in the design of the reactor is the thermal degradation (i.e. nickel sintering) of the catalyst [9]; to avoid this phenomenon, the process temperature has to be limited to 500-550°C. Therefore, the state of the art consists of a process carried out in a range of temperature and pressure of about 200-550 °C and 1-100 bars.

2.3.1 Reactor concepts

As previously analyzed, the CO₂ methanation is a highly exothermic reaction and this means that a great amount of heat has to be removed; for example, the direct conversion of CO₂ to CH₄ (Eq.[2-16]) releases 165,1 kJ_{th} per mole, equivalent to 1,8 kW_{th} for each m³ of methane produced per hour. Therefore, the control of the temperature inside the reactor during the process plays an important role to prevent thermodynamic problems (e.g. catalyst sintering). For this reason, different types of steady-state reactor have been designed and they can be found in the literature ([9], [12]):

- **Adiabatic fixed-bed reactors:** usually constituted by a series of 5-7 reactors with gas recirculation. The catalyst works in a huge temperature range (250-700°C) and can be subjected to cracking or sintering.
- **Fluidized-bed reactors:** can be considered almost isothermal reactors due to an efficient heat removal; however, the catalyst can be deactivated due to the attrition between the particles. Another great disadvantage is the formation of gas bubbles that causes an incomplete conversion of the CO₂.
- **Three-phase reactors:** the reaction occurs in a three-phase system (gas, liquid and solid) and the presence of the liquid phase allows a great efficiency of the heat removal due to the high heat capacity of this phase. The challenge of this type of reactor is in the gas-liquid mass transfer resistance and the evaporation and decomposition of the liquid phase.
- **Structured reactors:** very compact reactors with high heat transfer and small pressure drop. The disadvantages are the difficulty of replacing the catalyst when deactivated and also the complexity in the deposition of the catalyst on the metallic structure; finally, this configuration is also the most expensive one.
- **Cooled fixed-bed reactors** are an alternative to the adiabatic fixed-bed reactor where the reactor is defined as a shell and tube heat exchanger. The catalyst is inside the tubes of small diameter (1-4 cm), while the coolant flows externally to remove a great part of the heat. Usually, the cooling fluid is water at high temperature and pressure that evaporates; therefore, the result of the heat recovery is saturated steam at high pressure. The great disadvantage of this configuration is the higher cost with respect to a conventional fixed-bed reactor.

In this study, the last configuration is analyzed.

2.4 Introduction to the Power-to-X route

The penetration of renewable energy sources (RES) in the energy production systems is an important step that should lead to progressive decarbonization and thus, a reduction in the emission of greenhouse gases (GHG), fixed in a 40% cut (compared to 1990s emissions) by the European Commission in the 2030 Climate and Energy Framework [13]. In this perspective, the fluctuation and intermittent production of RES and subsequent mismatch between supply and electrical demand represent the great problems to be overcome. The possible solution to address these issues could be the increase of the storage capacity using different kind of electrical energy storage technologies (EESs).

Figure 2.6 provides a classification of the different EES systems divided according to the energy form; all these storage systems have the same purpose: converting electrical energy into another form of energy or in a carrier which can be stored easily. Among them, the most used worldwide form of energy to store electricity is the mechanical one; in particular, pumped hydroelectricity represents around 15.9% of the world's total electricity generation with a total global installed capacity of 1150 GW [14]. A hydroelectric plant is constituted mainly by a water reservoir and a power turbine located at different altitudes; when the water flows down through a duct (discharge phase), the starting potential energy of water is converted into electricity while in the charge phase the water in the lower tank is pumped to the upper-level to restore the initial potential energy of water. However, the great problem limiting the potential of this option is the topography of the region where it is installed. Compressed air storage could be an alternative solution to these problems; here, electricity is used to compress air and then store it in caves or other underground structures.

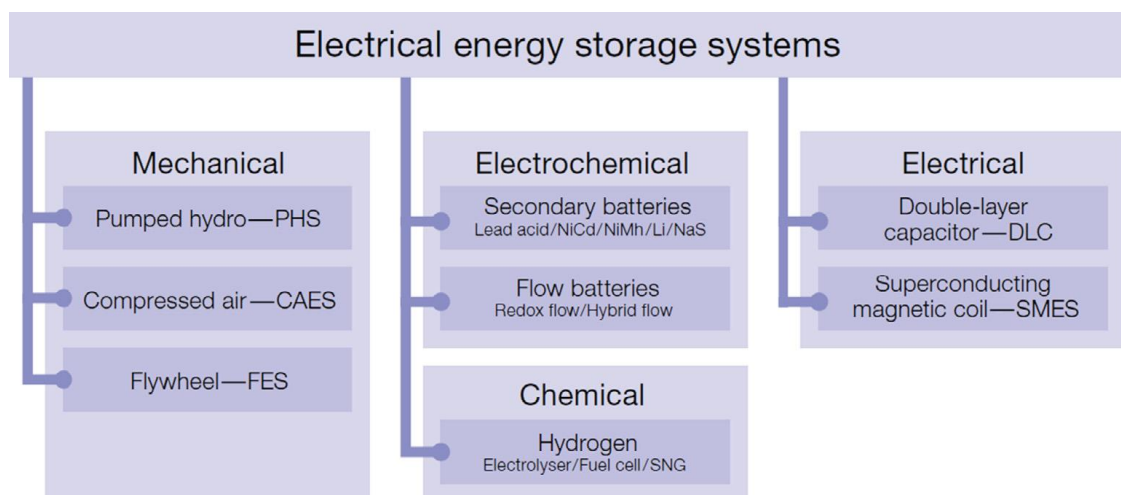


Figure 2.6 Schematic representation of the different kinds of EES systems divided by forms of energy [15].

The disadvantages related to this option are the huge volumes required to store energy (for example compared to H_2) and different specific geological constraints which limit the widespread of this technology.

In addition to these types of technologies, other forms of energy can be exploited, like electrochemical or electrical ones; batteries convert electricity into electrochemical energy while electrical energy systems include mainly superconductors and capacitors. All these first groups of systems enable the storage of electricity in a short-time period: for example, for small-size plants, batteries and capacitors are used, while larger systems rely on compressed air storage. On the other hand, a new concept has been designed for the large-size and long-term storage of electricity exploiting chemical energy, the so-called power-to-X scheme. In the following part, a brief overview of the power-to-X scheme is presented, focusing attention, especially on the power-to-gas pathway.

Figure 2.7 represents the schematic concept of power-to-X routes. The first possible output of the entire power-to-X route is hydrogen; as analysed in the previous paragraphs, this chemical fuel can be produced by water electrolysis using electricity to perform the reactions. In this way, renewable energy can be exploited and converted into a chemical form following the power-to- H_2 route, a subgroup of the complete process. Therefore, this chemical medium has a double effect: it enables the storage of huge amounts of electricity for long periods and it allows the reduction of the grid instabilities caused by the unpredictability of RES electric production surpluses. Moreover, H_2 can be employed also in other applications, for example in the transportation or industrial sector. A by-product of water electrolysis is the O_2 that is usually released into the atmosphere but sometimes can also be used for different purposes, for example as the oxidant for combustion processes or in the steel industry.

Following the route in *Figure 2.7*, the generated hydrogen can be mixed with pure carbon dioxide captured from exhausts of industrial or manufacturing processes through CO_2 capture systems (the CCS process has been analysed in *Paragraph 2.1*).

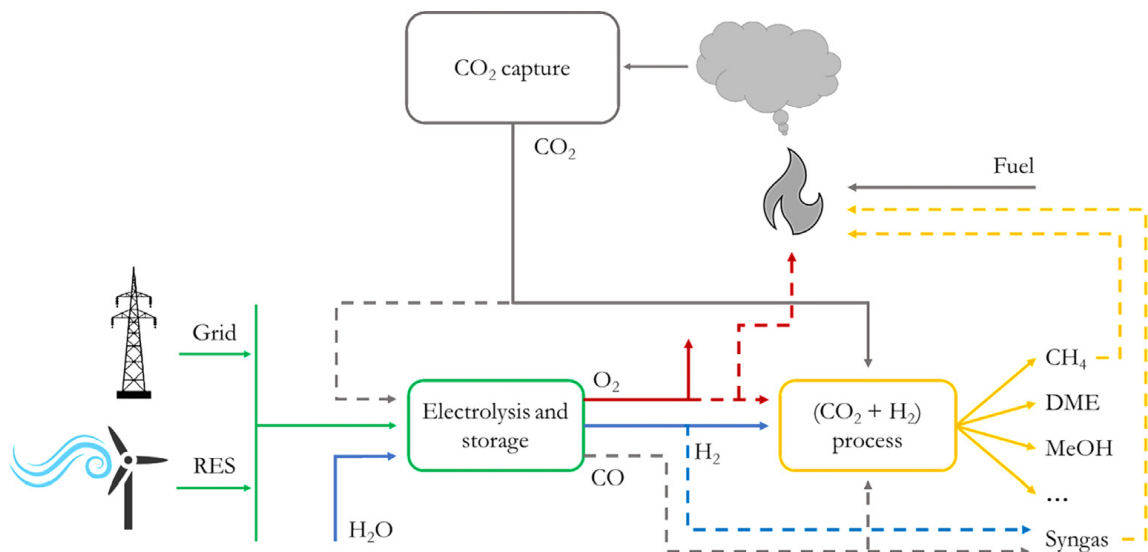


Figure 2.7 Schematic representation of power-to-X pathways [15].

The produced mixture of CO₂ and H₂ (or in case of co-electrolysis H₂ and CO) is transferred into the methanation section where CH₄ is finally generated. This last part of the power-to-X route is called power-to-gas (PtG) and is strictly related to the power-to-liquids and in general power-to-chemical categories that are parallel to the PtG concept. As a matter of fact, methane and in general synthetic natural gas (SNG) are not the only outputs of the whole process; there are also other commodities like liquid fuels (such as dimethyl ether, methanol, formic acid, etc.) or chemicals (esters, salicylic acid, etc.) that take part to the power-to-X scheme [16]. Finally, both the chemical and the gaseous products can be used directly or can be converted back to power (in the power-to-power concept) to shift the time of delivery power and thus, reducing the instability of the grid.

In the following paragraph, the PtG pathway is studied, pointing out the state of the art of this technology.

2.4.1 State of the art of power-to-gas systems

Power-to-gas consists of the chemical storage of electricity in the form of gaseous compounds like methane or hydrogen. From this perspective, power-to-gas can be defined as an extension of the power-to-H₂ route, in the sense that the production of synthetic natural gas (SNG) from H₂ and CO₂ compared to the production of only H₂ has the great advantage of being ready to be distributed via the natural gas grid; on the contrary, the hydrogen cannot be injected directly into the same network (in alternative H₂ can be used in the mobility sector, for instance).

Power-to-gas processes are all characterized by the same steps: first, electrolysis is performed producing pure hydrogen (from H₂O) or H₂+CO (if the feed reactant is a mixture of H₂O and CO₂) exploiting low-priced surplus electricity coming, for example, from RES. The second step consists of the methanation reaction which transforms H₂ and CO₂ (or H₂+CO) into methane. As a matter of fact, 2 main pathways for the power-to-gas route exist: one is the co-electrolysis of both H₂O and CO₂ and the following methanation of H₂ and CO, while the other one consists of simple electrolysis of H₂O and then the methanation involving CO₂ and H₂. The former process is defined by the following reactions:



Eq. [2-19] represents the overall reaction of co-electrolysis while *eq. [2-20]* is the methanation of CO.

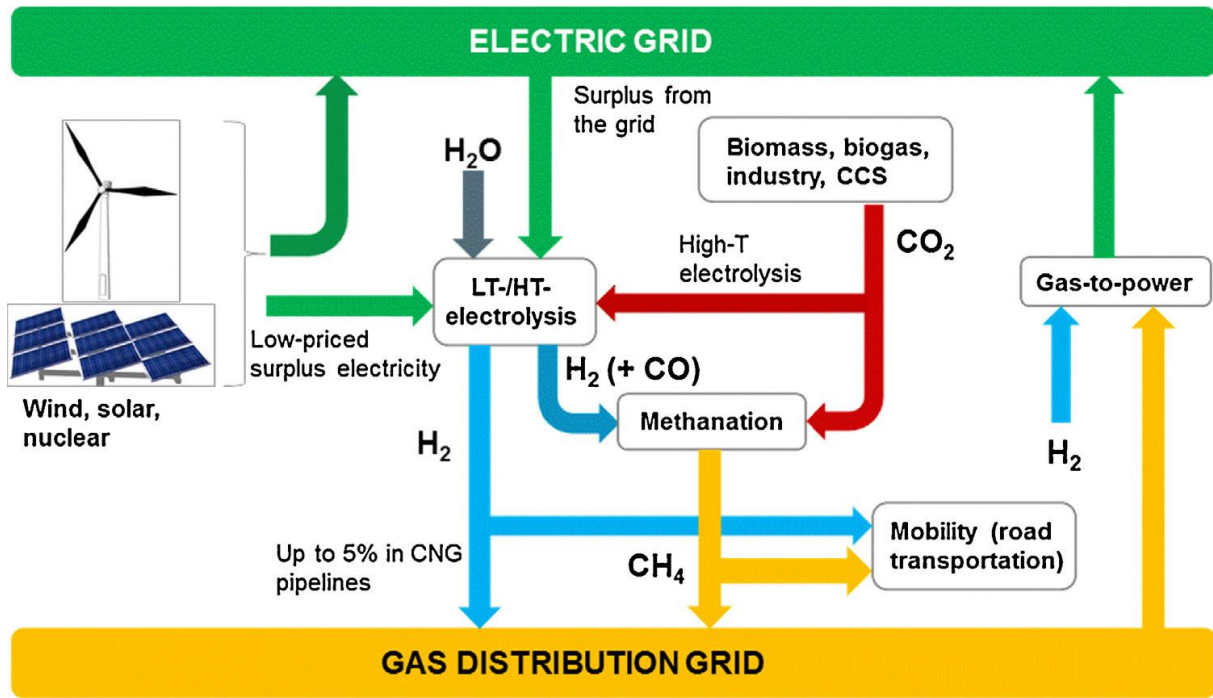
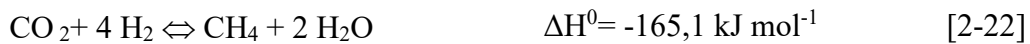


Figure 2.8 Schematic representation of PtG pathway [17].

Whereas, the second pathway is characterized by the following reactions:



Eq. [2-21] is the simple electrolysis, eq. [2-22] shows the CO_2 methanation.

Figure 2.8 shows a schematization of the entire power-to-gas route considering both pathways already analysed and different alternatives for the sources of the process (electricity to feed electrolyzers and CO_2 sent to methanation). Both two representations have the same starting and final point: from 2 moles of H_2O and 1 of CO_2 , 1 mole of CH_4 and 2 of O_2 are obtained (if the water is recovered from the methanation reaction). On the contrary, the difference between the two options is in the energy expenditures involved in the methanation process; as a matter of fact, simple electrolysis and co-electrolysis are endothermic processes with a similar enthalpy of formation (eq. [2-19] and [2-21]), while CO_2 methanation is less exothermic compared to CO methanation (eq. [2-20], [2-22]). Therefore, since the whole process is always endothermic, much less heat has to be supplied in the first pathway (involving co-electrolysis). This is translated into a higher efficiency from a thermodynamic point of view.

The actual state of the art of power-to-gas systems is strictly related to the type of technologies chosen to perform both electrolysis and methanation and also to the energy source used to feed the electrolyzer.

As previously analysed, both CO and CO₂ methanation can be performed; the former is a mature technology, especially for coal gasification while the latter is still under development with a lower overall efficiency but close to CO methanation (the achievable efficiencies are around 80%) [18].

For what concerns the section where electrolysis is performed, the cells that can be used are high or low temperature electrolyzers with all advantages and disadvantages already mentioned in *paragraph 2.2.1*. SOEC (high temperature) are promising technology suitable especially for co-electrolysis; in literature, there are many works in which the potentiality of this technology is analysed, studying its coupling, for example, with nuclear energy [19] or with Fischer-Tropsch process for the conversion of electricity into hydrocarbons [20]. On the other hand, low temperature electrolyzers (AEC and PEMEC) are mature and commercially available technology and thus, widely studied for the coupling with CO₂ methanation. A lot of different models are available in literature dealing with different technologies used for the power-to-gas pathway ([21],[17],[22]) and also other works, where power-to-gas pilot plants all over the world have been studied [23].

In conclusion is important to remember that the starting form of energy that is converted in chemical form is the electric surplus that, otherwise, would be curtailed; this virtuous coupling between RES and carbon dioxide sequestered from exhausts of different processes may lead to a new scenario of a circular economy, where CO₂ molecule can be reused many and many times.

3 Case study

The thesis deals with a techno-economic analysis of innovative solutions for the integration of processes aimed at implementing the decarbonization of power plants. In particular, the study is referred to a waste-to-energy plant and it is focused on the conversion of carbon dioxide contained into the exhaust of the plant into valuable products. In this perspective, two different and separate solutions for the conversion of CO₂ are addressed in this dissertation:

1. The **Power-to-gas system** (the operation of which has been introduced in the previous paragraphs) to produce synthetic natural gas (SNG) just from the CO₂ captured from the exhaust of the waste-to-energy plant and the H₂ produced by the electrolytic cell.
2. The **liquid CO₂ production plant** only for the sequestration of CO₂ contained into the exhaust of the waste-to-energy plant and its following storage in liquid form (liquefied gas by pressure) for the filling of a cylinder trailer every 2 days.

In the following paragraphs, an introduction to the operation of the two systems will be presented, showing a detailed representation of the different sections and the hypothesis made for the choice of the components. Moreover, the results of the annual simulations made by a previous study on the power-to-gas were reworked, adapting them to the two systems considered to obtain material and energy flows. With these results, firstly, a detailed analysis of the energy consumption is implemented to evaluate some important environmental and energy parameters among which also a preliminary sizing of the two systems. Secondly, a detailed economic analysis is performed, aimed at evaluating different economic indexes, such as the Levelized Cost of the different products, to understand the feasibility of the two solutions considered.

In the following paragraph, some important data on the annual emission of the waste-to-energy plant will be presented, targeting it at defining the annual hours of operation of the power-to-gas and liquid CO₂ production plant.

3.1 Input data from the waste-to-energy plant

Firstly, data from emissions of the waste-to-energy plant were provided by the emission monitoring system (SME) for 2019; they were used as input for the modelling of the power-to-gas and the liquid CO₂ production plant. In particular, the data considered are annual profiles, collected every 30 minutes, of the exhaust flow rate ejected from the chimney of one disposal line and their composition in terms of volume fractions of nitrogen, oxygen, carbon dioxide and water vapour.

Moreover, also the concentrations inside the exhausts of pollutants were provided, such as hydrochloric acid, hydrofluoric acid, ammonia, NO_x, SO_x, etc., that could cause degradation phenomena of the solvent. In *Figure 3.1* and *Figure 3.2* the annual profiles of the exhaust flow rate and its macro-composition in terms of volume fraction of different compounds respectively are shown; these two graphs were developed considering a first approximation on the data provided to remove those ones related to abnormal functioning of the system. In particular, the shutdown of the plant was imposed when the concentration of CO₂ in the exhaust was 0%_v and/or those of the O₂ was above 20%_v, even though the exhaust flow rate was not null; therefore, in these periods, the exhaust flow rate and its macro-composition were set equal to zero.



Figure 3.1 Annual profile of exhaust flow rate (kNm³/h) ejected from the line of the waste-to-energy plant



Figure 3.2 Annual profile of the exhaust's macro-composition (%v)

To find other periods of the year characterized by an unusual functioning of the plant, the annual profile obtained by this approximation was then overlapped to the annual profile of the net electric power produced by the steam turbine (*Figure 3.3*). As a matter of fact, in this study the hypothesis has been made that the waste-to-energy plant can work both on full electric and in Combine Heat and Power (CHP) mode. In particular, the hypothesis of the production of electricity from the turbine (full-electric) is used in the power-to-gas system while the production of both electricity and steam (CHP planning) is introduced in the study of the liquid CO₂ production plant considering a cogenerative ratio (λ) equal to 4.

In *Figure 3.3* it is possible to notice three main periods in 2019 in which the plant reduced its power production; in particular, there are two periods when the plant is subjected to a quite long stop: the first is between the 25th of August and the 3rd of September while the second between the 17th and the 18th of October. Moreover, the third period, characterized by a reduction in power production, is found between the 16th of June and the 13th of July. During these three intervals, the entire waste-to-energy system will be considered not in operation in this study.

In the rest of the year, there were also short intervals of time (lower than 12 hours), in which the exhaust flow rate coming from the waste-to-energy line was equal to zero (e.g. 10th of November or 20th of April) or the net power production decreased (e.g. during the 4th or 15th of February). In these intervals of time, it is not made the hypothesis of total shutdown of the plant, but different solutions will be considered (e.g. storage systems or purchase of electricity from the grid) to overcome the lack of exhaust flow rate or electricity production in the same periods. The techno-economic implication related to this hypothesis will be discussed in detail in their respective sections.

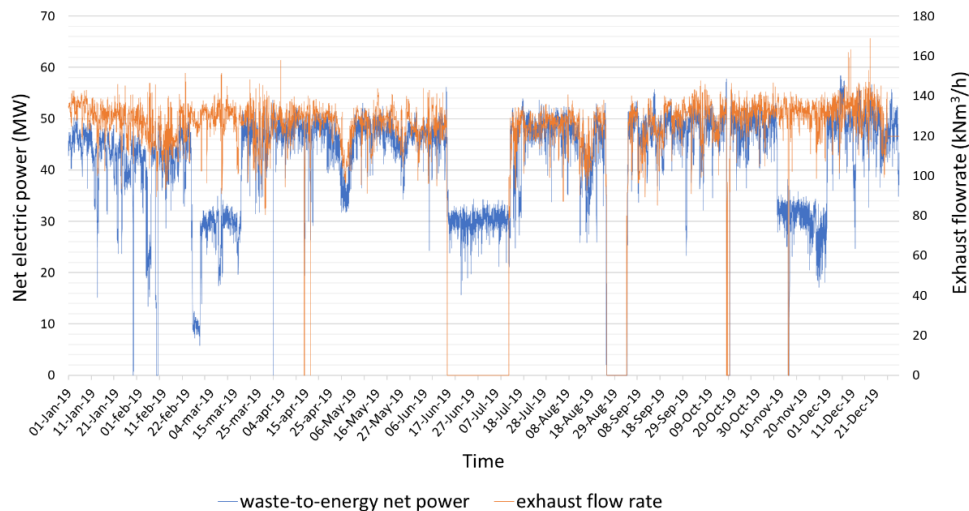


Figure 3.3 Yearly net power produced by the waste-to-energy plant vs exhaust flow rate

In conclusion, from the hypotheses already introduced on the shutdown of the waste-to-energy plant, the yearly operative hours of the two systems analysed are set equal to **7879 h/y**.

4 Methods for energy and environmental analysis

In this chapter the different inputs and technologies used for the modelling of the two systems are presented, analysing separately each main section. As previously introduced, the annual simulations made by a preceding study on the power-to-gas system are adapted to the solutions considered implementing a demand-to-production (D2P) method. It consists of setting a value for the products flow rate to size each component and calculating the energy and material flow exchanged between each section and with the outside, during one year of operation. With these results, some important energy and environmental parameters are evaluated to understand the technical feasibility of the systems.

4.1 Modelling of the power-to-gas plant

The power-to-gas system, outlined in *Figure 4.1*, is constituted by 3 main sections:

1. **CO₂ capture section**
2. **Electrolysis section**
3. **Methanation section**

In this paragraph, an introduction to the general analysis of the single sections which constitute the whole system is provided, focusing on the different technologies used (the main principles of the processes involved in each section have already been analysed in the first part of this work). It has been considered the stationary model, developed by a previous study with the software Aspen Plus; in particular, the case discussed in this work is referred to the production of 500 Nm³/h of SNG from the methanation section, that corresponds to the removal of 1 t/h of CO₂ from the exhaust of the waste-to-energy plant by the CO₂ capture system and the production of 180 kg/h of H₂ from the electrolysis system (nominal values). The specifications of the three main sections of the power-to-gas system are presented in the following part.

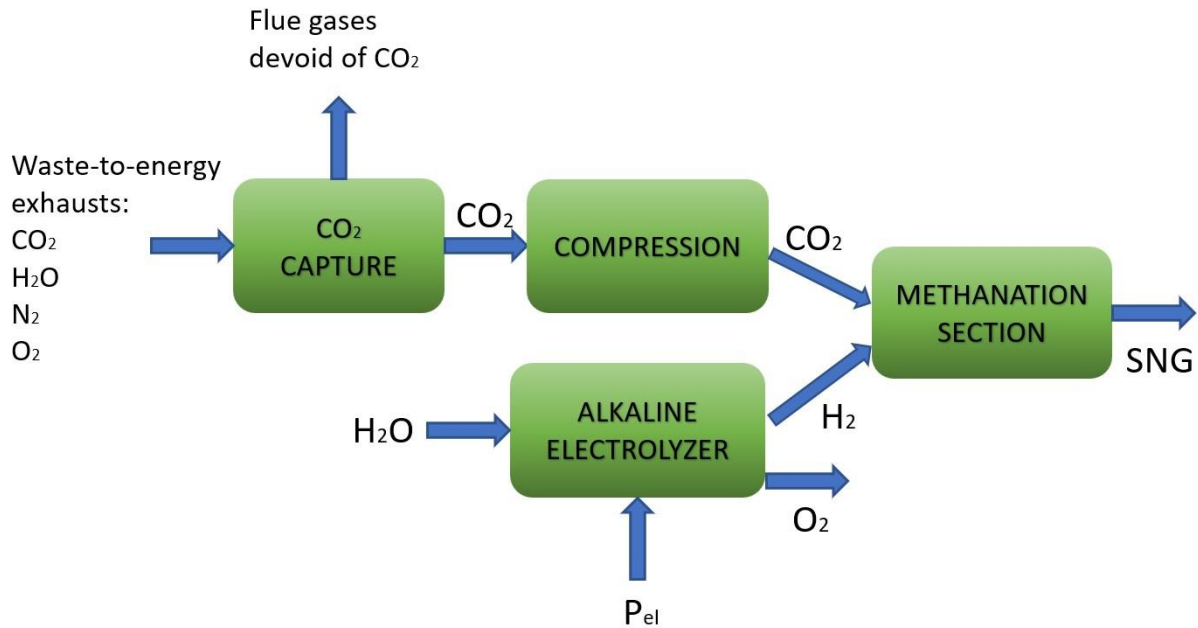


Figure 4.1 Process scheme of the power-to-gas system

4.1.1 CO₂ capture section

In the carbon capture section, the CO₂ is separated from the other gases composing the exhaust coming from the waste-to-energy plant and subsequently captured through a liquid or solid solvent. In this study, the post-combustion configuration for the CO₂ capture process from the exhaust of combustion has been considered (see paragraph 2.1.1); in particular, in the process of ab/desorption (see paragraph 2.1.2) the solvent used is a mixture of MEA and the ionic liquid [Bpy][BF₄] that constituted 30% in weight of the solvent. In Figure 4.2 there is a schematic representation of the entire capture system.

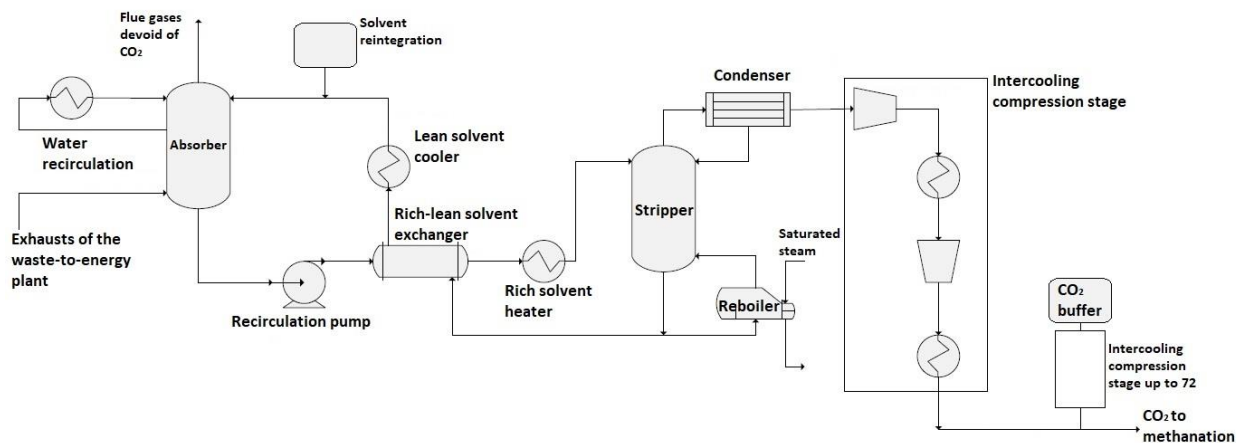


Figure 4.2 Scheme of the CO₂ capture section

The system has been implemented considering also other models as a starting point [24]. The main technologies composing this section are:

- An absorber equipped with an intercooler: this solution allows reducing the required amount of circulating solvent and, thus, the size of the equipment [25].
- A heat exchanger that enables the thermal recovery between CO₂ lean and rich solvent.
- A stripper column equipped with a reboiler and a condenser. The former was used to improve the purity of the solvent leaving the stripper and then recirculating back into the absorber, while the latter, was needed to improve the purity of the CO₂ concentrated stream headed to the methanation section, removing H₂O.
- Intercooling compression of CO₂ up to the methanation process pressure (15 bars)
- The solvent vessel installed to deal with the variations of the solvent flow rate, due to the continuous fluctuations of the exhaust's composition during the year. The tank is also used to collect the solvent, for example, in case of component maintenance.
- The CO₂ buffer placed upstream from the methanation section in order to solve problems related to the methanation reactors and to the capture system.
- The cooler for the lean solvent and a heater for the rich solvent.

The absorber and the stripper were designed like packing columns with a maximum value of flow rate imposed below 80% of the limit that causes the flooding. As a matter of fact, in absorption-desorption packed columns, if any or certain compositions of liquid or gas flow in combination with the reboiler heat pressure and too high stripper feed power, the column becomes flooded with the liquid; flooding is accompanied by a dramatic increase in pressure, resulting in inefficient operation and potential damage to equipment. Moreover, the hypothesis of a value of efficiency of the absorption process of 75% were made (typically it is between 75%-95%) so that a trade-off between economic and technical aspects is considered. In particular, the exhausts of the waste-to-energy plant are treated in their unaltered state, namely at 120 °C and 0.978 bar, although it is advisable to reduce their temperature to facilitate the absorption of the CO₂ by the solvent.

The intercooling compression is necessary because the desorption process takes place in the stripper at a pressure of 3,5 bars lower than the 15 bars at which the methanation process is carried out. The intercooling compression is chosen to reduce the compression work making it as much isothermal as possible.

As previously introduced, it is important to point out that in the study underlying this dissertation, a model is defined in order to estimate the almost pure CO₂ flow rate (99.6% w) to be constantly supplied to the methanation section varying the amount of exhaust from the waste-to-energy plant and sent to the absorber. Through this model it is possible to obtain the

annual simulation of the material and energy flow exchanged inside each component of the system.

Although phenomenon such as corrosion and degradation, caused by the MEA inside the solvent, can cause problems for the facility in terms of efficiency and maintenance, as a first approximation they are not treated in this study.

Sizing of the section

A preliminary sizing of the system is fundamental not only for the development of the model but also as an input for the following part of the economic analysis.

For what concerns the dimensions of the absorber and the stripper (assumed as cylindrical vessels), a height/diameter ratio is set equal to 10 and 8 respectively. From the simulations, the height for the two columns is defined equal to 15 m for the absorber and 4 m for the stripper. Moreover, the void fraction of the packed bed is fixed equal to 0.95 (both for absorber and stripper).

In addition, the volume of the solvent tank was preliminarily fixed equal to the sum of the volume of absorption and desorption vessels.

As previously introduced, a buffer for CO₂ was installed upstream from the methanation section; in particular, the option of a single vessel where CO₂ is stored in the liquid phase was chosen and the storage pressure and the range for the process of methanation were configured to a value of 72 bars and 12 hours respectively. The volume needed is evaluated dividing the mass of liquid CO₂ produced in 12 hours by the density (859.14 kg/m³ at 72 bars).

For the group of intercooling compression up to the value of 15 bars (representing the methanation pressure), it was assumed to cover an area of 3.1 m x 1.9 m with 2.4 m in height, values obtained from the catalogue of different suppliers. On the contrary, the shaft power of all the compressors is defined from the annual simulations.

The recirculation pump's size is neglected in the total footprint of the section, while its shaft power is derived from the simulations.

Finally, the sizing of the heat exchangers was considered; all of them, except for the heat exchanger used for the heat recovery between CO₂ lean and rich solvent stream, require an external heat source. The reboiler and the heater of the rich solvent need a source of heat at high temperature (it would be recovered from the vapour coming from the methanation section, see 4.1.4), while the coolant chosen for the others cooler in the section is water at 15°C with a ΔT of 10°C. Assuming a counter current heat exchanger for all the components analysed in this section, the log mean temperature difference (LMTD) and the maximum heat flux are estimated from the simulations. Moreover, from the software Aspen Exchanger Design and Rating, values of the global heat transfer coefficients for the different heat exchangers are estimated (*Table 4.1*).

From all these data it was possible to calculate the heat transfer area using the following formula:

$$A_{st} = \frac{Q_{max}}{U \cdot \Delta T_{log}} \quad [4-1]$$

where Q_{max} is the annual maximum heat flux (in kW) derived from the simulations, U is the global heat transfer coefficient (in kW/m²/K) and ΔT_{log} is the log mean temperature difference (in K). The value of A_{st} in m² obtained using *equation [4-1]* represents the starting point for the economic analysis in order to evaluate the cost of the heat exchangers (see *Table 5.7*).

Table 4.1 Global heat transfer coefficients for the different heat exchangers analysed

COMPONENT	GLOBAL HEAT TRANSFER COEFF. (kW/m ² /K)
Absorber Intercooler	1.45
Rich solvent heater	0.25
Stripper condenser	1.12
Reboiler	1.12
Solvent exchanger	1.68
Lean solvent cooler	1.78
Cooler#1 CO₂ compression	0.19
Cooler#2 CO₂ compression	0.11
Cooler#3 CO₂ compression	0.18

Once the heat transfer area is evaluated, a preliminary design of the heat exchangers is performed to compute the footprint of the entire capture section. Most of the following quantities are obtained from the simulations in Aspen Exchanger Design and Rating. In particular, the total footprint of each heat exchanger is defined using:

$$A_f = N_s \cdot N_p \cdot L_{ht} \cdot d_s \quad [4-2]$$

where N_s and N_p are the total numbers of tubes in series and parallel respectively, d_s is the diameter of the shell and L_{ht} is the length of each heat exchanger expressed both in meters and evaluated from:

$$d_s = \max\{0.1 \cdot L_{ht}; N_t \cdot P_t^2\} \quad [4-3]$$

$$L_{ht} = \frac{A_f}{N_s \cdot N_p \cdot N_t \cdot d_t \cdot \pi} \quad [4-4]$$

where N_t is the total number of tubes, P_t is the pitch fixed to 125% of the tube's diameter (d_t) that, as a first approximation, is set equal to 1 inch.

Therefore, having determined the net dimensions of the main components (absorber, stripper, buffers, exchangers, compressors), it was assumed to insert them inside a cabinet with a rectangular plan whose dimensions are determined assuming a certain arrangement of the components inside the cabinet, providing for an increase of 20% in both length and width.

4.1.2 Electrolysis section

In the electrolysis section, a certain amount of H_2 is produced from water and electric power mainly. Thus, the hydrogen is fed into the methanation section where the SNG is generated (see *paragraph 2.3*). The section is composed of 3 main components:

- The electrolysis system
- The water tank
- The water pump

At the same time, the electrolysis system is composed of the stack where the hydrogen is actually produced and all the balance of plant (BoP). This last part of the system consists of different compounds such as a power converter, purification system (water and gas) and water recirculation pump. Moreover, in this study, alkaline technology has been considered for the stack of the electrolysis system. The principal data for the alkaline electrolytic cell are shown in *Table 4.2*.

On the other side, the pump is used to replenish the water consumed by the electrolysis reaction. Furthermore, the tank is sized to have an autonomy of at least 12 hours while the specific consumed water by the electrolyzer is set equal to 15 L per kg of H_2 produced [26], whilst the shaft power of the pump is computed considering the efficiency of 0.7 and the pressure of electrolysis of 15 bars.

Table 4.2 Operative data for the alkaline cell

Operative temperature (°C)	70
Operative pressure (bar)	15
Nominal current density (A/cm²)	0.35
Minimum power	20% of nominal power

Modelling of the electrolyzer

A stack is composed of many cells in series, representing the basic unit to produce hydrogen starting from alternating current. When needed, stacks can be arranged in parallel or series to achieve the desired nominal capacity. The modelling follows a bottom-up approach: the single cell is first modelled, and then passed to the stack and system level.

To represent an electrolytic cell, it is necessary to know its polarization curve, which gives the relationship between current density and voltage. This curve, therefore, indicates how much voltage (V_{cell} in Volts) is required to generate a certain current density, which is directly proportional to the density of hydrogen produced.

The voltage of the electrolytic cell is defined as follows:

$$V_{cell} = V_{Nernst} + V_{ACT, AN} + V_{ACT, CAT} + V_{OHM} + V_{CONC, AN} + V_{CONC, CAT} \quad [4-5]$$

The term V_{Nernst} represents the Nernst voltage and derives from the thermodynamics of the electrochemical conversion process. In a real electrolyzer, in addition to the term V_{Nernst} , the presence of various overvoltage phenomena (which represent sources of inefficiency) must be considered. These losses can be grouped into three main contributions: activation (anodic and cathodic side), ohmic and concentration (anodic and cathodic side).

Faraday's law is used to relate the current density and the useful amount of hydrogen produced:

$$n_{H_2} = \frac{N_{H_2}}{A_{cell}} = \eta_F \cdot \frac{i}{2 \cdot F} \quad [4-6]$$

where N_{H_2} (in mol/s) corresponds to the flow rate of hydrogen produced, n_{H_2} is the flow rate of hydrogen produced per unit of active area (in mol/s/cm²), i (in A/cm²) represents the current density, A_{cell} (in cm²) constitutes the active cell area and F is the Faraday constant (equal to approximately 96485.33 C/mol). The term η_F represents Faraday efficiency and takes into consideration the fact that not all the hydrogen produced by the electrolysis reaction is a useful product for the end-user (a fraction of the hydrogen generated can, for example, react in secondary reactions or diffuse through the membrane that separates the anode from the cathode electrode). The following relationship is used for the calculation of Faraday's efficiency [27]:

$$\eta_F = 1 - \frac{2 \cdot F}{i} \cdot (n_{H_2, cross} + 2 \cdot n_{O_2, cross}) \quad [4-7]$$

where $n_{H_2,cross}$ and $n_{O_2,cross}$ (in mol/s/cm²) represent the specific total flow rate of H₂ and O₂ through the membrane of the AEC. These values are obtained through a mass balance of the different species in the anodic and cathodic compartment.

Moreover, the electrical power density consumed by the electrolytic cell to produce hydrogen p_{EL} (in kW/cm²) is evaluated using:

$$p_{EL} = V_{cell} \cdot i \cdot 10^3 \quad [4-8]$$

Moving from the modelling of the cell to that of the stack and the system, the total voltage of the stack is calculated as the sum of the voltages of all the cells that compose it:

$$V_{stack} = n_{cells} \cdot V_{cell} \quad [4-9]$$

where n_{cells} represents the number of electrolytic cells within the stack.

In conclusion, knowing the required amount of H₂ in order to produce 500 Nm³/h of SNG and the current density of the AEC (from *Table 4.2*), it is possible to evaluate A_{cell} from *equation [4-6]*; from this value, subsequently, the electrical power consumed by the electrolytic cell can be computed by multiplying p_{EL} by A_{cell} . In addition, it is necessary to take into account the electricity consumption due to the auxiliaries of the stack (e.g., control system, pumps, fans). In general, for alkaline electrolyzers, the electrical load required by the auxiliaries represents about 10% of the total electrical power [8]. This value can also be considered constant over the entire range of operation of the electrolyzer [8].

Electrolyzer power supply scenarios

Two different scenarios have been considered for what concerns the power supply of the electrolysis section:

- a. Using part of electricity produced by the waste-to-energy plant (**CASE A**).
- b. Considering surplus electricity coming from RES; in particular, in this second option, the hypothesis of zero cost of this energy has been made, considering the extreme case in which, otherwise, the electricity would be intended to curtailment (**CASE B**).

These two scenarios will be considered in the following part of the economic analysis to emphasize the importance of electricity on the total budget of the plant. Moreover, it is

important to point out that there are short intervals of time when the electric consumption of the electrolysis system is not met by the waste-to-energy plant (see *paragraph 3.1*): in those periods, in CASE A, the hypothesis has been made that the missing electricity is purchased from the grid so that the electrolyzer continues to produce hydrogen to be sent to the methanation section.

It is important to point out that, in both two cases, since the electricity is fed constantly to the electrolysis section, it is not necessary the installation of hydrogen storage; in case of maintenance or failure of the electrolyzer a small buffer of hydrogen could be regarded but in this study, to minimize the investment cost, it will not be considered.

Sizing of the section

For the electrolysis section, there are no data available for the direct estimation of the stack's size. The only way to obtain a preliminary approximation on the dimensions of the system is to retrieve the data from the manufacturers of other existing plants. Moreover, as a first approximation, the water pump and the water tank are not considered in the sizing of the section because their dimensions can be reasonably included inside the total system area derived by the manufacturers.

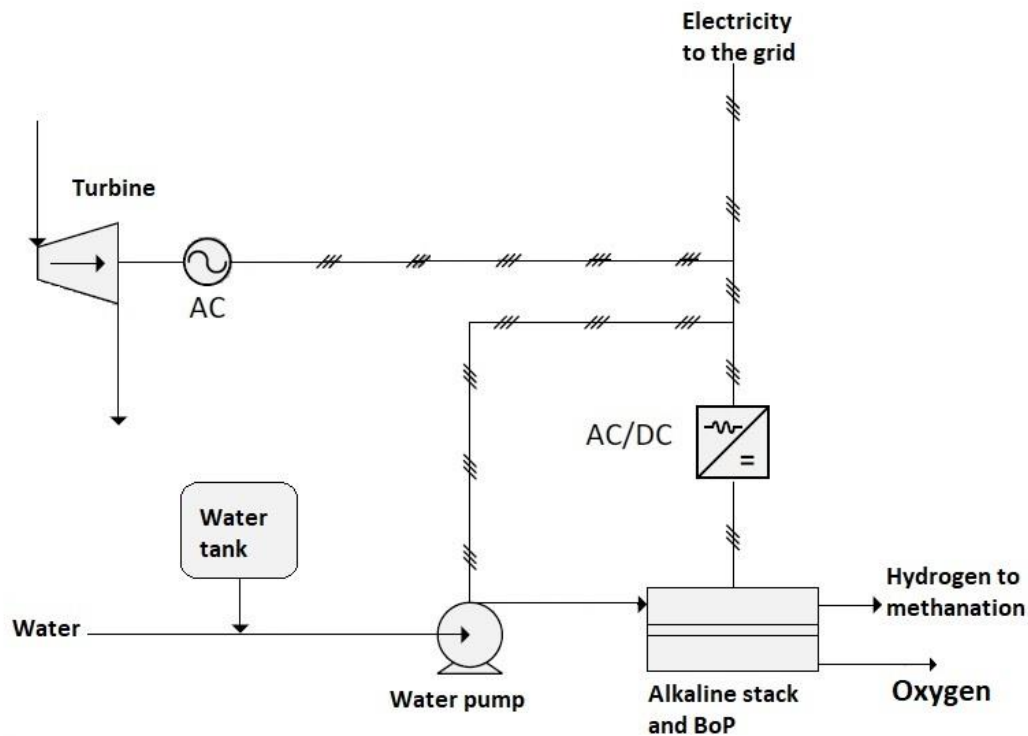


Figure 4.3 Schematic representation of the electrolysis section

4.1.3 Methanation section

The methanation section aims to produce SNG, composed mostly of CH_4 , starting from a mixture of CO_2 and H_2 . The product is then used for various purposes, such as for public transport, and its transportation can be carried out thanks to the national natural gas distribution network. The SNG produced into the methanation section can be injected into the existing grid only if it has particular properties defined by the laws in force. In *Table 4.3* the principal parameters of interest for SNG defined by SNAM [28] are shown. Traces of sulfur, mercury, ammonia, etc. are not considered in the process because they were already treated inside the waste-to-energy plant.

Table 4.3 Quality parameter of SNG (HHE and Wobbe index are referred to conditions of 15°C and 1 atm while the dew point is defined at 70 barg)

Properties	Acceptable range	Unit
Higher heating value	34.95÷45.28	MJ/Sm ³
Wobbe index	47.31÷52.33	MJ/Sm ³
Relative density	0.5548÷0.8	-
Water dew point	≤ -5	°C
Temperature	3÷50	°C
H ₂	≤ 0.5	% vol.
O ₂	≤ 0.6	% mol.
CO ₂	≤ 3	% mol.
CO	≤ 0.1	% mol.

Considering all the different options and configurations that can be found in literature ([17],[29],[30]), it has been implemented a process with 3 cooled-fixed bed reactors (*Figure 4.4*) at a pressure of 15 bars. The parallelization of the 3 reactors is considered to make the methanation section as flexible as possible. In particular, the cooling fluid of the reactors is boiling water at 270°C and 49,5 bars; in this way, the methanation reaction occurring inside the reactors produces heat in the form of saturated steam that can be recovered and used for the regeneration of the solvent at the reboiler (CO₂ capture section).

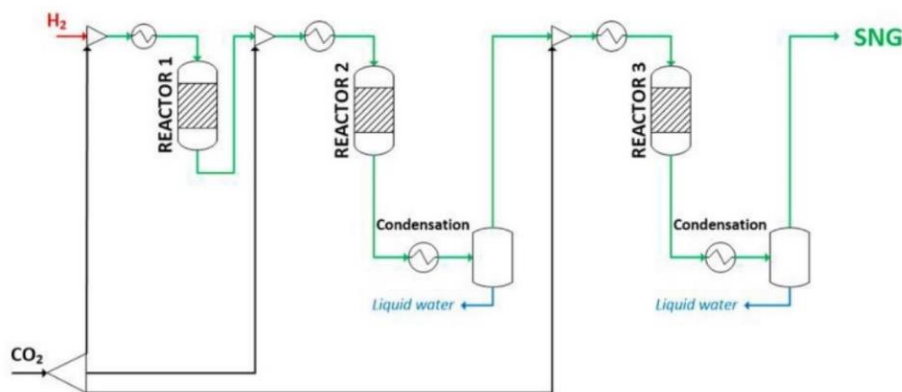


Figure 4.4 Schematization of the methanation process with 3 cooled-fixed bed reactors [29]

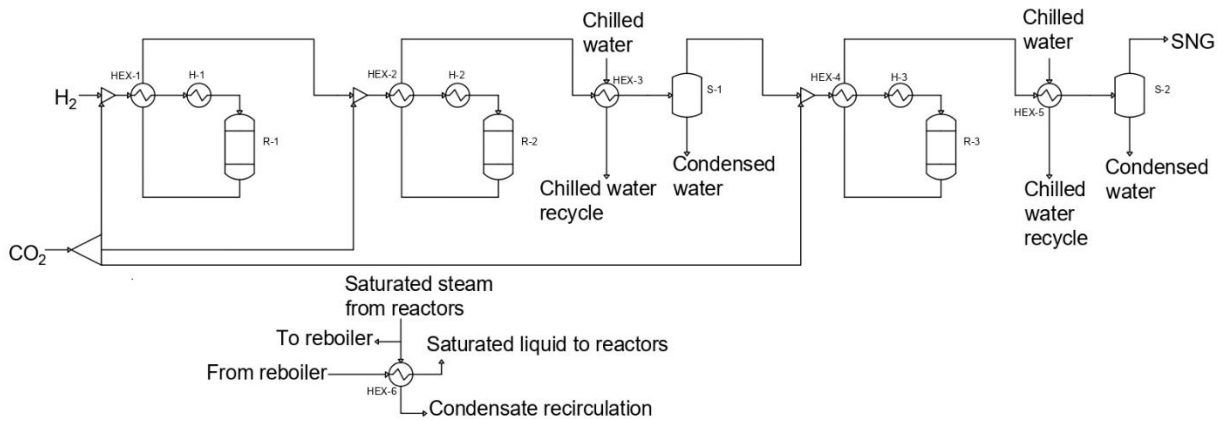


Figure 4.5 Schematic representation of the methanation section

In Figure 4.5 it is shown the representation of the entire methanation section. Hydrogen is fed entirely at the inlet of the process, while carbon dioxide is divided into three different streams (with different percentages) to better manage the production of heat inside the reactors.

In series with the reactors it is considered also a water removal stage by condensation, between the second and the third reactor. This water removal process allows to shift the condition of thermodynamic equilibrium to higher CO₂ conversions, favoring the production of CH₄ and reducing the unconverted gas fraction; in this way, it is possible to comply with the network legislation which provides for a maximum quantity of 3%_{mol} of CO₂ (see Table 4.3). The condensation of water between the second and third reactors and at the end of the methanation section is carried out using chilled water (4 °C ÷ 7 °C) and bringing the gases to 14 °C.

Moreover, the streams of CO₂ and H₂ at the inlet of the reactors are preheated using the residual heat in the gases at the outlet of the reactors themselves, using shell and tube exchangers. Furthermore, electric heaters have been provided to heat the preheated gases entering the reactors and bring them to the same temperature as the cooling fluid (270 °C).

In conclusion, the coolant of the reactors is heated to 270 °C using the steam produced by the reactors inside an economizer.

The catalyst used in the reactors is the Ni/ γ -Al₂O₃ composed of an active component in Nickel and a support material in aluminium oxide (Al₂O₃) in order to increase the surface of the catalyst, as previously introduced in paragraph 2.3. This catalyst is subjected to sintering phenomena if reaches high temperatures. For this reason, the most relevant aspect for the design of the reactors is the maximum temperature reached along their axis, which must not exceed 550 °C to avoid too sudden deactivation phenomena (see page 13). In particular, each reactor is designed to work inside a specific range of the nominal flow rate of the section (i.e. from 60% to 110%); in this study, the value of 100% of the nominal flow rate will be considered.

For what concerns the optimization of the entire process of methanation, another important goal is to minimize the pressure drops, minimizing the length of the reactors, in order to reach the outlet of the methanation section with a gas at a pressure higher than 12 bars (pressure of introduction into the natural gas' network). To do so, a sensitivity analysis is carried out by the study on which it is based this dissertation; therefore, in the following paragraphs, the results applied to the condition of 500 Nm³/h of SNG produced will be presented.

Sizing of the section

Concerning the sizing of the section, the method applied resembles the CO₂ capture section (see *paragraph 4.1.1*). In particular, the main components of the section are the heat exchangers, the reactors and the electric heaters while the two condensers are not considered in this preliminary sizing, as for the economic analysis.

All the heat exchangers are sized using the results of the simulations that give the numbers of exchangers in parallel and series, the number of tubes, the number of shell passes, etc. The same is for the three reactors that in this study are treated as shell and tube heat exchangers (as for the other exchangers in the section). From these parameters it is possible to evaluate the heat transfer area using:

$$A_{ht} = \pi \cdot d_t \cdot L \cdot N_t \quad [4-10]$$

where d_t is the outer tube diameter (in meters), L is the length of each tube (in meters) and N_t is the total number of tubes. For the electric heaters, the parameter used in the following economic analysis is the power input that is retrieved from the simulations.

For the preliminary evaluation of the section footprint, the real dimension of the different components is evaluated. For all the heat exchangers (except for the three reactors) the total area occupied is defined using:

$$A_f = d_s \cdot L \cdot N_s \quad [4-11]$$

where d_s is the internal diameter of the shell and N_s is the number of shells. As for the reactors, with no data available for the internal diameter of the shell, to evaluate d_s , it is assumed that the area of the shell is 50% higher than the total section area of the tubes; from this value, the shell diameter is obtained and, thus, A_f can be evaluated.

The area occupied by the three electric heaters is obtained from the technical specification of the manufacturer [31]. On the contrary, the electric power required by the heaters is derived from the annual simulations.

Once all the net dimensions of the main components are determined, it has been assumed to insert them inside a cabinet with a rectangular plan as for the carbon capture section; its dimensions are determined assuming that the components are arranged inside the cabinet like in *Figure 4.4*, providing for an increase of 20% in both length and width.

4.1.4 Thermal integration between the sections

The analysis of the individual processes and related technologies of the system highlighted the possibility of integrating the different sections of the power-to-gas system in order to optimize the thermal management.

In particular, as already introduced in *paragraph 2.3*, the CO₂ methanation is a high exothermic reaction that produces a huge amount of heat (resulting from the cooling of the three reactors) in the form of saturated steam. From this perspective, the steam produced at a temperature of 270 °C, represents a high quality thermal source which can be exploited to meet any needs within the power-to-gas system. The most interesting use is in the CO₂ capture section where the solvent regeneration requires a considerable amount of heat at a rather high temperature. In particular, from a previous study on the power-to-gas system, the required heat needed for the solvent regeneration is evaluated to be equal to 3.546 kJ/g_{CO₂} at a temperature of 140 °C. Therefore, it is possible to exploit the available steam coming from the reactors, producing a positive effect on the efficiency of the entire power-to-gas plant.

Figure 4.6 shows the scheme of the possible integration between the methanation and CO₂ capture section. A fraction of the saturated vapor produced by the methanation process is primarily exploited in the economizer for heating the condensate from the CO₂ capture system up to saturated liquid conditions before being re-used in the methanation section for the thermal control of the reactors. The amount of steam not exploited as a hot fluid in the economizer is used for the regeneration of the solvent in the CO₂ capture section.

From a study on the power-to-gas readapted to the case discussed in this thesis has emerged that the three methanation reactors produce 4 kJ/g_{CO₂} in form of saturated steam at 270 °C; this amount is sufficient to meet the requested heat by the reboiler of 3.546 kJ/g_{CO₂} at 140 °C and simultaneously also the amount requested by the economizer. In particular, the reactors produce 2361 kg/h of saturated steam, of which 1763 kg/h are used to feed the reboiler, while the remaining 598 kg/h are used inside the economizer. In that way, the CO₂ capture section could be considered self-sufficient.

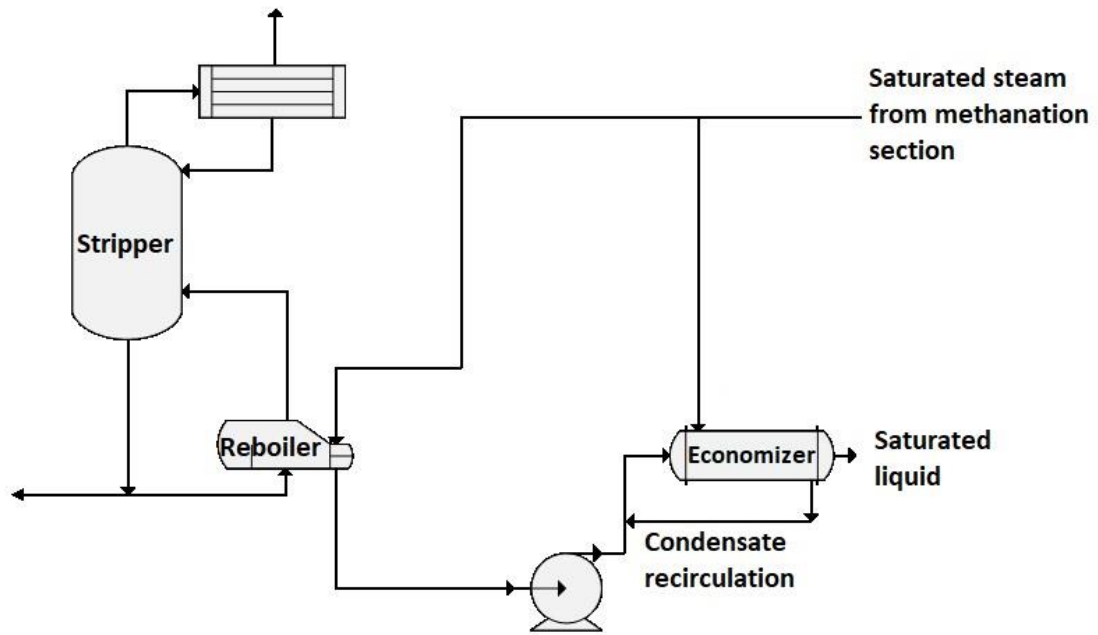


Figure 4.6 Scheme of the thermal integration between the methanation and the CO₂ capture section

4.2 Modelling of the liquid CO₂ production plant

The liquid CO₂ production plant resembles the CO₂ capture section of the power-to-gas plant already analysed (see *paragraph 4.1.1*). The aim of the section is always to capture the CO₂ inside the combustion exhausts of the waste-to-energy plant and store the carbon dioxide inside a tank. In this system, the CO₂ is stored in liquid form (liquefied gas by pressure) in a cylindrical tank that is sized to maintain the liquid for 48 hours. Every 2 days, the tank is emptied in order to fill a cylinder trailer managed by an external owner (i.e. retailer of technical gases). In this paragraph the main component of the system will be introduced and then the hypothesis made. The aim is to assess the operation of the plant, computing the energy and environmental performances, and evaluate the levelized cost of the liquid CO₂ produced, comparing it with the market values to understand the economic potentiality of the technology.

4.2.1 Data and technologies considered

The case treated is always the capture of 1 t/h of CO₂ from the exhausts of the waste-to-energy plant and the main technologies composing the section are the same as for the carbon capture introduced on *page 24*. The only differences are:

- The intercooling compression
- The tank of liquid CO₂

Figure 4.7 shows the scheme of the liquid CO₂ production plant; all the energy and economic study will be related to the analysis of the entire section without considering the cylinder trailer.

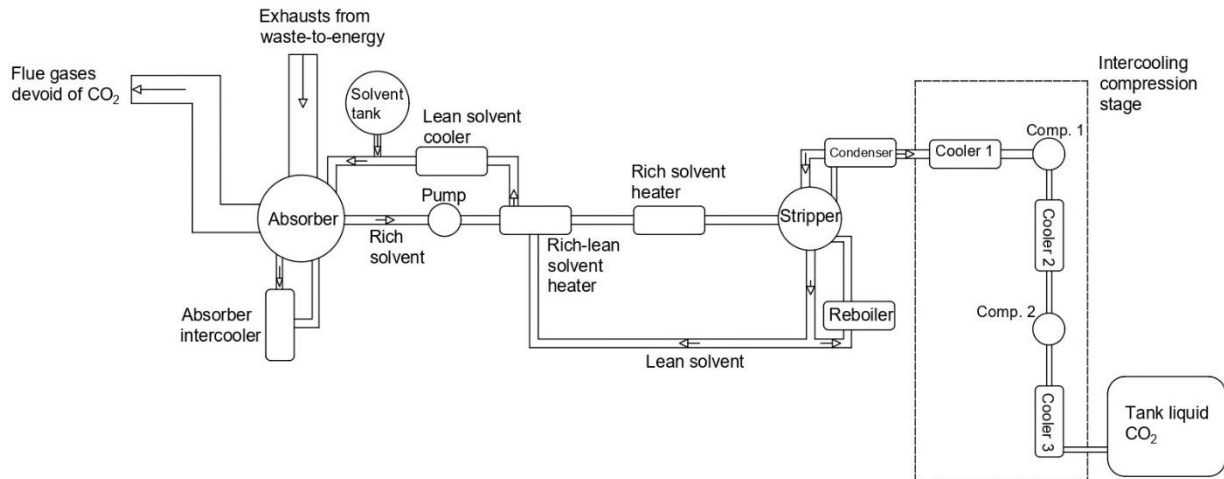


Figure 4.7 Schematic representation of the entire liquid CO₂ production plant

The stage of intercooling compression, here, brings the CO₂ from the pressure of the absorption process (3,5 bars) to the pressure selected for the storage in liquid form inside the tank. In particular, the storage conditions are set equal to 72 bars and 15 °C because carbon dioxide condensates very quickly (for example at 15 °C the saturation pressure is of about 53 bars) with a critical point fixed to 73,77 bars and 30,98 °C (see Figure 4.8). For this reason, to handle potential issues related to the variation of the temperature inside the tank due, for example, to seasonal temperature changes, is chosen a point inside the liquid region of the phase diagram (Figure 4.8) not so close to the saturation conditions. Moreover, at 72 bars and 15 °C the liquid CO₂ has a density of 859 kg/m³, much higher than the value in the gaseous form resulting in a tank less spacious, on equal substance contained.

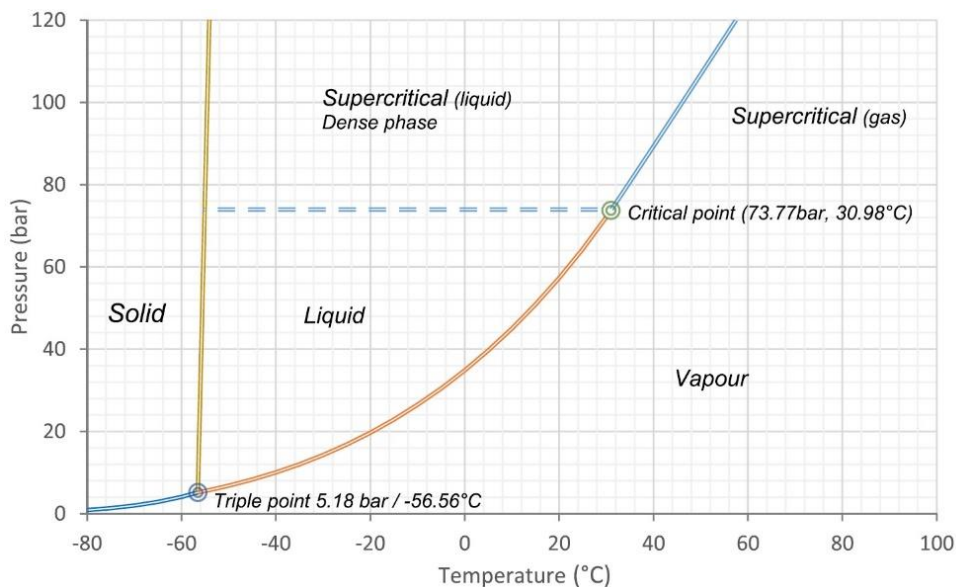


Figure 4.8 Phase diagram of CO₂ [32]

The intercooling compression stage is modeled using the software Aspen Plus. Since the other components of the system are sized according to the results of the study on the power-to-gas plant, only the two stages of compression are considered inside this model. As already analysed, the compression up to 72 bars is performed using the intercoolers to decrease the compression work; this happens because the work of the second compressor is reduced proportionally to the temperature reduction in the intercooling stage.

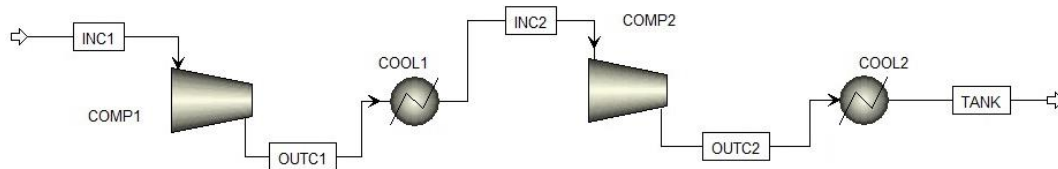


Figure 4.9 Aspen Plus scheme of the intercooling compression section

The input data to be used inside the software are shown in *Table 4.4*. In particular, an important parameter is the intermediate pressure between the first and second stage that is set equal to 15.87 bars; this value was chosen to remind that the best configuration is obtained when:

$$\beta_{1,opt} = \beta_{2,opt} = \sqrt{\beta_{tot}} \quad [4-12]$$

where β is the compression ratio and the subscripts 1 and 2 are referred to the first and second stage of compression.

Moreover, for the cooler, the coolant chosen is the same as for the other cooler inside the section, namely water at 15°C with a ΔT of 10°C.

Table 4.4 Input parameters for the model

INPUT PARAMETERS	VALUE
T_{inlet} (Compressor 1)	38 °C
P_{inlet} (Compressor 1)	3.5 bars
P_{outlet} (Compressor 1)	15.87 bars
T_{outlet} (Cooler 1)	38 °C
P_{outlet} (Compressor 2)	72 bars
T_{outlet} (Cooler 2)	15 °C
Isentropic efficiency of the compressors	0.72

4.2.2 Configurations for the waste-to-energy plant

An important difference between the carbon capture section of the power-to-gas plant and the liquid CO₂ production plant is the absence of a thermal integration for the solvent regeneration at the reboiler because, obviously, in this last system the methanation section is no more considered. For this reason, to solve the problem, two different cases are treated in the study:

- The waste-to-energy plant produces only electricity through the steam turbine (**full-electric** mode) and the solvent is regenerated using an electric heater with a power-to-heat efficiency of 95% and fed, precisely, by a fraction of the electricity produced by the waste-to-energy plant
- The waste-to-energy plant is in a **Combined Heat and Power** (CHP) mode and this would provide a steam flow rate at a thermal level consistent with that required for the solvent regeneration.

In the second case, part of the steam conveyed to the district heating network can be withdrawn from the turbine and brought to the reboiler. The CHP mode required the installation of discharge and return pipes from the turbine and towards the reboiler and vice versa. The length of the two pipelines is supposed to be 2x146 m. Moreover, the diameters depend on the heat to be supplied and are determined by imposing a speed of the steam v_{vap} in discharge and of the condensate v_{liq} in return of 20 m/s and 1 m/s respectively using the following equations:

$$D_{discharge} = \sqrt{\frac{4 \cdot \dot{Q}_{diff,max}}{\pi \cdot v_{vap} \cdot \rho_{vap} \cdot q_{lat}}} \quad [4-13]$$

$$D_{return} = \sqrt{\frac{4 \cdot \dot{Q}_{diff,max}}{\pi \cdot v_{liq} \cdot \rho_{liq} \cdot q_{lat}}} \quad [4-14]$$

where $\dot{Q}_{diff,max}$ is the maximum heat flux to be supplied to the reboiler during the year obtained from the simulations, ρ is the density in kg/m³ and $q_{lat} = 2163$ kJ/kg is the latent heat of condensation of the steam at 3 bars.

4.2.3 Sizing of the section

For the sizing of the system, the data from the main components remain the same as for the carbon capture section of the power-to-gas system (see *paragraph 4.1.1*).

As a first approximation, also the group of intercooling compression up to the value of 72 bars was assumed to cover an area of 3.1 m x 1.9 m with 2.4 m in height, as for the carbon capture section of the power-to-gas. Moreover, for the two compressors, the shaft power is derived from the simulations with Aspen (*Figure 4.9*) considering that this value is constant during the annual operation.

The tank of the liquid CO₂ is assumed to be a cylindrical vessel with a high/diameter ratio set equal to 2.9. In particular, the two dimensions of the vessel are evaluated from its volume considering that liquid CO₂ at 72 bars has a density of 859.14 kg/m³ and that the tank is emptied every 48 hours.

In conclusion, all the heat exchangers are sized as already introduced in *paragraph 4.1.1* and, in particular, the same process is applied for the estimation of the global heat transfer coefficient for the two coolers inside the intercooling compression group. Therefore, from the software, Aspen Exchanger Design and Rating the data in *Table 4.5* for the first and second cooler are obtained. From these values and the annual fluxes derived from the simulation with Aspen (*Figure 4.9*) assumed to be constant during the annual operation of the system, the total heat transfer area of the two coolers is computed from the *equation [4-1]*.

Table 4.5 Data for the two coolers

	COOLER 1	COOLER 2
Global heat transfer coeff. [kW/m²/K]	0.113	0.62
Log mean temperature difference [K]	74.61	29.46

Concerning the electric heater, used only in the full-electric configuration, its contribution to the total footprint of the system is not considered on a first approximation. On the contrary, its power consumption is set equal to the sum of the power required from the reboiler and the heater of the rich solvent during the annual operation.

4.3 Energy and environmental indicators

From the study of the energy and material annual flow of the systems, different indicators are determined for the assessment of the energy and environmental performance of the two solutions considered.

The main indicators evaluated for both the power-to-gas and liquid CO₂ production plant are:

- Specific Primary Energy Consumption for CO₂ Avoided (SPECCA) in MWh/tCO₂
- Water consumption (cooling and process water) in t/y
- Mass of CO₂ avoided in t/y
- Occupation land in m²

The SPECCA represents the energy consumption for the carbon dioxide capture; it is computed using:

$$SPECCA = \frac{E_{elCO_2} + Q_{thCO_2}}{m_{CO_2}} \quad [4-15]$$

where E_{elCO_2} and Q_{thCO_2} are the electrical and thermal energy spent by the entire two systems to capture a certain amount of carbon dioxide (m_{CO_2} in tonnes) used for the production of the SNG in the power-to-gas plant and the liquid CO₂ for the liquid CO₂ production plant. From *equation [4-15]* the electrical and thermal forms of energy are assumed at the same energy level, while in reality, the electrical form is more “valuable” than the thermal one. Despite this consideration, the SPECCA represents anyway an important indicator for the evaluation of the performances of the plant.

Moreover, the other two values of water consumption and the CO₂ saved emission are derived from the results of the material flow inside the sections of the two plants.

Furthermore, only for the power-to-gas plant are evaluated other two important parameters. The first is the plant global efficiency expressed by the ratio between the chemical energy of the SNG produced and energy consumption:

$$\eta_{global} = \frac{n_{SNG} \cdot LHV(HHV)_{SNG}}{E_{el_{sys}} + Q_{th_{sys}}} \quad [4-16]$$

where n_{SNG} is the SNG flow rate in kg/s while $E_{el_{\text{sys}}}$ and $Q_{th_{\text{sys}}}$ are the electrical and thermal energy consumption of the entire power-to-gas system in MW (also in this case are valid the comments already made in the *equation [4-15]*). The global efficiency can be determined also on a lower heating value (LHV) or high heating value (HHV) bases, both expressed in MJ/kg. The second parameter is the Wobbe Index expressed in MJ/Sm³ defined as:

$$I_w = \frac{HHV}{\sqrt{\rho}} \quad [4-17]$$

where ρ is the specific density of the SNG compared to the air density. This parameter, together with others already shown in *Table 4.3*, is important to understand if the SNG produced by the power-to-gas system can be injected into the existing infrastructure for the transportation of the natural gas.

In conclusion, land occupation is evaluated by adding together all the values of the systems' sections.

5 Methods for the economic analysis

In this paragraph the methods applied for the economic analysis of the two solutions will be presented, introducing the hypothesis made for the detailed estimation of the CAPEX and cash flow of each section of the plant; with these results, some important economic indexes for the evaluation of the plant performances will be evaluated. In particular, these economic analyses are focused on the assessment of the Levelized cost of the outcomes, which represents the average revenue per unit of product required to have a balance between incomes and outcomes at the end of the lifetime of the system. In this respect, the time-horizon of the entire economic analysis is set equal to 30 years.

5.1 CAPEX estimation

The method applied for the estimation of the capital expenditure (CAPEX) is expressed in *Figure 5.1*, defined in the guidelines from the National Energy Technology Laboratory (NETL) [33]. In particular, the process applied is a bottom-up approach, where the cost of the main components is calculated from the annual simulation of the system in order to compute, subsequently, the size of each one; then, using cost functions, the final cost of each component is determined.

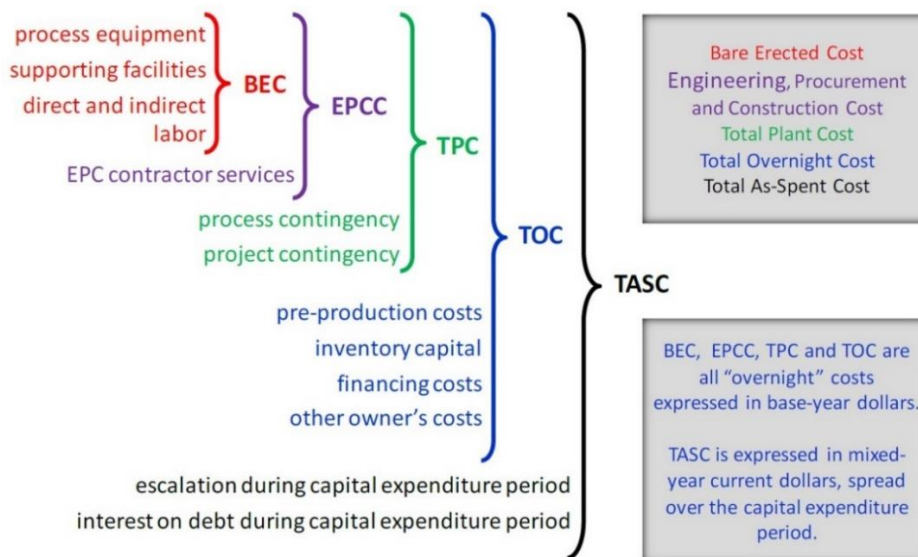


Figure 5.1 Capital cost levels and their elements [33]

To calculate the total amount of capital expenditure, the study will be focused on the estimation of the total overnight capital (TOC) neglecting the last part related to the total as-spent capital (TASC). Moreover, it is relevant to remember that all these costs are “overnight” costs (so without considering any kind of interest during the construction of the plant) and are defined in “base-year” euros (in particular the “base-year” considered in this analysis is 2019).

5.1.1 Estimation of process equipment cost

The first step of the economic analysis is the calculation of the process equipment cost, defined also as the bare module cost (C_{bm}). The technique applied for the major components of the system is that one described in Turton et al. [34] based on the use of cost functions; *equation [5-1]* represents the general cost functions considered, obtained by doing regressions on real data about the cost of components and defined in a certain range in terms of capacity, pressure, etc.

$$C_{bm} = C_P^0 \cdot F_{bm} \quad [5-1]$$

where C_P^0 is the purchased cost of the equipment in a base condition and F_{bm} is the bare erected module cost factor accounting for specific materials constructions and operating conditions.

Equation [5-2] represents the cost function defined in [34] in order to calculate C_P^0 at ambient pressure and making the hypothesis that the material used for the construction of the component is carbon steel:

$$\log_{10} C_P^0 = K_1 + K_2 \cdot \log_{10} A + K_3 \cdot [\log_{10} A]^2 \quad [5-2]$$

where K_1 , K_2 and K_3 are constant parameters defined to fit the equation to the real cost of the equipment, while A represents the capacity or size parameter chosen as reference for the device considered. In particular, the fitting parameters K_1 , K_2 and K_3 are defined as a function of A and they are valid only inside a specific range $[A_{min}; A_{max}]$ provided by Turton et al, for each component. On the contrary, if A falls outside of this range then C_P^0 can be calculated as:

$$C_P^0 = \begin{cases} C_P^0(A_{min}) \cdot \left(\frac{A}{A_{min}}\right)^n & \text{if } A < A_{min} \\ C_P^0(A_{max}) \cdot \left(\frac{A}{A_{max}}\right)^n & \text{if } A > A_{max} \end{cases} \quad [5-3]$$

where n is a cost exponent that can be obtained from [35] or, if there are no data available, it can be set equal to 0.6.

As previously said, in order to account for the real operation conditions of the components, the value of F_{bm} needs to be evaluated; in particular, for components like heat exchangers, pumps and process vessels the cost function in order to calculate the bare module factor is:

$$F_{bm} = B_1 + B_2 \cdot F_m \cdot F_p \quad [5-4]$$

where B_1 and B_2 are constants while F_m and F_p are the material factor and the pressure factor respectively. In particular, the value of F_p accounts for the operating pressure of the equipment and it is calculated in two different ways: for horizontal and vertical process vessels of diameter D in meters, an operating pressure of P_g in barg and a wall thickness of at least 0,0063 m the value of F_p is given by:

$$F_{p,vessel} = \frac{\frac{(P_g + 1) \cdot D}{2 \cdot [850 - 0,6 \cdot (P_g + 1)]} + 0,00315}{0,0063} \quad [5-5]$$

while for all the remaining process equipment it is given by the following general formula:

$$\log_{10} F_p = C_1 + C_2 \cdot \log_{10} P_g + C_3 \cdot [\log_{10} P_g]^2 \quad [5-6]$$

where C_1, C_2 and C_3 are constants defined in [34] for a specific range of P_g . Moreover, the value of F_m , accounting for the different choice of construction material of the components, and the constant values B_1 and B_2 are always given by [34] for components like heat exchangers, pumps and process vessels; for all the other components, it gives directly the value of the bare module cost F_{bm} .

It is important to point out that all the values given in the tables in Turton et al. are referred to 2001, so in the end, the purchased cost calculated with this method provides a value normalized to that year. In order to convert this cost into one accurate for the present time considering also changing in economic conditions, the following formula will be applied:

$$\frac{C_2}{C_1} = \frac{I_2}{I_1} \quad [5-7]$$

where the subscript 2 is referred to the time when the cost is desired while 1 to the time when the cost is known, C is the purchased cost of the equipment and I is the cost index which considers the effect of inflation and escalation. In *Table 5.1* the “Chemical engineering plant cost index” (CEPCI) used in this analysis is shown in order to get the cost to 2019.

Table 5.1 CEPCI indexes referred to 2001 and 2019

CEPCI (2001)	CEPCI (2019)
394	603

Finally, it is also important to remember that the prices of the components defined by Turton et al. are in \$ so in order to convert it into € an exchange euro-dollar of 1.145 is considered (1€=1.145\$).

In the following paragraphs, the assumption made for the estimation of the bare module cost of each component of the two systems studied will be presented.

5.1.2 Definition of different scenarios for the estimation of the CAPEX

Most of the techno-economic analysis is intended for the purpose of a feasibility study, considering a range of accuracy by which the final value of the CAPEX falls into. In this analysis, 3 different scenarios are treated:

1. Optimistic scenario
2. Realistic scenario (based on real projects and literature research)
3. Pessimistic scenario

In general, the optimistic and pessimistic scenarios are set, respectively, equal to -10% and +15% compared to the value evaluated for the realistic case. In the following paragraphs, the different percentages and hypotheses considered for the 3 scenarios are listed in specific tables.

5.1.3 Estimation of bare erected cost (BEC)

Following the method explained in the previous section, the overall bare module cost of the main component of the system ($C_{bm,main}$) will be evaluated by adding each value of C_{bm} . In order to evaluate also the cost of the minor components, a certain percentage of the total bare module cost ($C_{bm,tot}$) is considered; for each of the 3 scenarios, the contributions of minor components and main components on $C_{bm,tot}$ are expressed in *Table 5.2*.

Table 5.2 Hypothesis for the estimation of the cost of the minor component expressed in percentage of $C_{bm,tot}$

	OPTIMISTIC SCENARIO	REALISTIC SCENARIO	PESSIMISTIC SCENARIO
$C_{bm,main}$	71.2%	68%	63.1%
Piping, valves, fittings	18.0%	20.0%	23.0%
Process instruments & controls	6.3%	7.0%	8.1%
Electrical components	4.5%	5.0%	5.8%
$C_{bm,tot}$	100%	100%	100%

Once the value of $C_{bm,tot}$ is evaluated, the Bare erected cost is defined adding also the cost for the installation of the components and the construction, materials and labor costs. As for the minor components, also for these costs, their values are expressed in percentage of the BEC (*Table 5.3*).

Table 5.3 Hypothesis for evaluation of BEC

	OPTIMISTIC SCENARIO	REALISTIC SCENARIO	PESSIMISTIC SCENARIO
$C_{bm,tot}$	71.2%	68%	63.1%
Installation	21.6%	24.0%	27.6%
Construction, materials and labour costs	7.2%	8.0%	9.2%
BEC	100%	100%	100%

5.1.4 Estimation of the Total Overnight Capital (TOC)

The last part related to the CAPEX analysis is focused on the definition of the total overnight cost that, in this study, represents precisely the value of the initial invested capital. As shown in *Figure 5.1*, after the evaluation of the BEC, the values of the EPCC, TPC and finally the TOC need to be calculated. In *Table 5.4* there are the percentages considered in order to evaluate the final TOC in each of the three scenarios. Process and project contingencies are included in the analysis accounting for unknown costs that are omitted due to a lack of complete project definition and engineering. Process contingencies are strictly related to the maturity and the development status of the technology considered, so in the following paragraphs, the hypothesis made for each section of the solutions analysed will be presented. Furthermore, project contingencies for the realistic scenario are taken from a European project (CEMCAP [36]). All the other values in *Table 5.4* are defined from [33].

Table 5.4 Hypothesis for the evaluation of the TOC

		OPTIMISTIC SCENARIO	REALISTIC SCENARIO	PESSIMISTIC SCENARIO
EPCC	EPC contractor services (%BEC)	15.0%	17.5%	20.0%
TPC	PC-Process contingencies (%BEC)	TBD	TBD	TBD
	Project contingencies (%(EPCC+PC))	15.0%	15.0%	30.0%
TOC	Pre-production costs (%TPC)	1.8%	2.0%	2.3%
	Inventory capital (%TPC)	0.45%	0.50%	0.58%
	Financing costs (%TPC)	2.4%	2.7%	3.1%
	Other owner's costs (%TPC)	13.5%	15.0%	17.3%

5.2 OPEX and cash flow analysis

The annual budget of the system related to the k-th period after the year of investment (defined as year 0) is evaluated from:

$$B_k = \sum R_i - \left| \sum S_j \right| \quad [5-8]$$

where R_i and S_j are the revenues and the expenditures, respectively, of each section of the plant. In particular, in this study, the revenues are not considered because the aim is not to obtain the payback time but the Levelized cost of the products, as previously defined. On the contrary, the items of expenditures are different according to each section of the plant. In this perspective, the only item that is common to each part is the electricity price referred to electricity produced by the waste-to-energy plant and consumed by the different sections; the two annual profiles used for the electricity price are the PUN and the PZN (both in €/MWh and referred to 2019) where:

- “Prezzo Unico Nazionale” (PUN) is the price of the electricity drawn from the grid (surcharged 105% for system’s burden) when the waste-to-energy plant cannot be able to sustain the electric demand coming from the power-to-gas system (this happens in a few periods of time for the electrolysis section only). In this study, the excise duties are not applied to the electricity’s price.
- “Prezzo Zona Nord” (PZN), instead, is the price at which the electricity produced by the waste-to-energy plant is fed into the Italian grid (the price is referred to as the northern area of the country).

In addition to the PZN, it is considered also the contribution of the so-called “ex Certificati Verdi” (CV) provided until 2028 (not included). The final sell price of the electricity is defined by:

$$p_{el,sell} = PZN + 0,51 \cdot CV \quad [5-9]$$

where CV is the bonus related to the “ex-C.V.”, set equal to 92,11 €/MWh for 2019 and assumed to be constant until 2028 (it is equal to 0 from 2028 included).

As defined in the previous paragraphs the waste-to-energy plant can work in both full-electric or in CHP mode. When the second option is considered, the price of the heat fed into the district heating follows the principle expressed by *equation [5-9]*:

$$p_{heat} = \frac{PZN + 0,51 \cdot CV}{\lambda} \quad [5-10]$$

It is important to remember that the electricity and the heat produced by the waste-to-energy plant are used by the different sections of the two systems analysed and are not fed into the grid; in this way, the electricity and heat price calculated with [5-9] and [5-10] belong to the expenditures inside the *equation* [5-8] (they are defined as a missed revenue).

Moreover, another important expenditure belonging to the cash flow analysis is the cost for the ordinary maintenance of the system that is defined from:

$$OC_k = 3\% \cdot TPC \quad [5-11]$$

This equation is valid for all the sections except for the electrolysis, for which the hypothesis considered in order to evaluate the cost of maintenance will be presented in the next paragraphs.

After performing the maintenance costs, the “Earnings Before Interest, Taxes, Depreciation and Amortization” (EBITDA) is evaluated:

$$EBITDA_k = B_k - |OC_k| \quad [5-12]$$

The EBITDA is an important index of profitability of society and, in particular, is based only on the operational management, thus without considering any kind of interests or depreciation rate but only the business of the company under study.

The next step is the evaluation of the net free cash flow (FCF) that is defined as:

$$FCF_k = EBITDA_k - |IRES_k| \quad [5-13]$$

where IRES is the “Imposta sul reddito di società” which in that study is set equal to zero because it is defined only when the “Earnings before interest and taxes” (EBIT) is positive and in this analysis is always negative; in this way, FCF coincides with the EBITDA.

In conclusion, by adding each year the value of the FCF, the cumulative free cash flow (CFCF) is evaluated:

$$CFCF = -|CAPEX| + \sum_{k=1}^{n_{life}} FCF_k \quad [5-14]$$

where n_{life} is the lifetime of the plant set equal to 30 years.

In addition to the values just presented, also the Discounted cash flow (DCF) and the Net present value (NPV) could be evaluated:

$$DCF = \frac{FCF}{(1 + WACC)^k} \quad [5-15]$$

$$NPV = -|CAPEX| + \sum_{k=1}^{n_{life}} DCF_k \quad [5-16]$$

where WACC is the Weighted Average Cost of Capital. Since in the two plants there are only expenditures, the evaluation of these two terms become pointless.

In *Table 5.5* there is a summary of the main hypothesis made for the definition of the cash flow analysis (they are constant for the three different scenarios considered); other specific hypotheses will be introduced in the following paragraphs where all the sections of the two systems are investigated separately.

Table 5.5 Summary of the hypothesis made for the cash flow analysis

	VALUE
Weighted average cost of capital (WACC)	6.6%
Surcharge on the electricity drawn from the grid	105%
Certificati Verdi (CV) [€/MWh]	92.11
Fixed annual water withdrawal fee [€/year] [37]	499.61
Water consumption fee [€/m³] [37]	3.36
Operation maintenance	3% of TPC
Plant lifetime [years]	30

5.3 Economic analysis applied to the power-to-gas

The generic scheme followed for the development of the economic analysis is described in *paragraphs 5.1* and *5.2*. In this section, a focus on the power-to-gas system will be presented, analysing one by one each section, showing more details and hypotheses for the complete economic analysis. The same procedure will be applied for the case of the liquid CO₂ production plant.

5.3.1 CO₂ capture section

Coefficients for the evaluation of the C_{bm}

Table 5.7 shows the parameters used in order to calculate the bare module cost for the major components of the CO₂ capture section (from *Equation [5-1]*).

In addition to the costs for the main component of the capture section, there is also the cost related to the initial solvent (blending of MEA and the ionic liquid [Bpy][BF₄]); it is defined making the hypothesis that the entire solvent is constituted for 30% of [Bpy][BF₄], 40% of MEA and the remaining 30% of water (all expressed in % of solvent's weight). In *Table 5.6* the hypotheses for the price of the MEA and the ionic liquid derived from [38] are shown, while the price for water is presented in *Table 5.5*.

Table 5.6 Hypothesis for the price of MEA and the ionic liquid (constant for all three scenarios)

	VALUE
Price of MEA [€/kg]	1.09
Price of ionic liquid ([BPY][BF ₄]) [€/kg]	5.74

Process contingencies

As previously said, the process contingencies are related to the maturity of the technology analysed. There are different CO₂ capture plants around the world on an industrial scale, but the process is not adopted on a commercial level. The values chosen for the process contingencies, with respect to *Table 5.4*, are 5%, 17.6% and 20% of the BEC for the optimistic, realistic and pessimistic scenario respectively [1].

Table 5.7 Parameters used for the estimation of the bare module cost of the components composing the CO₂ capture section

Components	Component description	A	A _{min}	A _{max}	K ₁	K ₂	K ₃	P _g (barg)	C ₁	C ₂	C ₃	F _p	Material	F _m	B ₁	B ₂	F _{bm}	n[35]
Absorber	Packed tower	Volume [m ³]	0.3	520	3.4974	0.4485	0.1074	0	0	0	0	1	SS clad	1.7	2.25	1.82	-	0.85
Packing absorber	Packing (loose)	Volume [m ³]	0.03	628	2.4493	0.9744	0.0055	0	0	0	0	1	-	-	-	-	7.1	0.6
Stripper	Process Vessel	Volume [m ³]	0.3	520	3.4974	0.4485	0.1074	2.5	0	0	0	1	SS	3.1	2.25	1.82	-	0.35
Packing stripper	Packing (loose)	Volume [m ³]	0.03	628	2.4493	0.9744	0.0055	2.5	0	0	0	1	-	-	-	-	7.1	0.6
Reboiler	Kettle	Area [m ²]	10	100	4.4646	-0.5277	0.3955	< 40	0	0	0	1	SS shell / SS tube	2.7	1.63	1.66	-	0.5
Heat exchanger*	Fixed Tube	Area [m ²]	10	1000	4.3247	-0.303	0.1634	< 40	0	0	0	1	SS shell / SS tube	2.7	1.63	1.66	-	0.65
	Double pipe	Area [m ²]	1	10	3.3444	0.2745	-0.0472	< 40	0	0	0	1	**	**	1.74	1.55	-	0.65
Pump	Centrifugal	Shaft power [kW]	1	300	3.3892	0.0536	0.1538	<10	0	0	0	1	SS	2.3	1.89	1.35	-	0.52
Compressor	Rotary	Shaft power [kW]	18	950	5.0355	-1.8002	0.8253	-	0	0	0	1	CS	-	-	-	2.7	0.79
Solvent tank	Tank-API fixed roof	Volume [m ³]	90	30000	4.8509	-0.3973	0.1445	<0.07	0	0	0	1	SS	3.1	1.49	1.52	-	0.68
CO ₂ vessel	Process vessel	Volume [m ³]	0.1	628	3.5565	0.3776	0.0905	71	-	-	-	13.399	CS	1	1.49	1.52	-	0.65

*For the heat exchanger considered in this study the heat transfer area is evaluated and it is used as the parameter A. If A is lower than 10 m² the component installed is a shell and tube double pipe heat exchanger, while if the area is higher than 10 m² then it is used as a fixed tube heat exchanger. In the study, the only fixed tube installed is the rich-lean solvent heat exchanger.

**For the intercooler of the absorber, the condenser of the stripper, and the cooler of the lean solvent the materials chosen are Carbon Steel (CS) for the shell and Stainless Steel (SS) for the tubes, in order to avoid corrosion phenomena due to the hot fluid; for these types of heat exchangers F_m=1.8. Moreover, for the heater of the rich solvent Stainless Steel (SS) is used for both the shell and the tube so in this case F_m=2.7. Finally, for the 4 coolers of the CO₂ coming from the stripper F_m=1 because the heat exchanger is entirely in Carbon Steel.

Annual budget

As introduced in *paragraph 5.2* the only items considered for the definition of the annual budget of the system are the expenditures; in the carbon capture section the different items composing the annual budget are (all values in €):

1. Loss of revenue due to the self-consumption of electricity produced by the waste-to-energy plant and used in the CO₂ capture section
2. Contribution of the “ex Certificati Verdi” (until 2028 not included)
3. Cooling water withdrawal
4. Withdrawal of water for the refill of solvent
5. Refill of MEA

The first two items are evaluated considering the *equation [5-9]* already presented and multiplying it for the total energy consumed by the capture section.

For the water consumption, the price is evaluated considering both the fix and variable annual fee (both expressed in €/year):

$$C_{H_2O} = C_{H_2O,fix} + C_{H_2O,var} \quad [5-17]$$

where $C_{H_2O,fix}$ is defined in Table 5.5 while the variable part ($C_{H_2O,var}$) is evaluated using:

$$C_{H_2O,var} = c_{H_2O,cons} \cdot V_{H_2O} \quad [5-18]$$

where $c_{H_2O,cons}$ is the specific cost for the water annual consumption (*Table 5.5*) and V_{H_2O} is the annual water consumption of the section in m³.

Moreover, for what concerns the use of water for the refill of solvent it is considered only the variable water fee, that is multiplied for the annual consumption of solvent derived from the simulations.

Lastly, the cost for the refill of MEA is derived by multiplying the specific cost in *Table 5.6* for the MEA refill weight from the simulations.

It is important to point out that, like other ionic liquids, [Bpy] [BF₄] is also characterized by low volatility (i.e., the vapor pressure is extremely low). Therefore, it can be assumed that the loss of ionic liquid and the consequent refill are negligible for the purposes of the techno-economic analysis.

5.3.2 Electrolysis section

Evaluation of the CAPEX

The components included in the economic analysis are the electrolysis system, the water tank and the pump for the refill of water. The hypothesis and the method used to evaluate the CAPEX of this section will be presented, considering that the value computed for the electrolysis system represents the total bare module cost ($C_{bm,tot}$) while for the other components of the section the $C_{bm,main}$ will be shown.

1. *Electrolysis system*

Firstly, the electrolysis' system is constituted by the stack and all the balance of the plant (i.e. power converter, water purification systems, recirculation pump, etc). The specific investment cost for an alkaline electrolyzer is derived from the literature. In [39] a specific price for a single-stack of 2 MW is set equal to 750 €/kW; in the case of multi-stack, this value tends to decrease with the increase of the power input following the behavior in *Figure 5.2*.

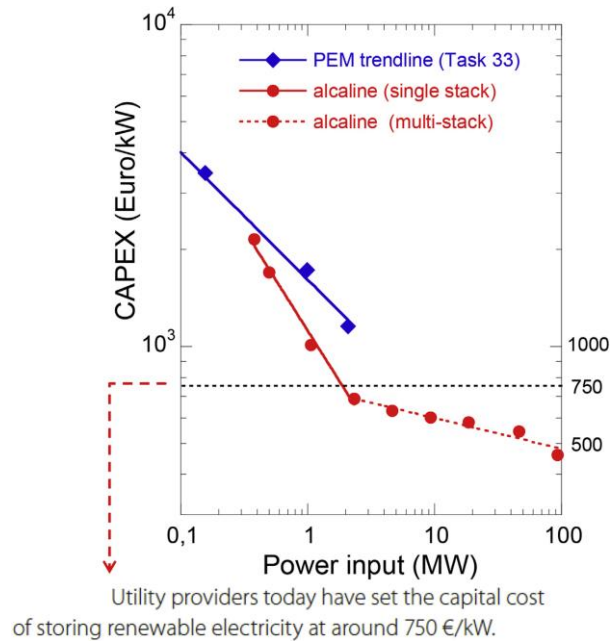


Figure 5.2 CAPEX data for PEM and alkaline electrolyzers; for the alkaline solution, data are based on a single stack of 2.13MW [39]

For multi-stack systems, as for the case considered in this study, the specific investment cost can be evaluated by fitting the results presented in [39] using the following equation:

$$C_{bm,tot,alc} = 1437.1 \cdot P_{nom,alc}^{-0.095} \quad [5-19]$$

where $C_{bm,tot,alc}$ is the specific cost of the alkaline electrolyzer system in €/kW while $P_{nom,alc}$ is the nominal power of the electrolysis system in kW.

A significant aspect to emphasize is the part of the electrolysis' system cost related to the stack price. Typically, this cost contributes to 20-35% of the total cost of the electrolyzer system; from the literature, the following formula is used [40]:

$$C_{stack,alc} = \frac{2 \cdot C_{bm,tot,alc} \cdot 0.4}{3} \quad [5-20]$$

where $C_{stack,alc}$ is the specific cost of the alkaline stack in €/kW. Therefore, this value represents the substitution cost for the stack that needs to be considered because, during the operation, the stack can be damaged, or its efficiency can drop below a certain threshold. In particular, from a similar study [26], the hypotheses for the estimation of the substitution time have been obtained using the following equation:

$$Lifetime_{stack,alc} = \frac{h_{tot}}{h_{op,year}} \quad [5-21]$$

where h_{tot} are the hours of continuous operations of the stack until it can be substituted while $h_{op,year}$ is the hours of real operation of the stack evaluated from the simulations. From [26] h_{tot} is set equal to 77000 hours, considering that above this value the efficiency of the stack goes below 90%.

2. Water pump and tank

The $C_{bm,main}$ for the water pump is evaluated considering the previously analysed method discussed by Turton et al (*paragraph 5.1.1*). The type of component chosen is a “reciprocating pump” and the coefficients used for the estimation of the bare module cost are shown in *Table 5.8*. In particular, the value of the shaft power is derived from the water flow rate considering the specific water consumption by the electrolyzer of 15 L per kg of H₂ produced (see *4.1.2*). It is useful to point out that the pump for the water recirculation, which is used to control the thermal balance inside the stack, is not assessed because already considered inside [5-19].

The cost function selected for the water storage tank, that is sized to ensure an autonomy of 12 hours, is defined by [41]:

$$C_{bm,tank} = 5941.7 \cdot V_{H_2O}^{-0.389} \quad [5-22]$$

where $C_{bm,tank}$ is the specific cost of the water tank in €/m³ while V_{H_2O} is the volume of the tank in m³ and derived from the specific consumption of water already defined (15 L/kg of H₂) and considering the autonomy of 12 hours.

Table 5.8 Coefficients for the estimation of the C_{bm} of the water pump (operating pressure of 15 bar)

A	A_{min}	A_{max}	K_1	K_2	K_3	C_1	C_2	C_3	$Mater$	F_m	B_1	B_2
Shaft power [kW]	0.1	200	3.8696	0.3161	0.122	-0.245382	0.259016	-0.01363	CS	1.5	1.89	1.35

Process contingencies

Here the process contingencies are set equal to 5%, 10% and 15% of the BEC for the optimistic, realistic and pessimistic scenarios respectively [42].

Operation and maintenance costs

The O&M cost (in €) for the electrolysis system (stack+BoP) is constituted by a fix and a variable term:

$$O\&M_{tot} = O\&M_{var} + O\&M_{fix} \quad [5-23]$$

where:

$$O\&M_{fix} = \frac{1}{3} \cdot \left(\frac{3}{10} \cdot C_{bm,tot,alc} \cdot P_{nom,alc} \right) \quad [5-24]$$

$$O\&M_{var} = \frac{2}{3} \cdot \left(\frac{3}{100} \cdot C_{bm,tot,alc} \cdot P_{nom,alc} \right) \cdot \frac{h_{op,year}}{8760} \quad [5-25]$$

For the other two components, the O&M cost is expressed in percentage of the Total Plant Cost (TPC); their values are shown in Table 5.9.

The values calculated with these procedures represent the term OC_k inside the equation [5-11].

Table 5.9 Assumption for the evaluation of the O&M cost of pump and water tank.

	VALUE
Water tank	2% of TPC
Water pump	3% of TPC

Annual budget

The annual budget is composed of the following items of expenditure (all values in €):

1. Loss of revenue due to the self-consumption of electricity produced by the waste-to-energy plant and used by the electrolysis system
2. Contribution of the “ex Certificati Verdi” (until 2028 not included)
3. Electricity withdrawal from the grid due to short shutdown
4. Water withdrawal for the normal operation of the electrolyzer

The first two items are evaluated as already mentioned in the carbon capture section (see *page 55*).

The cost for the withdrawal of electricity from the grid is considered because, as already analysed in *Figure 3.3*, there are short periods of the year in which the net power produced by the waste-to-energy plant decreases consistently due to, for example, forced shutdown of the plant or to its maintenance. When the power produced is below the power required by the electrolysis system it is useful to purchase the electricity from the grid. On these occasions, the price of the electricity is evaluated considering the PUN, increased by 105% due to system charges, as already mentioned in *paragraph 5.2*.

Finally, the cost for the water withdrawal is always evaluated as for the capture section using *equation [5-17]*. The value of the water consumption of the electrolysis system is assumed to be equal to 15 L per kg of H₂ produced (see *page 57*).

5.3.3 Methanation section

Coefficients for the evaluation of the C_{bm}

The components considered in the economic analysis are the heat exchangers, the 3 reactors, the pump, and the three electric heaters. For what concerns the reactors they are assumed to be modeled as a heat exchanger for the estimation of their bare module cost. Therefore, the coefficients used for the evaluation of the bare module cost of the heat exchangers have been already defined in *Table 5.7*; from the simulations, the parameter A is calculated and, depending on that value, a double pipe or a fixed tube type of model is chosen.

For the electric heaters and the pump, the coefficients considered are shown in *Table 5.10*. As a first approximation, the electric heaters are considered hot water heater, although their aim is to pre-heat a mixture of H₂ and CO₂.

The two flash separators are not considered in this economic analysis.

Moreover, in this section, there is also the cost of the chilled water; the cost function used for the estimation of the bare module cost of the chilled water is derived from [43]:

$$C_{bm, chilled\ water} = \dot{Q} \cdot (a \cdot CEPCI + b \cdot C_{el}) \quad [5-26]$$

where \dot{Q} is the chilled water energy consumption in kJ/y derived from the simulations, CEPCI is defined for 2019 from *Table 5.1*, while a and b are constant set equal to $1 \cdot 10^{-9}$ €/kJ_{th} and $6.73 \cdot 10^{-7}$ GJ_{el}/kJ_{th}.

Process contingencies

The process contingencies are set equal to 5%, 17.6% and 20% for the optimistic, realistic and pessimistic scenarios respectively (as for the carbon capture section).

Annual budget

The annual budget is composed by the following items of expenditure (all values in €):

1. Loss of revenue due to the self-consumption of electricity produced by the waste-to-energy plant and used by the methanation section
2. Contribution of the “ex Certificati Verdi” (until 2028 not included)
3. Annual substitution of the catalyst

The first two are evaluated as in the previous sections (see *page 55*).

The Ni/γ-Al₂O₃ catalyst is supposed to be replaced every year at a specific price of 2000 €/t [44].

Table 5.10 Parameters used for the estimation of the bare module cost of the components composing the methanation section

<i>Components</i>	<i>Component description</i>	<i>A</i>	<i>A_{min}</i>	<i>A_{max}</i>	<i>K₁</i>	<i>K₂</i>	<i>K₃</i>	<i>P_g</i> (barg)	<i>C₁</i>	<i>C₂</i>	<i>C₃</i>	<i>F_p</i>	<i>Material</i>	<i>F_m</i>	<i>B₁</i>	<i>B₂</i>	<i>F_{bm}</i>	<i>n</i>
<i>Heat exchanger*</i>	Fixed Tube	Area [m ²]	10	1000	4.3247	-0.303	0.1634	>5	0.039	-0.113	0.082	**	SS shell / SS tube	2.7	1.63	1.66	-	-
	Double pipe	Area [m ²]	1	10	3.3444	0.2745	-0.0472	< 40	0	0	0	1	CS shell / SS tube	1.8	1.74	1.55	-	-
<i>Electric heater</i>	Hot water heater	Heat duty [kW]	650	10750	2.083	0.907	-0.024	14	-0.016	0.057	-0.009	1.09	-	-	-	-	2.2	0.6
<i>Pump</i>	Centrifugal	Shaft power [kW]	1	300	3.3892	0.0536	0.1538	47	-0.3935	0.3957	-0.00226	1.83	SS	2.2	1.89	1.35	-	-

*For the heat exchanger considered in this study the heat transfer area is evaluated and it is used as the parameter A. If A is lower than 10 m² the component installed is a shell and tube double pipe heat exchanger, while if the area is higher than 10 m² then it is used as a fixed tube heat exchanger. In the study, the only double pipe heat exchanger installed is HEX-5.

**The value of pressure is different depending on the type of component; for the three reactors and the economizer (HEX-6) P_g=47 barg while for all the other component P_g=14 barg. The correspondent values of F_p (evaluated with equation [5-6]) are equal to 1.2 and 1.04 respectively.

5.4 Economic analysis applied to the liquid CO₂ production plant

For this specific system, two different cases are considered as defined in *paragraph 4.2.2*. In this perspective, all the economic analysis separating the two situations will be presented.

5.4.1 Waste-to-energy in CHP configuration

Coefficients for the evaluation of the C_{bm}

The coefficients used for the evaluation of the $C_{b,main}$ are the same as the carbon capture section of the power-to-gas system so they are shown in *Table 5.7*.

In the case of steam integration, it is necessary to implement a junction constituted by delivery and return pipes from the turbine and towards the reboiler and vice versa. Once the diameter D and the length L of this junction are defined (see *paragraph 4.2.2*) the bare erected cost of the two pipe sections can be evaluated from:

$$BEC_{pipe} = (a_0 + a_1 \cdot D + a_2 \cdot D^2) \cdot y \cdot L \quad [5-27]$$

where a_0 , a_1 and a_2 are coefficients fitted from construction data and set equal to 11.7 €/m, 113.7 €/m² and 1575 €/m³ respectively, $y=2.7$ is a coefficient that takes into account construction (laying) and other costs.

Process contingencies

The percentages considered in the three scenarios are equal to those defined in the carbon capture section (see *paragraph 5.3.1*).

Annual budget

The annual budget is constituted by the following terms:

1. Loss of revenue due to the self-consumption of electricity produced by the waste-to-energy plant and used in the liquid CO₂ production plant
2. Loss of revenue due to decreasing of electric productivity by the waste-to-energy plant in order to produce heat and send it to the reboiler

3. Contribution of the “ex Certificati Verdi” (until 2028 not included)
4. Loss of revenue due to the self-consumption of heat produced by the waste-to-energy plant and used in the liquid CO₂ production plant (sent to the reboiler)
5. Cooling water withdrawal
6. Withdrawal of water for the refill of solvent
7. Refill of MEA

Items 1,3,5,6 and 7 have already been presented in the carbon capture section of the power-to-gas system (see 5.3.1).

In addition to these terms, there is the contribution due to the steam integration. It is constituted by two parts:

- The first is related to the decreasing of the electric productivity (item number 2) of the waste-to-energy plant because in this case, the plant is in a CHP configuration. In order to account for this term, the reduction of electric productivity in kW is firstly evaluated (following the annual profile):

$$P_{el,red} = \frac{P_{ext,integr}}{\lambda} \quad [5-28]$$

where $P_{ext,integr}$ is the external power to be provided to the reboiler for the solvent regeneration and to the heater of the rich solvent, while λ is the cogenerative ratio. To compute the loss of revenue related to that value in €, the PZN is used (see *paragraph 5.2*).

- The second is constituted by the loss of revenue due to the consumption of heat otherwise destined to the district heating (term number 4). This value is computed following the procedure previously analysed (*equation [5-10]*).

5.4.2 Waste-to-energy in full-electric configuration

Coefficients for the evaluation of the C_{bm}

Also in this case the components considered are almost the same compared to the carbon capture section of the power-to-gas system. The only difference is that the reboiler is replaced by an electric heater; the coefficients used for this last component are already shown in *Table 5.10*. The steam integration with the two pipe junctions is, obviously, not considered.

Process contingencies

The percentages considered in the three scenarios are equal to those defined in the carbon capture section (see *5.3.1*).

Annual budget

The annual budget is the same already presented in the carbon capture section of the power-to-gas system (see *page 55*). In the term related to the electric energy consumed, it is considered also the electricity for the electric heater.

5.5 Economic indicators

For each section of the two systems considered different economic indicators are evaluated, derived from the analysis explained in the previous paragraphs; they are:

1. Capital expenditure (CAPEX)
2. Earnings Before Interest, Taxes, Depreciation and Amortization (EBITDA)
3. Cumulative free cash flow (CFCF)
4. Levelized cost of the products

The Levelized cost of the different outcomes produced in the different sections is evaluated from:

$$LC_{product} = \frac{CFCF}{m_{product} \cdot n_{life}} \quad [5-29]$$

where $LC_{product}$ is the Levelized cost of the CO₂, the H₂, the SNG and the liquid CO₂ usually in €/kg; $m_{product}$ is the mass of the corresponding product usually expressed in kg/year and n_{life} is the lifetime of the two systems set equal to 30 years.

It is useful to point out that the two most important values are the Levelized cost of the SNG for the power-to-gas system and the Levelized cost of the liquid CO₂ produced by the liquid CO₂ production plant; as a matter of fact, these two quantities represent the most important feasibility indicators for the two systems analysed.

In particular, for the evaluation of LC_{SNG} , the CFCF in the *equation [5-29]* holds the terms of the annual budget already defined in *paragraph 5.3.3*, to which the price for the annual consumption in the methanation section of CO₂ and H₂ must be added (produced by their respective sections). These two values are implemented by multiplying the value of the levelized cost of CO₂ and H₂ (in €/kg) by the annual production of CO₂ and H₂ (in kg/year).

6 Results and discussion

In this chapter the results of the energy and economic analysis will be shown, considering both the two systems separately. The aim is to provide different parameters to understand the feasibility of the solutions examined.

6.1 Power-to-gas system: energy and environmental analysis

In this paragraph the results of the energy and environmental analysis for the power-to-gas are shown, considering each section of the plant. Firstly, the annual material flows and then the energy consumptions of each component will be presented. These values are used in the following economic analysis for the evaluation of the operating expense during each year of the plant's operation. In conclusion, the results of the preliminary sizing of the system are introduced.

6.1.1 CO₂ capture section

Material and energy flow

In *Table 6.1* the main results of the material's flows of the carbon capture section are listed. The relevant result is the annual amount of CO₂ extracted from the exhaust of the waste-to-energy plant; this value represents the mass of CO₂ avoided and it is useful to the evaluation of the energy parameters expressed in the previous paragraphs. Moreover, the final molar composition of the flux that goes to the methanation section consists of 99.2%_{mol} of CO₂ and the remaining 0.8%_{mol} of H₂O.

Table 6.1 Material flows of the CO₂ capture section

	Unit	Value
Exhaust expelled from the waste-to-energy	kNm ³ /y	997206
Exhaust treated by the CO₂ capture section	%	6.57
Total water consumption	t/y	2754.5
MEA consumption (refill)	t/y	13.59
CO₂ to the methanation section	t/y	7740

Table 6.2 Electric and thermal annual energy consumption of the CO₂ capture section's components

COMPONENT	Thermal energy consumption [MWh _{th} /y]
Absorber Intercooler	-1148.8
Stripper's condenser	-1031.3
Rich solvent heater	124
Reboiler	7519.3
Solvent exchanger	5504.5
Lean solvent cooler	-3206.7
Cooler#1 CO ₂ compression	-80.3
Cooler#2 CO ₂ compression	-190.9
Cooler#3 CO ₂ compression	-227.8
Electric energy consumption [MWh_{el}/y]	
Pump and compressors	331.6

In Table 6.2 the results of the annual simulations for the evaluation of the thermal and electric energy consumptions of each component of the section are shown. From a first look, electric energy represents a small fraction of the entire annual energy consumption.

For the thermal consumptions, it is fundamental to point out that the energy required for the solvent regeneration at the reboiler and the heating of the rich solvent is entirely covered by the steam produced in the reactors of the methanation section (see *paragraph 4.1.4*). Moreover, for the solvent exchanger, the value in the table represents the thermal energy exchanged between the rich and lean solvent and for this reason it is not part of the total energy consumption of the section.

Furthermore, for the electricity consumption, the energy for the compression of the CO₂ up to 72 bars for its storage in liquid form inside the CO₂ buffer is not considered; as a matter of fact, this value is difficult to predict because depends on the operation of the buffer that is strictly related to possible shut-downs of the system.

Sizing of the section

The results of the preliminary sizing of the section will be presented following the method already explained on *page 27*. Table 6.3 shows the results of the footprint of each component composing the section. On the contrary, the values of the parameters used inside the cost functions for the evaluation of the bare module cost of each component will be presented in the paragraph related to the economic analysis together with the relative costs (the same will be for the other sections of the power-to-gas plant).

Table 6.3 Footprint of the components composing the carbon capture section

COMPONENT	Dimension	Value
Absorber	Height [m]	15
	Diameter [m]	1.5
Stripper	Height [m]	4
	Diameter [m]	0.5
Absorber cooler for water recirculation	Area [m ²]	6.49
Rich solvent heater	Area [m ²]	0.38
Stripper's condenser	Area [m ²]	0.16
Reboiler	Area [m ²]	1.14
Solvent exchanger	Area [m ²]	6.18
Lean solvent cooler	Area [m ²]	2.52
Intercooled compression train	Area [m ²]	5.89
Solvent tank	Area [m ²]	10.88
CO ₂ buffer	Area [m ²]	39.18

Table 6.4 presents the total dimensions of the container inside which the components are supposed to be placed. The total surface is evaluated considering that the different units inside the section are arranged as shown in *Figure 6.1*. In particular, the width is evaluated as the CO₂ buffer diameter while the length is the sum of the lengths of the absorber cooler, the lean solvent cooler, the stripper condenser, the width of the intercooling compression stage and the diameter of the CO₂ buffer. Both the two dimensions are increased by 20% to evaluate the final value of the surface occupied by the container. In conclusion, the height of the container is supposed to be equal to the height of the absorber, increased by 20%.

Table 6.4 Dimensions of the container for the CO₂ capture section

	Value [m ²]
Total footprint of the components (increased by 10%)	82.18
Total footprint of the container (increased by 20%)	213
Height of the container (increased by 20%)	18

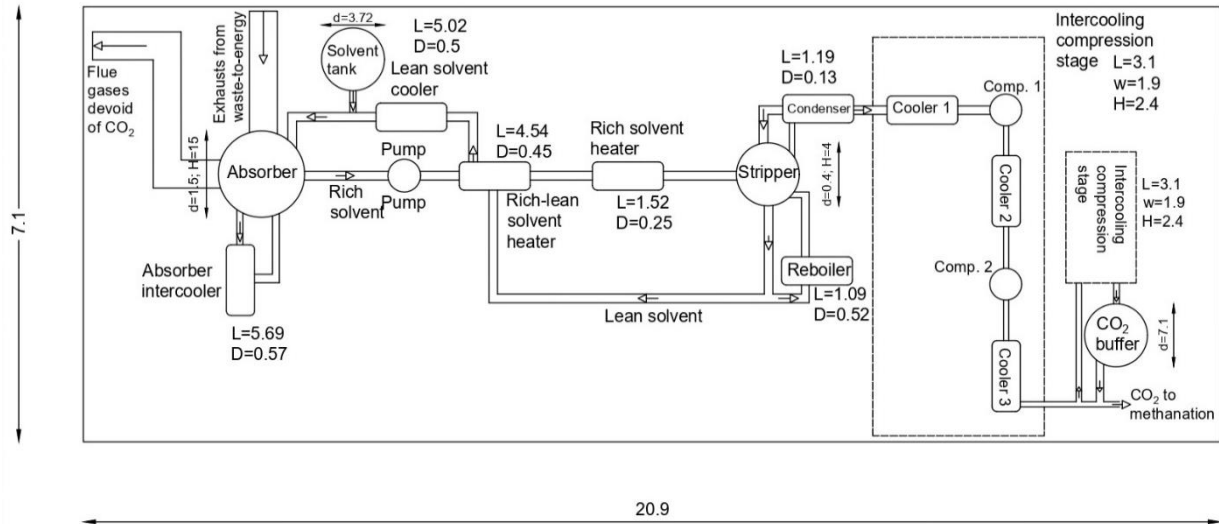


Figure 6.1 Arrangement of the components inside the carbon capture section (dimensions in meters)

6.1.2 Electrolysis section

Material and energy flow

From the simulations of the study applied to the case of 500 Nm³/h of SNG, the installation of an alkaline electrolyzer of nominal power of 10 MW is necessary. The power required from the waste-to-energy plant is about 10.6 MW.

Table 6.5 shows the material and energy flows. As already defined in paragraph 4.1.2 the electric energy consumption is constituted by the self-consumption of electric energy produced by the waste-to-energy plant and the purchased electricity from the grid when the electric demand is not met by the waste-to-energy plant. The former represents the major quantity, about 82.28 GWh_{el}/y while the latter is only 410 MWh_{el}/y.

Table 6.5 Material and energy annual flows of the electrolysis section

	Unit	Value
H₂ produced	t/y	1394.5
Water consumption	t/y	20917
Electric energy consumption	GWh _{el} /y	82.69

Sizing of the section

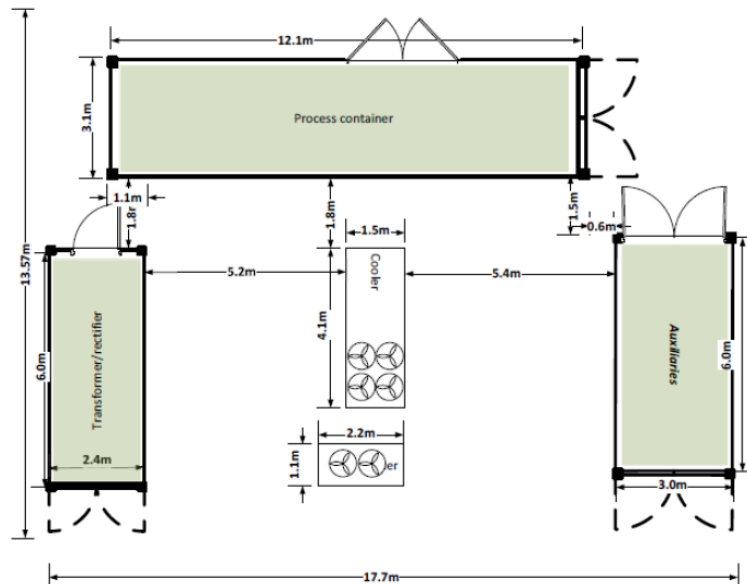
Usually, the entire electrolysis system, composed of the alkaline electrolyzers and all the BoP, is provided in large containers of specific dimensions according to the input power required and, thus, the produced hydrogen. For example, some manufacturers provide the dimensions of the single container of 500 kW_{el} each [45]; on the contrary, other manufacturing companies provide different solutions and configurations for the direct construction of a plant composed of multi-units of power input higher than 2 MW_{el} each [46].

In this study, an interval for the area occupied by the electrolysis system (included all the BoP) is evaluated taking into account the different configurations depending on how the single block composing the electrolysis section can be assembled.

Taking into account that the nominal power of the alkaline electrolyzer is 10 MW, the left-hand boundary of the interval is evaluated considering the installation of about 20 containers of 500 kW_{el} each. From the manufacturer schedule, each module is composed of a 40 ft container (12.19 m x 2.44 m) so in the end, the total area occupied could be **600 m²**.

On the contrary, the right-hand side of the interval's boundary is defined considering 5 multi-unit modules of 2 MW_{el} each. The dimensions of each module are 13.57 m x 17.7 m (*Figure 6.2*) resulting in a total footprint area of approximately **1200 m²**.

In conclusion, the higher value of 1200 m² largely reflects the real footprint of the section, because it resembles the dimensions of existing plants of a nominal power closest to 10 MW.



Layout of a McLyzer 400-30 – not contractual / for reference only – actualization of layout will be provided with basic design informations.

Figure 6.2 Dimensions of a 2 MW_{el} unit by McPhy [46]

6.1.3 Methanation section

Material and energy flow

Table 6.6 shows the main material flows of the section. The water consumption is represented by the cooling water needed to condensate the water inside the SNG. Moreover, the SNG is produced at 14 °C and 13.9 bars; the composition of this gas expressed in Table 6.6 reveals that the percentage of H₂ is too high with reference to the limits imposed by the owner of the natural gas grid (Table 4.3). In order to fulfil the requirements for the injection into the network, it is necessary to clean the SNG using different technologies. In this study, the purification of the SNG is not investigated.

Table 6.6 Material flows of the methanation section

	Unit	Value
Water consumption	t/y	74500
Catalyst mass Ni	kg/y	327.6
SNG produced	t/y	2812
SNG molar composition	% _{mol} CH ₄	97.5
	% _{mol} H ₂	2
	% _{mol} CO ₂	0.5
	ppm H ₂ O	16

Concerning the energy flows, Table 6.7 shows the thermal balance of the entire section and the annual electric energy consumption. In terms of thermal energy, the values in the table represent the energy exchanged inside each component of the methanation section (except for the chilled water energy consumption) and they don't constitute an annual energy expense; as already introduced in paragraph 4.1.3, the entire section could be considered thermally self-sufficient thanks to the heat generated inside each reactor. In particular, Table 6.7 represents also the thermal energy produced and recovered inside the three reactors as saturated steam at 270 °C; it is used partially to heat the water used as a coolant from 50 °C to 270 °C, and the remaining part is sent to the carbon capture section to regenerate the solvent.

On the other hand, the annual electric consumption represented in Table 6.7 is mainly due to the three electric heaters installed to pre-heat the mixture of CO₂ and H₂ entering the reactors and bring it to 270 °C.

Table 6.7 Thermal energy exchanged inside the exchangers and reactors and electric consumption of the methanation section

COMPONENT		Thermal energy exchanged [MWh _{th} /y]
Heat exchangers	HEX-1	1236.2
	HEX-2	1135.4
	HEX-3	212.7
	HEX-4	614.6
	HEX-5	49.6
	HEX-6	5271.1
Reactors	R-1	2855
	R-2	3739
	R-3	1532
Chilled water energy consumption		261.4
Electric energy consumption [MWh _{el} /y]		
Electric heaters		1059
Pump		22.7

Sizing of the section

For the methanation section, the footprint of each component is evaluated following the method already explained on *page 34*. The results are shown in *Table 6.8*.

Table 6.8 Footprint of the components composing the methanation section

COMPONENT		Footprint [m ²]
Heat exchangers	HEX-1	3.2
	HEX-2	2.8
	HEX-3	0.93
	HEX-4	2.8
	HEX-5	0.74
	HEX-6	2.5
Reactors	R-1	0.76
	R-2	0.89
	R-3	1.0
Electric heaters	H-1	17.68
	H-2	17.68
	H-3	7.68

From the results obtained, firstly the total footprint of the components is evaluated, providing an increase of this value of 10%; afterwards, as already explained in the carbon capture section, the components are supposed to be placed inside a container following the same arrangement of *Figure 4.5*. In particular, the length of the container is 18.3 m while its width is 10.9 m.

Table 6.9 shows the total area occupied by the container evaluated increasing the width and the length of the container by 20%.

Table 6.9 Dimensions of the container for the methanation section

	Value [m²]
Total footprint of the components (increased by 10%)	64.7
Total footprint of the container (increased by 20%)	286.1

6.2 Liquid CO₂ production plant: energy and environmental analysis

The method followed to explain the results of this system is the same as that applied to the power-to-gas system. Firstly, the main results of the Aspen model on the compression stage will be presented. Secondly, the annual material and energy flows will be shown, taking into account the two configurations considered for the waste-to-energy plant (see *paragraph 4.2.2*). In conclusion, a preliminary sizing of the section will be proposed.

6.2.1 Results of the simulation for the intercooling compression stage

Table 6.10 shows the main results of the simulations for the intercooling compression stage that brings the CO₂ from 3.5 bars up to 72 bars. The thermal and electric power required for the compressors and the coolers respectively are presented; these values contribute to the total annual electric and thermal energy consumption of the system, considering that they remain constant during the year.

Table 6.10 Results from the Aspen simulation of the intercooling compression

	Unit	Value
Power required (compressor 1)	kW _{el}	39.1
Power required (compressor 2)	kW _{el}	36.7
Power required (cooler 1)	kW _{th}	-42.2
Power required (cooler 2)	kW _{th}	-109.1
T_{OUT} (compressor 1)	°C	194.6
T_{OUT} (compressor 2)	°C	197.7

6.2.2 Material and energy flow

The results for the material and energy flows mostly resemble those shown in the carbon capture section of the power-to-gas system (see *paragraph 6.1.1*).

Table 6.11 shows the main material flows of the section. In particular, the liquid CO₂ produced is the same quantity of the total CO₂ avoided from the power-to-gas plant.

Table 6.11 Material flows of the liquid CO₂ production plant

	Unit	Value
Total water consumption	t/y	2820
MEA consumption (refill)	t/y	13.59
Liquid CO₂ produced	t/y	7740

Table 6.12 represents the energy consumption during one year of operation of the section. As already defined in paragraph 4.2.2 two different configurations are considered for the waste-to-energy plant. In particular, the results for the thermal energy consumption of the components are quite the same as for the carbon capture section of the power-to-gas (see Table 6.2) except for the coolers of the compression stage. Moreover, for the CHP configuration, the total heat provided by the waste-to-energy plant is 7643.3 MWh_{th}/y to the reboiler and the rich solvent heater.

The annual electricity consumption is defined in the same table; for the CHP configuration the total amount of electricity is used for the pump and compressors and this value is higher with respect to that one of the power-to-gas plant due to the high compression work. On the other hand, for the full-electric mode it is also added the electric energy required for the solvent regeneration and the heating of the rich solvent by the electric heater.

Table 6.12 Electric and thermal annual energy consumptions for the two configurations of the waste-to-energy plant

COMPONENT	Thermal energy consumption [MWh _{th} /y]	
	CHP configuration	Full-electric configuration
Absorber Intercooler	-1148.8	-1148.8
Stripper's condenser	-1031.3	-1031.3
Rich solvent heater	124	124
Reboiler	7519.3	-
Solvent exchanger	5504.5	5504.5
Lean solvent cooler	-3206.7	-3206.7
Cooler stripper's condenser	-80.3	-80.3
Cooler#1 CO₂ compression	-331.8	-331.8
Cooler#2 CO₂ compression	-857.3	-857.3
	Electric energy consumption [MWh _{el} /y]	
	CHP configuration	Full-electric configuration
Pump and compressors	638.2	638.2
Electric heater	-	8045.6

6.2.3 Sizing of the system

The sizing of the system follows the same procedure defined for the carbon capture section of the power-to-gas system. The results are already expressed in *Table 6.3* except for the CO₂ tank that in this system is a cylindrical vessel with a total area occupied of 6.56 m².

The same procedure is also applied for the estimation of the container's dimensions following the arrangement described in *Figure 6.3*. As a first approximation, the sizing of the system is made considering only the CHP configuration.

Table 6.13 Dimensions of the container for the liquid CO₂ production plant.

	Value [m ²]
Total footprint of the components (increased by 10%)	46.3
Total footprint of the container (increased by 20%)	153.15
Height of the container (increased by 20%)	18

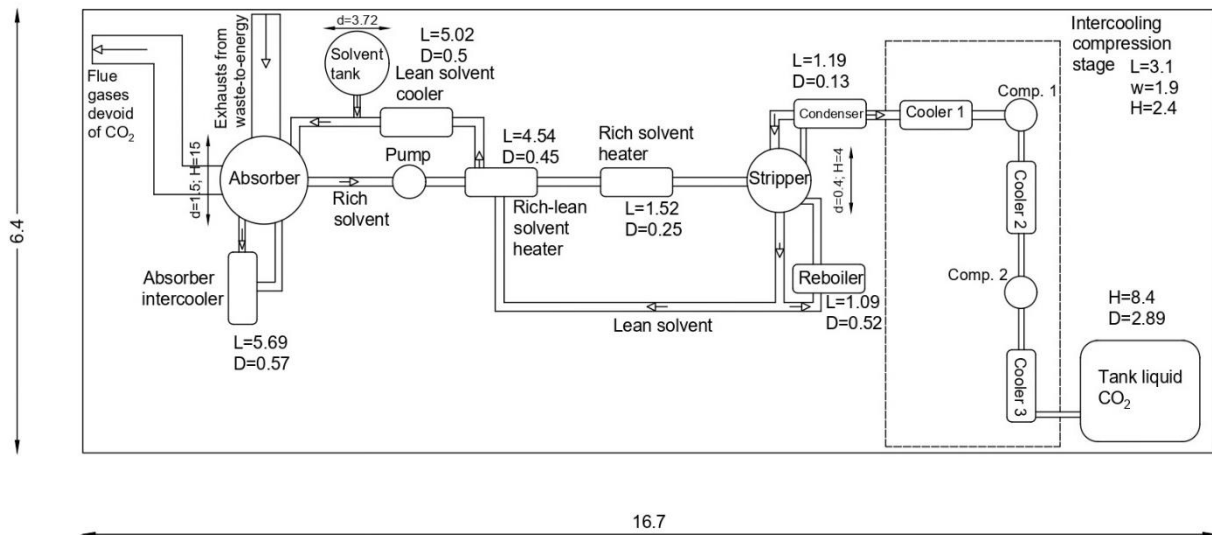


Figure 6.3 Arrangement of the components inside the liquid CO₂ production plant (dimensions in meters)

6.3 Energy and environmental indicators: results and comments

From the results of the energy and environmental analysis, the principal indicators are evaluated. They are shown in *Table 6.14* for both the power-to-gas and the liquid CO₂ production plant.

For the power-to-gas system, the global efficiency is evaluated using the *equation [4-16]* on a high heating value (HHV) and lower heating value (LHV) bases. In the equation, LHV and HHV are evaluated as a weighted average on the mass fraction of H₂ and CH₄ present inside the SNG produced and considering that for the pure H₂ the HHV is 141.8 MJ/kg and LHV is 120 MJ/kg while for the pure CH₄ is 55.5 MJ/kg (HHV) and 50 MJ/kg (LHV); the final values for the SNG are 55.02 MJ/kg (HHV_{SNG}) and 49.55 MJ/kg (LHV_{SNG}). Moreover, $E_{el_{sys}}$ is equal to 10.57 MW while $Q_{th_{sys}}$ is equal to zero, because each section of the power-to-gas plant is thermally self-sufficient.

The Wobbe index is evaluated from *equation [4-17]* where ρ is the specific density of the SNG equal to 0.55 and HHV is 36.5 MJ/Sm³ considering that the SNG density is 0.663 kg/Sm³.

Table 6.14 Energy and environmental indicators for both the two solutions considered

	Power-to-gas	Liquid CO ₂ production plant
SPECCA [MWh/tco₂]	0.0428	1.07 (CHP) 1.12 (full-electric)
m_{co₂} avoided [t/y]	7740	7740
Water consumption [t/y]	98170	2820
η_{global}	0.465 (LHV) 0.511 (HHV)	-
WOBBE INDEX [MJ/Sm³]	49.3	-
Footprint [m²]	213 (CO ₂ capture) 600÷1200 (electrolysis) 286 (methanation)	153

From the results in *Table 6.14*, it is possible to obtain some relevant considerations on the operation of the two systems.

Firstly, the SPECCA is considerably lower (for the same quantity of CO₂ captured) for the power-to-gas plant because, here, the carbon capture section is self-sufficient due to the thermal recovery from the methanation section. On the contrary, for the liquid CO₂ production

plant at the numerator of *equation [4-15]*, there is also the thermal consumption of almost 7643 MWh_{th}/y for the solvent regeneration and this explains very well how the thermal recovery influences the final value of the SPECCA. Moreover, the SPECCA does not change a lot for the two configurations of the waste-to-energy plant (CHP or full-electric); this is due to the fact that the values of electric and thermal consumption are quite the same in the two configurations and, thus, the numerator of *equation [4-15]* is almost the same. The problem already explained in *paragraph 4.3* is that the thermal and electric energy is assumed to be at the same energy level in *equation [4-15]* and in this way the comparison between the two values of SPECCA in the liquid CO₂ production plant could be pointless.

Furthermore, water consumption is higher for the power-to-gas system due to the largest number of components with respect to the liquid CO₂ production plant. The CO₂ captured and avoided is the same for the two systems and it is greater than 7.7 million kilos per year.

For the power-to-gas system, the global plant efficiency states that the plant is not so performant. Different studies in the literature analyse the power-to-gas pathway with different configurations of the various sections. For instance, [29] consider a SOEC stack instead of alkaline technology and this leads to an increase of the global plant efficiency up to 80% (on HHV bases). Nevertheless, the downside is the cost of this solution that could be very consistent with respect to the alkaline one.

Concerning the Wobbe index, it is inside the limit interval expressed in *Table 4.3* as for all the other values except for the H₂ volume fraction that needs to be decreased (see *page 71*) if the SNG is intended to be injected into the existing grid.

In conclusion, the land occupied by the two systems is variable especially for the power-to-gas plant, where the electrolysis system represents the biggest section of the plant.

6.4 Power-to-gas system: economic analysis

In this paragraph, the results of the economic analysis of the power-to-gas will be shown. Firstly, each section will be analysed separately, presenting the CAPEX, OPEX, the cash flows and the levelized cost of each product. Finally, a paragraph will be dedicated to a general overview of the results of the entire plant focusing the attention on the levelized cost of SNG and making a comparison with the price of other commodities.

6.4.1 CO₂ capture section

Estimation of the TOC

Table 6.15 shows the bare module cost for the main components of the section based on the evaluation of parameter A as already defined in paragraph 5.1.1.

Table 6.15 Results of the bare module cost of the main components of the CO₂ capture section derived from the parameter A

	Parameter A	C _{bm,main} [k€]
Absorber	26.5 m ³	161.2
Packing absorber	1.3 m ³	3.51
Stripper	0.8 m ³	29.84
Packing stripper	0.039 m ³	0.12
Absorber intercooler	4.2 m ²	18.99
Rich solvent heater	7.5 m ²	28
Stripper's condenser	1.7 m ²	15.4
Reboiler	46.96 m ²	398.1
Solvent exchanger	20.0 m ²	131.6
Lean solvent cooler	7.1 m ²	21.21
Cooler#1 CO₂ compression	4.2 m ²	13.78
Cooler#2 CO₂ compression	5.0 m ²	14.34
Recirculation pump	1.7 kW	17.09
Compressor #1	29.0 kW	53.17
Compressor #2	28.7 kW	52.76
Solvent tank	27.0 m ³	154.7
CO₂ buffer	13.8 m ³	92.74
Compressor #3	21.6 kW	45.7
Compressor #4	21.6 kW	45.7
Cooler#3 CO₂ compression	5.0 m ²	14.34
Cooler#4 CO₂ compression	5.0 m ²	14.34
Initial solvent	-	56.8

For the estimation of the bare module cost of the CO₂ buffer, an approximation has been considered. The cost function expressed in Turton et Al. is not appropriate for a tank of liquid CO₂; as a matter of fact, if the bare module cost is evaluated from the volume of the tank using the common cost function expressed by *equation [5-1]*, the final cost will be too high. For this reason, it was considered a correction of the cost function taking into account the cost of an existing tank of H₂ in carbon steel from a manufacturer. The cost of the vessel containing 96 kg of hydrogen at 28 bars (volume of 41 m³) is 102 k€; if the condition of this vessel was applied to the cost function from Turton et Al., *equation [5-1]* would give a value of 408 k€. In conclusion, it is possible to evaluate the correction factor (equal to 0.25) that allows bringing back the cost evaluated with the cost function expressed by Turton et Al. to a much realistic cost of the vessel.

Following the procedure already introduced in *paragraph 5.1*, it is possible to estimate the Total Overnight Cost (that is the CAPEX) of the carbon capture section. In *Table 6.16* the TOC and the other main costs for the three different scenarios are shown.

Table 6.16 TOC and other main costs of the CO₂ capture section in k€ for the three different scenarios

	Optimistic	Realistic	Pessimistic
C_{bm,main} [k€]	1383	1383	1383
C_{bm,tot} [k€]	1943	2034	2189
BEC [k€]	2729	2992	3463
EPCC [k€]	3138	3515	4156
TPC [k€]	3766	4648	6303
TOC [k€]	4450	5587	7767

Estimation of the annual budget (EBITDA)

Table 6.17 shows the items of the annual budget of the section that are the same for the three scenarios considered. The values are estimated starting from the results of the energy and material flows already introduced in the energy analysis in *paragraph 6.1.1*.

In order to determine the EBITDA, also the contribution of the Operation & Maintenance cost that changes depending on the scenario should be considered; it is 113 k€, 139k€ and 189 k€ for the optimistic, realistic and pessimistic scenario respectively.

In *Table 6.18* the final values of the EBITDA for the three different scenarios are represented considering two periods, until and after 2028, because the contribution of the “ex Certificati Verdi” is set equal to zero after 2028.

Table 6.17 Expenditures composing the annual budget of the carbon capture section

	Expenditure [k€]
Self-consumption of electricity	-16.9
“ex certificati verdi” (until 2028)	-15.6
Cooling water	-2.2
Water for solvent's refill	-7.6
MEA refill	-14.8

Table 6.18 EBITDA of the CO₂ capture section for the three scenarios

	Optimistic	Realistic	Pessimistic
EBITDA (until 2028) [k€]	-170	-196	-246
EBITDA (after 2028) [k€]	-154	-181	-231

Cash flow and levelized cost of the CO₂ produced

Adding, year by year, the EBITDA to the CAPEX, it is possible to estimate the cumulative free cash flow during the entire life of the plant fixed in 30 years. The trend of CFCF is shown in *Figure 6.4*. Moreover, since the section has only expenditures in the annual budget, it is useless to evaluate the Net Present Value (NPV) and, thus, the Pay Back Time.

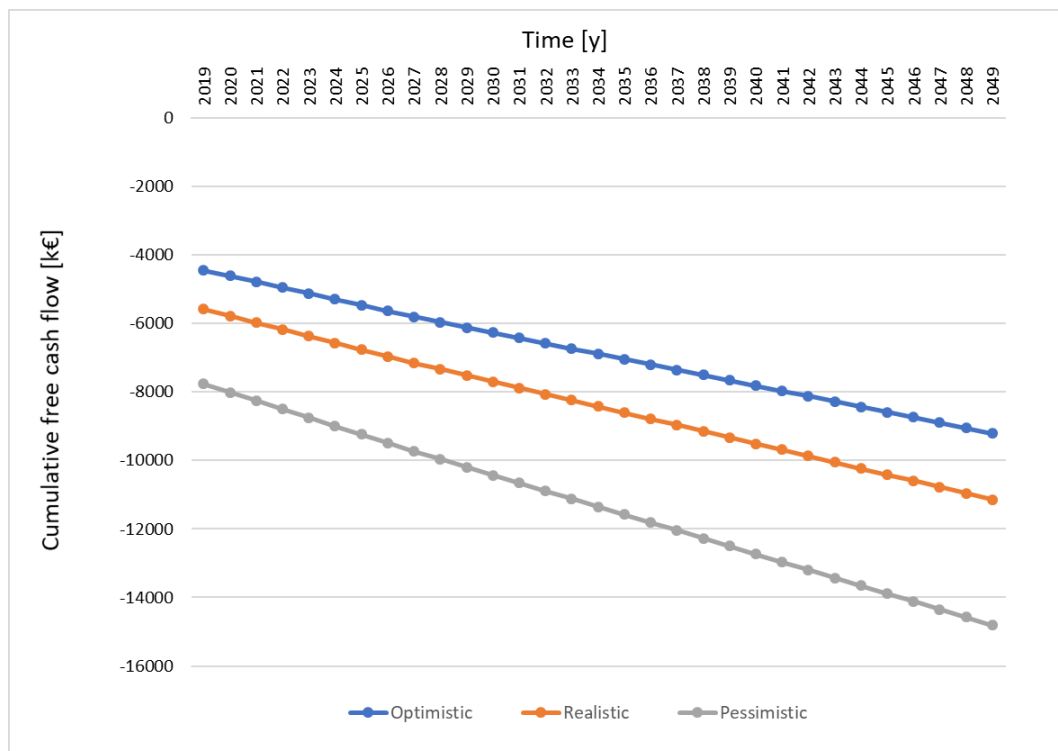


Figure 6.4 Cumulative free cash flow of the CO₂ capture section for the three scenarios

Once the CFCF is evaluated, it is possible to know the levelized cost of the CO₂ avoided. The values obtained for the three scenarios are presented in *Table 6.19*. In particular, the levelized cost in the realistic scenario reflects the value for similar systems; for instance, for carbon capture systems coupled with fossil fuel power plants, the resulting cost of 47.96 €/tCO₂ is inside the interval of values estimated by [47] of 37 €/tCO₂ for coal power plants and 90 €/tCO₂ for natural gas plants.

Table 6.19 Levelized cost of CO₂ for the three scenarios

	Optimistic	Realistic	Pessimistic
Levelized cost of CO₂ [€/tCO₂]	39.65	47.96	63.77

6.4.2 Electrolysis section

Estimation of the TOC

Table 6.20 introduces the bare module costs of the components of the section. They represent the $C_{bm,main}$ except for the electrolysis system that is a $C_{bm,tot}$, namely, all the minor component costs (i.e. Piping, valves, process instruments & controls, etc) have already been considered inside that value.

$C_{bm,tot,alc}$ is evaluated starting from the nominal power of the stack (10 MW_{el}), while $C_{bm,pump}$ and $C_{bm,tank}$ are computed from their volume and shaft power that are 32.1 m³ and 1.5 kW respectively (see *paragraph 5.3.2*).

Table 6.20 Bare module cost of the components of the electrolysis section

	VALUE [k€]
Electrolysis system ($C_{bm,tot,alc}$)	6305
Water pump ($C_{bm,pump}$)	44.8
Water tank ($C_{bm,tank}$)	49.5

Table 6.21 shows the results of the TOC and the other main costs for the three scenarios considered, tested following the procedure already introduced in *paragraph 5.1*.

Table 6.21 TOC and other main costs of the electrolysis section for the three scenarios.

	Optimistic	Realistic	Pessimistic
$C_{bm,main}$ [k€]	6399	6399	6399
$C_{bm,tot}$ [k€]	6438	6444	6454
BEC [k€]	9042	9476	10213
EPCC [k€]	10398	11135	12255
TPC [k€]	12477	13895	17923
TOC [k€]	14746	16701	22087

In addition, the substitution cost of the stack is appraised from *equation [5-20]* considering that the hours of annual operation of this component are 7879. From *equation [5-21]* it is possible to evaluate the lifetime of the stack that is 10 years (rounded up). Therefore, the stack is replaced every 10 years with a cost of 1681 k€ ($C_{stack,alc}$).

Estimation of the annual budget (EBITDA)

As already explained in *paragraph 4.1.2* two different scenarios were considered for the power supply of the electrolysis section. *Table 6.22* shows the items of expenditure composing the annual budget of the section, taking into account both the case of consumption of electricity from the waste-to-energy plant (**CASE A**) and the case of zero-cost energy from RES (**CASE B**). In particular, in **CASE B** the only expenditure on the budget is due to the water withdrawal because the other items are related to the cost of the electricity that in this scenario was considered null. The values in the table are estimated starting from the results of the energy and material flows already introduced in the energy analysis in *paragraph 6.1.2*.

Table 6.22 Expenditures composing the annual budget of the electrolysis section

	Expenditure [k€]	
	CASE A	CASE B
Self-consumption of electricity	-4207	-
“ex certificati verdi” (until 2028)	-3865	-
Electricity withdrawal from the grid	-53.18	-
Water withdrawal	-70.78	-70.78

Moreover, the O&M costs of the section are presented in *Table 6.23* considering that for the two cases of power supply these values remain the same.

Table 6.23 O&M costs of the electrolysis section

	Optimistic	Realistic	Pessimistic
Electrolysis system O&M [k€]	175.5	175.5	175.5
Pump and tank O&M [k€]	6.35	7.4	10.25
Total O&M cost [k€]	181.9	182.9	185.8

From the annual budget and the O&M costs, it is possible to obtain the EBITDA defined in Table 6.24 for the three scenarios and the two cases considered, pointing out that for CASE A the contribution of the “ex Certificati Verdi” exists until 2028 (not included).

Table 6.24 EBITDA of the electrolysis section for the three scenarios and the 2 cases of power supply

		Optimistic	Realistic	Pessimistic
CASE A	EBITDA (until 2028) [k€]	-8378	-8379	-8382
	EBITDA (after 2028) [k€]	-4513	-4514	-4517
CASE B	EBITDA [k€]	-252.7	-253.7	-256.6

Cash flow and levelized cost of the H₂ produced

The behavior of the CFCF for both the two cases of power supply of the electrolysis system is shown in Figure 6.5 and Figure 6.6 (for CASE A and CASE B respectively).

Firstly, from the two figures, it can be noticed that there is a change in the slope of the lines in all the three scenarios; this is due to the contribution of the alkaline stack replacement that needs to be added every 10 years for both the CASE A and CASE B.

Moreover, the values in the two figures are extremely different. Although the CAPEX is the same in both the two cases, the difference lies in the annual operating costs and in particular in the electricity cost. As a matter of fact, in CASE B, where the annual expenditures for the electricity are set equal to zero (assumption of zero cost of electricity), the annual EBITDA is 253.7 k€ for the realistic scenario, a value much lower compared to 8379 k€ for the CASE A (after 2028 is 4514 k€). This huge difference between the two cases demonstrates the importance of the electricity cost that contributes to a value higher than 90% on the total economic balance of the section. From this perspective, the assumption of zero cost of energy from RES (CASE B) is made precisely to emphasize this contribution, even knowing that it is an extreme and maybe not feasible hypothesis.

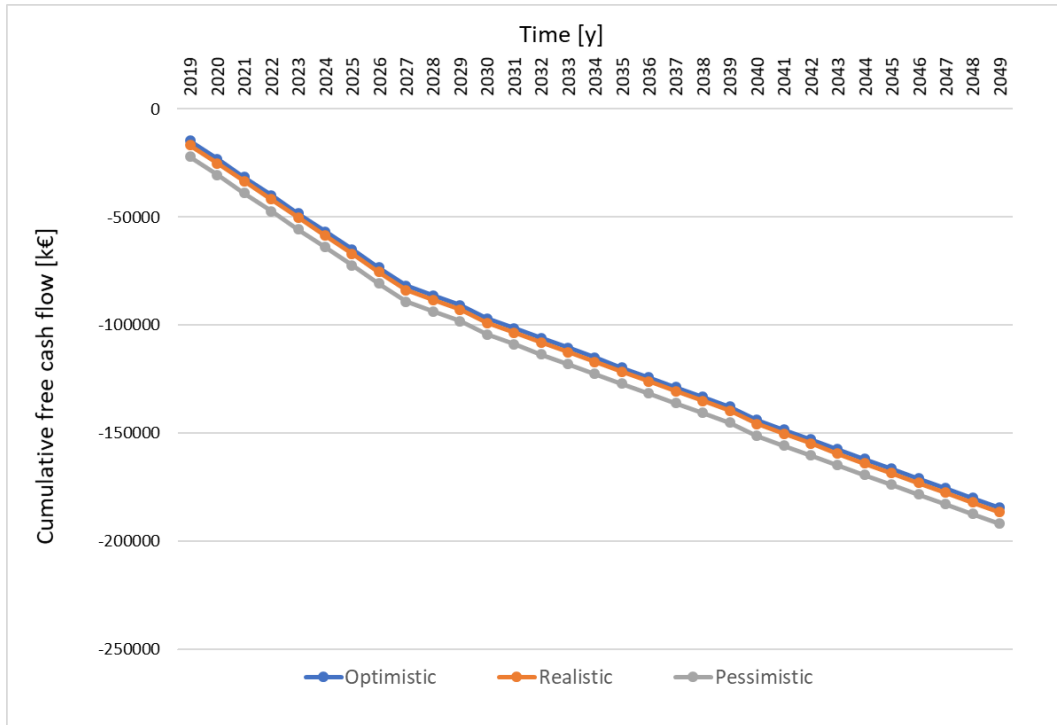


Figure 6.5 CFCF of the electrolysis section for the three scenarios (CASE A)

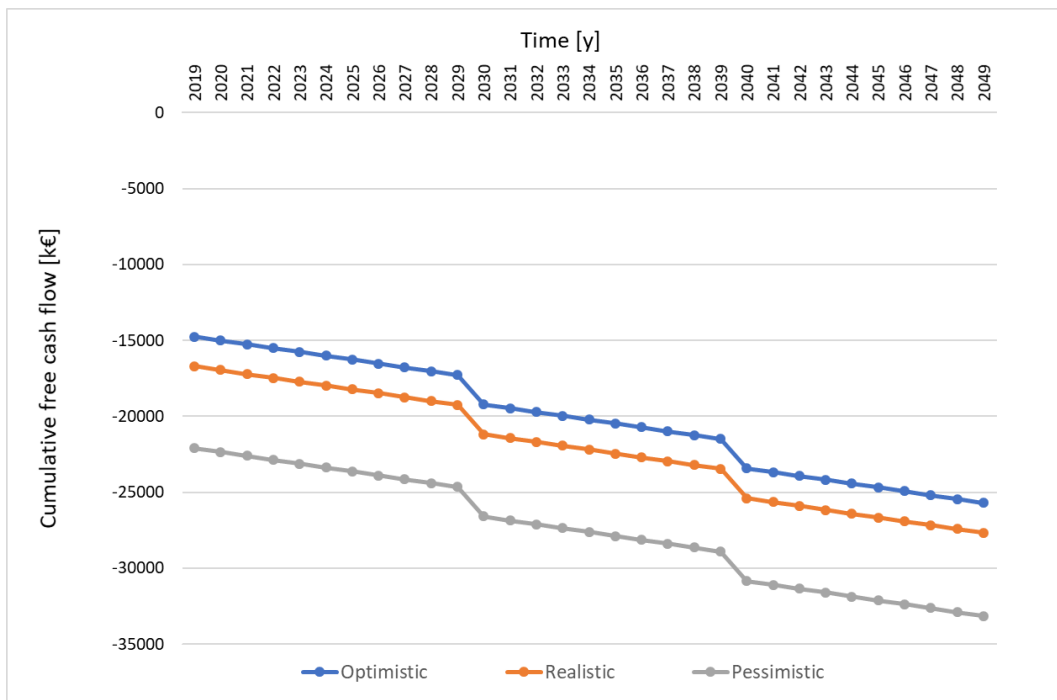


Figure 6.6 CFCF of the electrolysis section for the three scenarios (CASE B)

The importance of the electric energy in the electrolysis section is reflected in the value of the levelized cost of the hydrogen (LCOH) produced. Table 6.25 shows the results obtained for the two cases and the different scenarios considered.

These values reflect the results obtained from various studies in literature, although the final cost is closely linked especially to the electricity cost. [48] for example, calculates the LCOH produced by alkaline water electrolysis for different scenarios, based on the price of electricity and other parameters; for electricity prices of about 0.06 \$/kWh (i.e. about 0.05 €/kWh, a value roughly corresponding to that used in this thesis) the LCOH is around 4 \$/kg_{H₂} (about 3.4 €/kg_{H₂}) while for zero cost of electricity an LCOH of about 0.5 €/kg_{H₂} is obtained. Comparing these values with the results in *Table 6.25* it can therefore be stated that in both cases the results are in line with the data in the literature. It is important to emphasize that, in general, in case A, the goal set by the United States Department of Energy to reach an LCOH of 2.3 \$/kg_{H₂} (i.e. 2 €/kg_{H₂}) by 2020 can only be achieved if the price of electricity is reduced as much as possible.

Table 6.25 Levelized cost of the H₂ produced for the two cases and the three different scenarios

	Optimistic	Realistic	Pessimistic
Levelized cost of H₂ - CASE A [€/kg_{H₂}]	4.41	4.46	4.59
Levelized cost of H₂ - CASE B [€/kg_{H₂}]	0.61	0.66	0.79

6.4.3 Methanation section

Estimation of the TOC

Table 6.26 shows the bare module cost of the main components ($C_{\text{bm,main}}$) of the methanation section evaluated from parameter A (see *paragraph 5.3.3*). The chilled water cost is derived from *equation [5-26]* where the annual chilled water energy consumption has already been introduced in *Table 6.7*.

Table 6.26 Results of the bare module cost of the main components of the methanation section derived from the parameter A

	Parameter A	$C_{\text{bm,main}}$ [k€]
HEX-1	42.5 m ²	309.3
HEX-2	30.6 m ²	289.2
HEX-3	13.6 m ²	130.6
HEX-4	30.6 m ²	289.2
HEX-5	7 m ²	21.13
HEX-6	131.8 m ²	244.5
R-1	12.3 m ²	144.6
R-2	13.4 m ²	145.3
R-3	22 m ²	152.7
H-1	50.6 kW	19.22
H-2	53.9 kW	19.96
H-3	27.2 kW	13.24
Pump	2.9 kW	27.33
Chilled water	-	9.51

Following the same procedure already defined in the previous paragraphs, it is possible to estimate the TOC in the three different scenarios considered. The results are shown in *Table 6.27*.

Table 6.27 TOC and other main costs of the methanation section in k€ for the three different scenarios

	Optimistic	Realistic	Pessimistic
$C_{\text{bm,main}}$ [k€]	1816	1816	1816
$C_{\text{bm,tot}}$ [k€]	2339	2397	2484
BEC [k€]	2550	2670	2873
EPCC [k€]	2933	3137	3448
TPC [k€]	3519	4149	5229
TOC [k€]	4159	4987	6443

Estimation of the annual budget (EBITDA)

Table 6.28 shows the items of the annual budget of the section estimated from the results of the energy and material flows already introduced in the energy analysis in *paragraph 0*. These values are the same for the three scenarios considered.

To determine the EBITDA also the contribution of the Operation & Maintenance cost should be considered; it is 105.6 k€, 124.5 k€ and 156.9 k€ for the optimistic, realistic and pessimistic scenario respectively.

In Table 6.29 the final values of the EBITDA for the three different scenarios are represented considering two periods, until and after 2028 (the contribution of the “ex Certificati Verdi” is null after 2028).

Table 6.28 Expenditures composing the annual budget of the methanation section

	Expenditure [k€]
Self-consumption of electricity	-67.6
“ex certificati verdi” (until 2028)	-61.96
Substitution of the catalyst	-0.66

Table 6.29 EBITDA of the methanation section for the three scenarios

	Optimistic	Realistic	Pessimistic
EBITDA (until 2028) [k€]	-236	-255	-287
EBITDA (after 2028) [k€]	-174	-193	-225

Cash flow and levelized cost of the SNG produced

In Figure 6.7 the cumulative free cash flow of the methanation section is shown for the three scenarios. In particular, this graph is made considering the EBITDA already defined in Table 6.29. On the contrary, if the levelized cost of the SNG produced aims at being evaluated, it is necessary to add to the CFCF already mentioned the expenditures for the H₂ and the CO₂ consumed by the methanation section each year (see *paragraph 5.5*).

The results of the levelized cost of the SNG are defined in Table 6.30 considering that the value expressed in €/MWh is derived from the LHV of the SNG (in MJ/kg) already defined on page 77. Since the levelized cost of the SNG is evaluated considering also the levelized cost of CO₂ and H₂, the results are expressed for both the two cases of power supply of the electrolysis system (CASE A and CASE B).

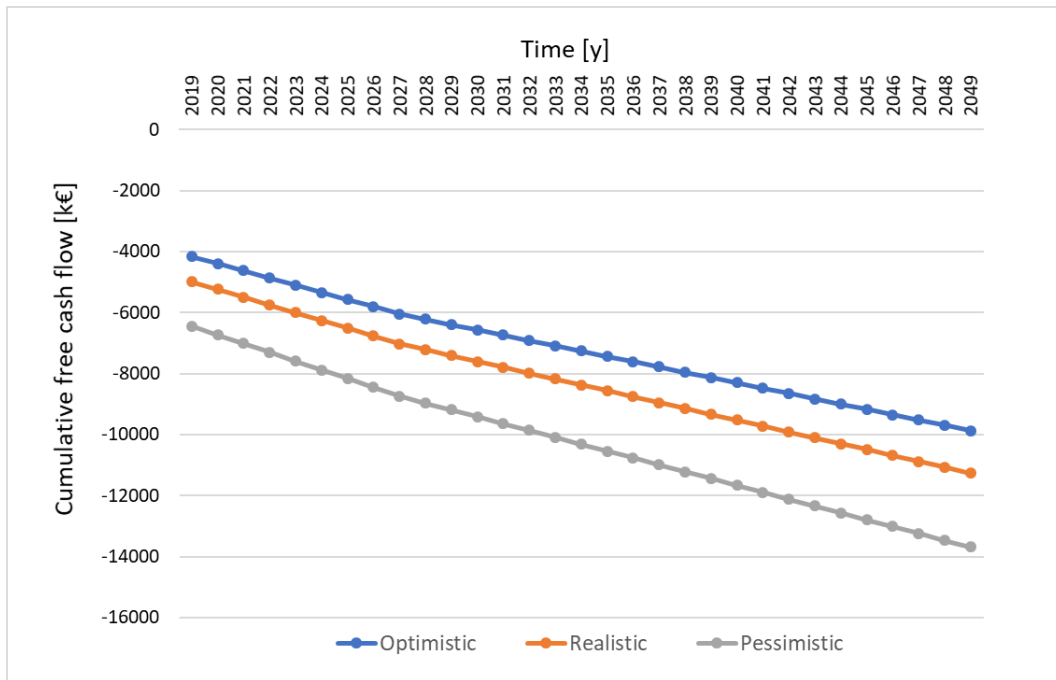


Figure 6.7 CFCF of the methanation section for the three scenarios

Table 6.30 Levelized cost of the SNG produced for the two cases and the three different scenarios

		Optimistic	Realistic	Pessimistic
CASE A	Levelized cost of SNG [€/kg]	2.42	2.49	2.62
	Levelized cost of SNG [€/Nm ³]	1.73	1.77	1.87
	Levelized cost of SNG [€/MWh]	176.14	180.64	190.48
CASE B	Levelized cost of SNG [€/kg]	0.53	0.59	0.72
	Levelized cost of SNG [€/Nm ³]	0.38	0.42	0.52
	Levelized cost of SNG [€/MWh]	38.31	42.81	52.65

6.4.4 General overview of the results for the entire power-to-gas plant

In this paragraph a general overview of the results obtained for the economic analysis will be presented, focusing the attention on the economic contribution of the single sections on the entire power-to-gas plant.

Firstly, the capital expenditure of the entire power-to-gas plant is obtained adding the CAPEX of each section in the three different scenarios. The results are 23.4 M€, 27.3 M€ and 36.3 M€ for the optimistic, realistic and pessimistic scenario respectively. *Figure 6.8* shows the contribution of each section on the CAPEX of the entire power-to-gas plant; from this graph, it is possible to state that the electrolysis section contributes to more than 60% of the total capital expenditure of the plant.

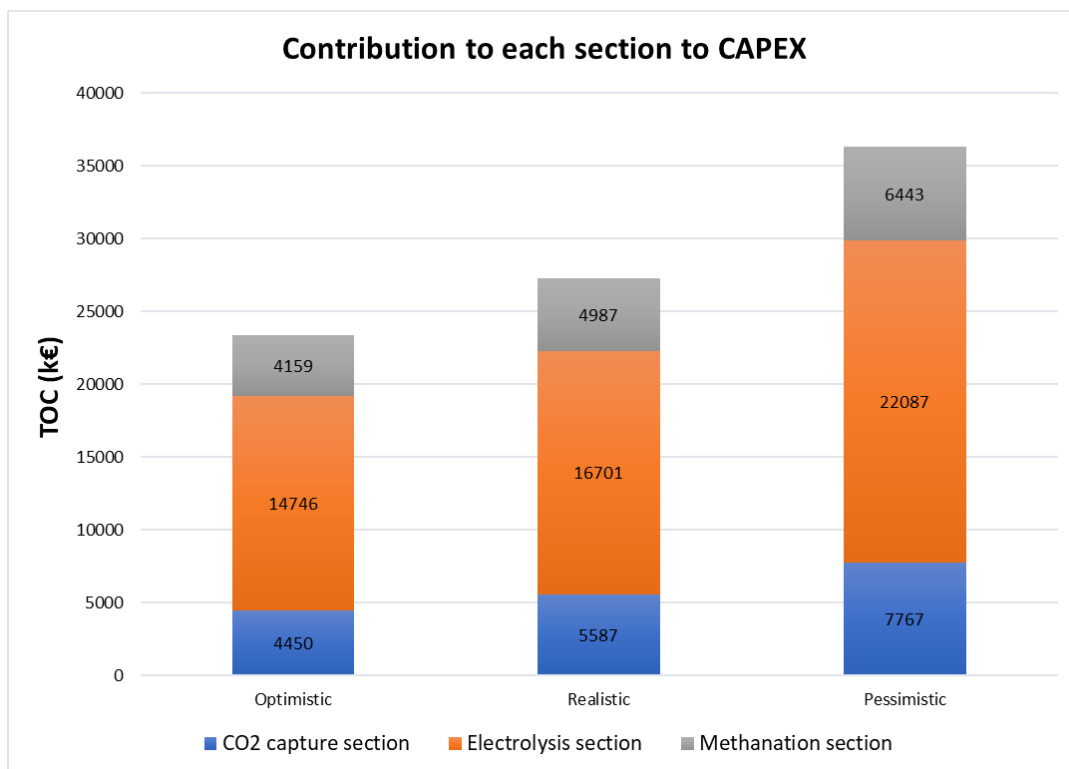


Figure 6.8 Contribution of each section to the CAPEX of the entire power-to-gas plant in the three scenarios

Moreover, the annual operation costs of the entire plant are evaluated starting from the EBITDA of the single section (remember that in this analysis the EBITDA coincides with the annual FCF). *Figure 6.9* and *Figure 6.10* represent the contribution of each section on the annual operating costs of the power-to-gas, considering both the two cases of power supply of the electrolysis system (CASE A in *Figure 6.9* and CASE B in *Figure 6.10*) and the three scenarios. In addition, the distinction between the EBITDA of the plant before and after 2028

is made depending on whether the contribution of “ex Certificati Verdi” is considered or not. Furthermore, the contribution of the stack replacement every 10 years needs to be considered in both two cases after 2028.

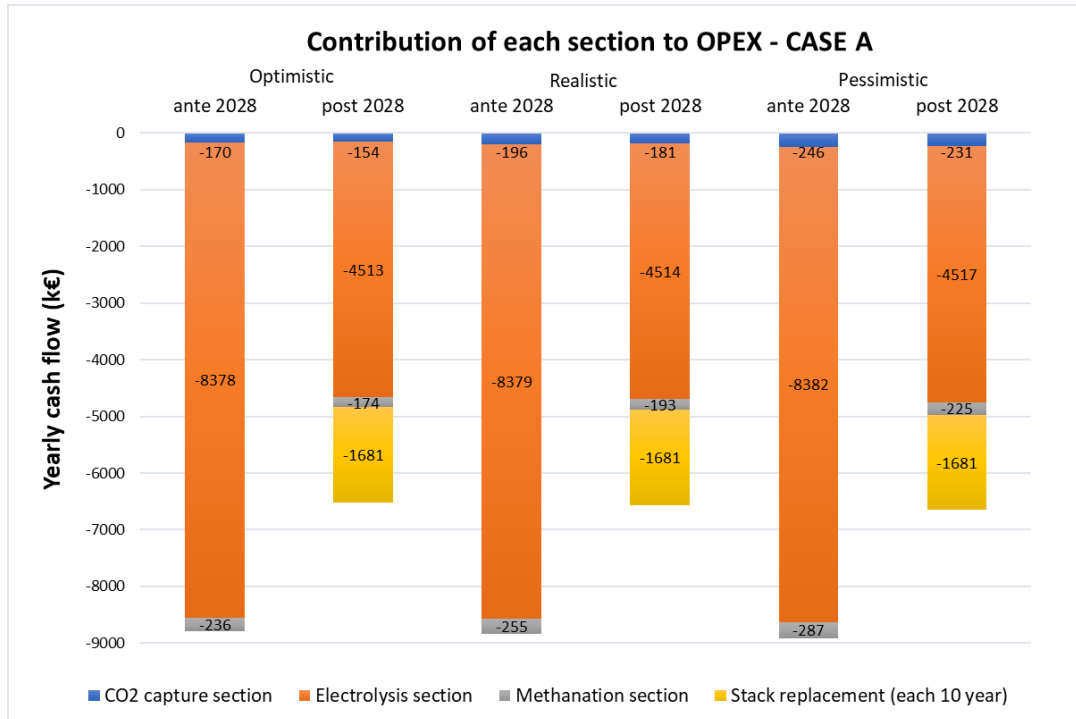


Figure 6.9 Contribution of each section to the OPEX of the entire power-to-gas plant (CASE A)

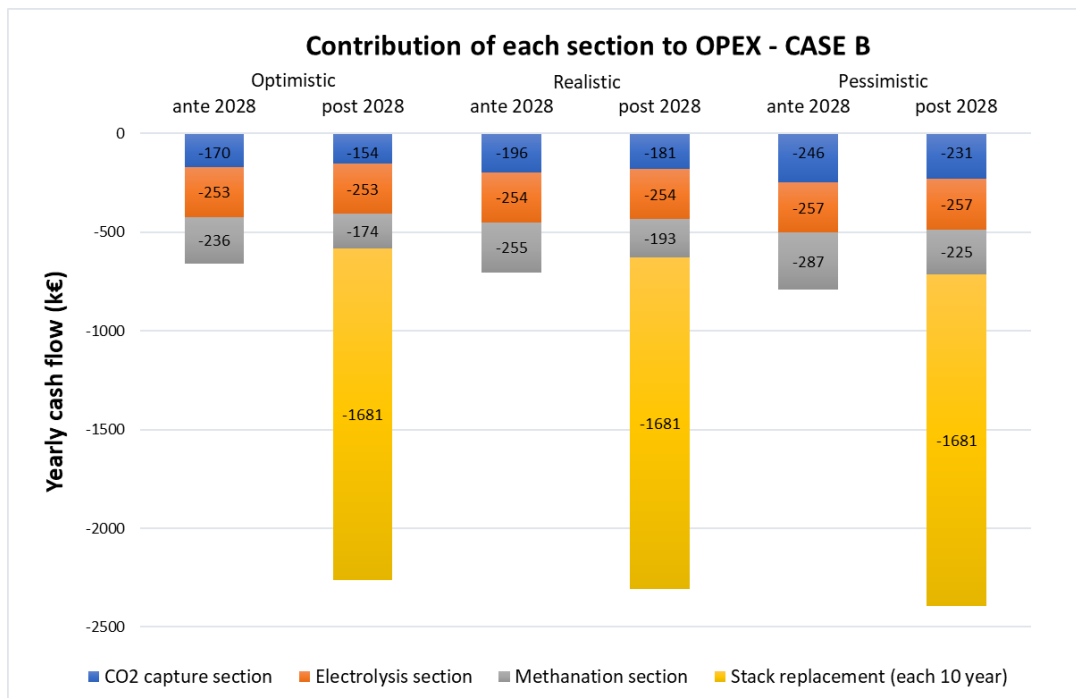


Figure 6.10 Contribution of each section to the OPEX of the entire power-to-gas plant (CASE B)

From these two figures, it is evident that the electrolysis section almost totally contributes to the operating cost of the entire plant both before 2028 and after 2028. As already explained in *paragraph 6.4.2*, the cost for electricity in the electrolysis system constitutes the major part of the expenditures inside this section and this impacts also on the total operating cost of the entire plant. As a matter of fact, the EBITDA for the electrolysis section (before 2028) goes from an annual cost of more than 8 M€ in CASE A to a cost of just over 250 k€ in CASE B only setting the cost of electricity equal to zero. Therefore, in CASE B shown in *Figure 6.10*, the total operating costs are more affordable with respect to CASE A and this can bring also the levelized cost of the SNG to a more competitive level.

6.4.5 Comparison of the LC_{SNG} with prices of other commodities

As already introduced in the previous chapters, the levelized cost of the SNG is the most important indicator of the feasibility and profitability of the plant. In order to understand if the value obtained for the SNG could be defined competitive, it is useful to compare the result to the selling price of other commodities. In this study two products are considered as a price benchmark: natural gas and biomethane.

The price of natural gas is obtained from the 2019 Annual Relation of ARERA [49]. In particular, the final natural gas price after tax for domestic and industrial consumers in Italy for 2019 is presented, taking into account a precise consumption band. For domestic use, the second band is considered because the typical household consumer is regarded as a family with independent heating and annual consumption of 1400 m³/y; on the contrary, for industrial use, the selling price of natural gas is obtained considering the annual production of the power-to-gas plant (almost 4 million m³ per year) and using this value in the tables of ARERA. The result is **0.61 €/Nm³** for domestic use and **0.27 €/Nm³** for industrial use.

Figure 6.11 shows the comparison between the levelized cost of the SNG already introduced in Table 6.30 for both CASE A and CASE B, and the two values of the natural gas selling price just explained. Focusing on the realistic scenario only, the LC_{SNG} in CASE A is 1.77 €/Nm³, a value too high compared to both the domestic and industrial natural gas prices. On the contrary, if the CASE B is considered, the value obtained is 0.42 €/Nm³ that is inside the range of 0.27 €/Nm³ for industrial use and 0.61 €/Nm³ for domestic use.

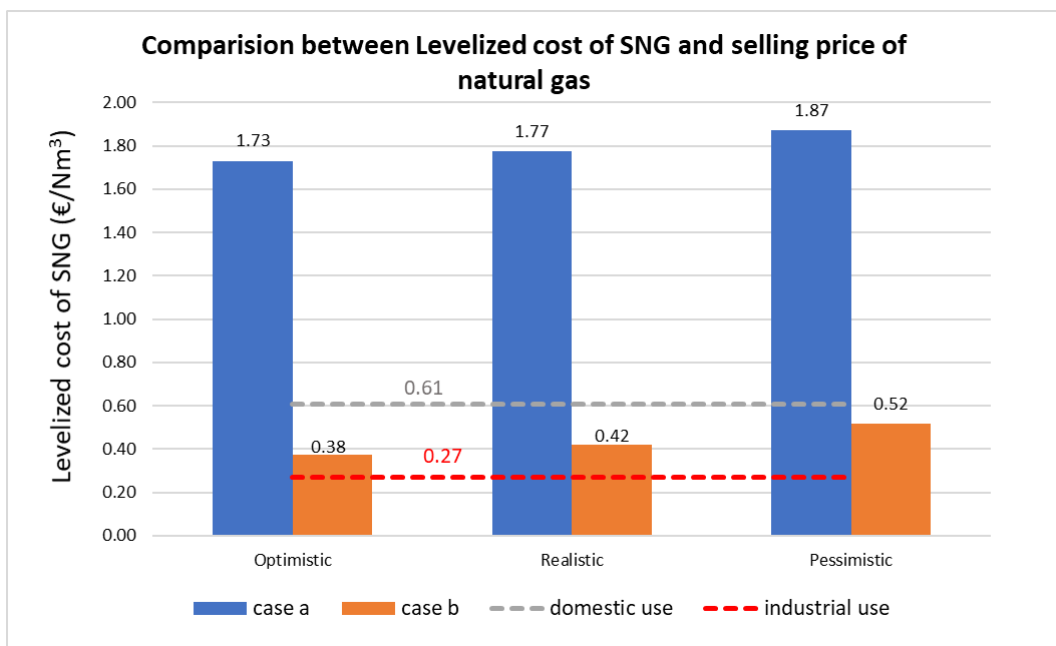


Figure 6.11 Comparison between levelized cost of SNG and selling price of natural gas

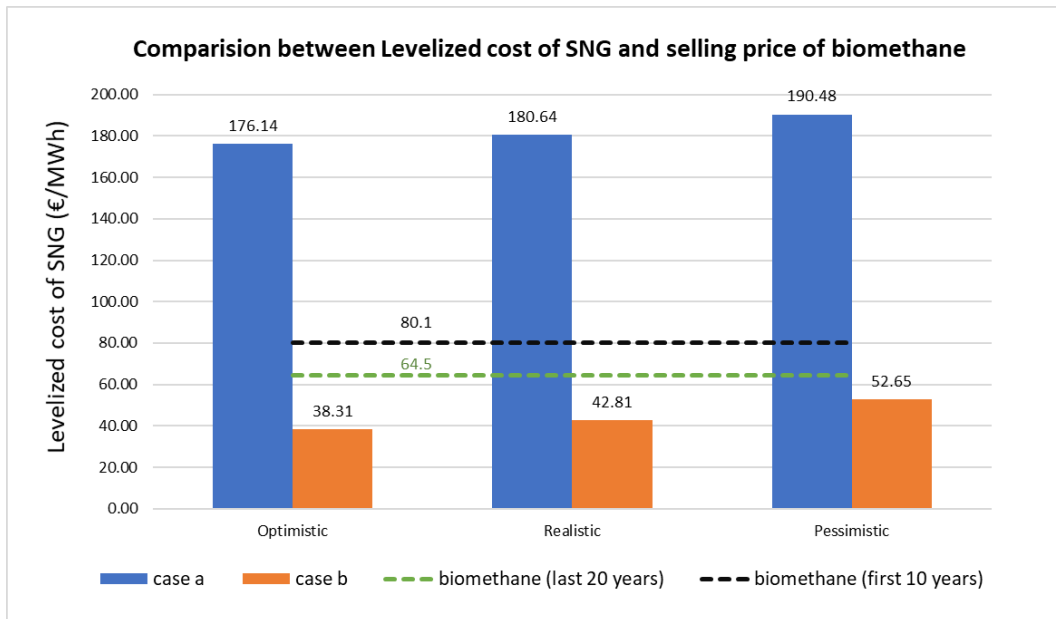


Figure 6.12 Comparison between levelized cost of SNG and selling price of biomethane

For the biomethane, the selling price is evaluated from the “Decreto 2 marzo 2018-Promozione dell'uso del biometano e degli altri biocarburanti avanzati nel settore dei trasporti” [50] and considering that the power-to-gas plant produces SNG that falls into the category of “Biometano avanzato” (the procedure can be found also in [51]). The total selling price of the biomethane is implemented from the “Certificati di immissione in consumo” (CIC), evaluated from the energy eligible for incentives (computed by multiplying the LHV by the annual quantity of SNG produced). From this perspective, for advanced biomethane manufacturers, the accreditation of 375 €/CIC has been envisaged, as well as the possibility of a surplus due to the withdrawal by the “Gestore servizi energetici” (GSE) of the advanced biomethane at a fixed price, decided every month by the same GSE. This procedure is applied for the first 10 years of operation of the plant; after that period, only the CIC can be sold to other operators at a price that depends on the biomethane market (in this study it has been considered the price of 375 €/CIC for a lack of information). Therefore, the final selling price of the biomethane is 80.1 €/MWh for the first 10 years and 64.5 €/MWh for the last 20 years of plant operation.

Figure 6.12 shows the comparison between the levelized cost of SNG (from Table 6.30) and the selling price of the biomethane just introduced. As in Figure 6.11, also in this graph a huge difference can be found between the LC_{SNG} and the biomethane price in CASE A while for CASE B the result is more attractive from an economic point of view.

Therefore, what can be observed from both the comparisons is that to have a competitive levelized cost of the SNG produced and, thus generate a possible gain during the entire lifetime of the plant, it is necessary to reduce the electricity cost by exploiting the electric energy surplus coming from RES as much as possible.

6.5 Liquid CO₂ production plant: economic analysis

In this paragraph, the results of the economic analysis of the liquid CO₂ production plant will be shown. As already introduced in *paragraph 5.4*, the analysis is implemented separating the two operative configurations of the waste-to-energy plant (CHP and full-electric). In conclusion, few comments on the results obtained and a comparison of the levelized cost of the liquid CO₂ produced with market values will be discussed.

6.5.1 CHP configuration: economic results

Estimation of the TOC

Table 6.15 shows the bare module cost for the main components of the system based on the evaluation of parameter A.

Table 6.31 Results of the bare module cost of the main components of the liquid CO₂ production plant derived from the parameter A (CHP configuration)

	Parameter A	C _{bm,main} [k€]
Absorber	26.5 m ³	161.2
Packing absorber	1.3 m ³	3.51
Stripper	0.8 m ³	29.84
Packing stripper	0.039 m ³	0.12
Absorber intercooler	4.2 m ²	18.99
Rich solvent heater	7.5 m ²	28
Stripper's condenser	1.7 m ²	15.4
Reboiler	46.96 m ²	398.1
Solvent exchanger	20.0 m ²	127.54
Lean solvent cooler	7.1 m ²	21.21
Cooler#1 CO₂ compression	5 m ²	14.34
Cooler#2 CO₂ compression	5.9 m ²	14.85
Recirculation pump	1.7 kW	17.09
Compressor #1	39.1 kW	65.82
Compressor #2	36.7 kW	62.62
Solvent tank	27.0 m ³	154.7
Liquid CO₂ tank	55 m ³	343
Initial solvent	-	56.8

For the estimation of the bare module cost of the CO₂ vessel, the same correction factor (0.25) already defined for the carbon capture section of the power-to-gas plant in *paragraph 6.4.1* is considered. Moreover, the price of the delivery and return pipes for the thermal integration, derived from *equation [5-27]*, is equal to 27.46 k€ (it represents a BEC).

In *Table 6.32* the TOC and the other main costs for the three different scenarios is shown.

Table 6.32 TOC and other main costs of the liquid CO₂ production plant in k€ for the three different scenarios for CHP configuration

	Optimistic	Realistic	Pessimistic
C_{bm,main} [k€]	1533	1533	1533
C_{bm,tot} [k€]	2153	2254	2426
BEC [k€]	3052	3343	3866
EPCC [k€]	3509	3928	4639
TPC [k€]	4211	5194	7035
TOC [k€]	4977	6243	8670

Estimation of the annual budget (EBITDA)

Table 6.33 shows the items of the annual budget of the system that are the same for the three scenarios considered. The values are estimated starting from the results of the energy and material flows already introduced in the energy analysis in *paragraph 6.2.2*.

To determine the EBITDA also the contribution of the Operation & Maintenance costs for the three scenarios should be considered: they are 126 k€, 156 k€ and 211 k€ for the optimistic, realistic and pessimistic scenario respectively.

In *Table 6.34* the final values of the EBITDA for the three different scenarios are represented considering two periods, until and after 2028, depending on whether the contribution of “ex Certificati Verdi” is considered or not.

Table 6.33 Expenditures composing the annual budget of the liquid CO₂ production plant for CHP configuration

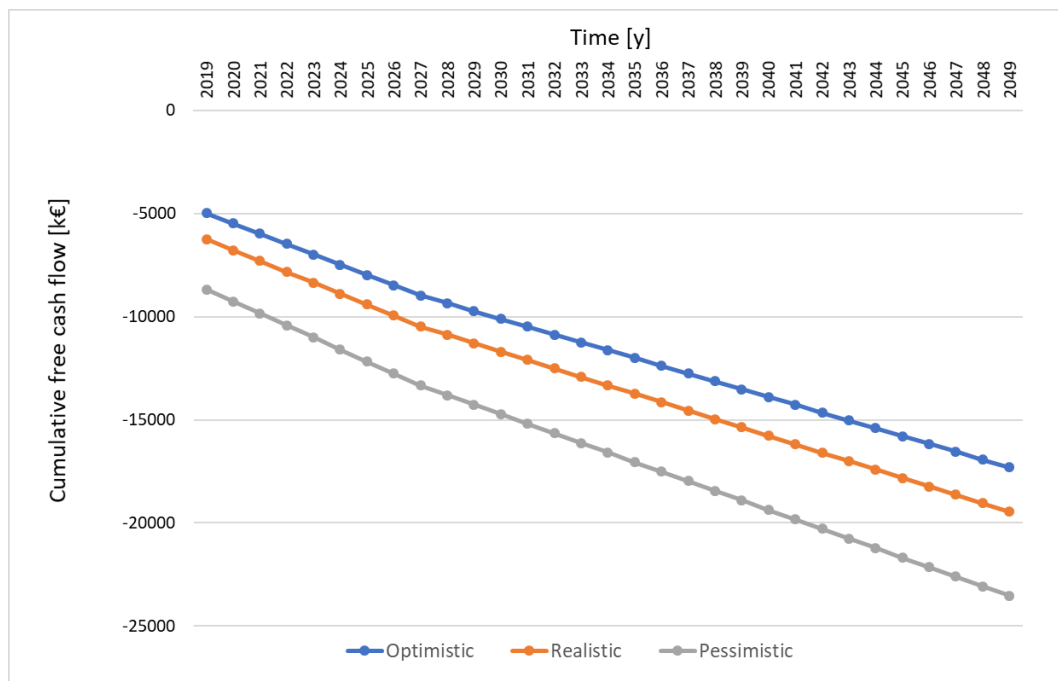
	Expenditure [k€]
Self-consumption of electricity	-32.4
Decreasing of electric productivity	-97.7
“ex certificati verdi” (until 2028)	-30.0
Self-consumption of heat (until 2028)	-187.5
Self-consumption of heat (after 2028)	-97.7
Cooling water	-2.4
Water for solvent's refill	-7.6
MEA refill	-14.8

Table 6.34 EBITDA of the liquid CO₂ production plant for the three scenarios for CHP configuration

	Optimistic	Realistic	Pessimistic
EBITDA (until 2028) [k€]	-499	-528	-583
EBITDA (after 2028) [k€]	-379	-408	-464

Cash flow and levelized cost of the CO₂ produced

Figure 6.13 shows the cumulative free cash flow of the system during the entire lifetime of the plant. From equation [5-29] it is possible to evaluate the levelized cost of the liquid CO₂ produced; the results are introduced in Table 6.35 for the three scenarios.

Figure 6.13 CFCF for the liquid CO₂ production plant in the three scenarios for CHP configurationTable 6.35 Levelized cost of liquid CO₂ for the three scenarios (CHP configuration)

	Optimistic	Realistic	Pessimistic
Levelized cost of liquid CO ₂ [€/tCO ₂]	74.51	83.77	101.36

6.5.2 Full-electric configuration: economic results

Estimation of the TOC

In the full-electric configuration of the waste-to-energy plant, the reboiler is replaced by an electric heater in order to regenerate the solvent. Therefore, the results of the bare module cost of the main components of the system are those already introduced in *Table 6.31* except for the reboiler that is replaced by the parameter A and the $C_{bm,main}$ of the electric heater that are 1021.1 kW and 115.3 k€ respectively. In *Table 6.36* the TOC and the other main costs for the three scenarios is shown.

Table 6.36 TOC and other main costs of the liquid CO₂ production plant in k€ for the three different scenarios for full-electric configuration

	Optimistic	Realistic	Pessimistic
C_{bm,main} [k€]	1250	1250	1250
C_{bm,tot} [k€]	1756	1839	1978
BEC [k€]	2466	2704	3130
EPCC [k€]	2836	3177	3756
TPC [k€]	3403	4201	5697
TOC [k€]	4022	5049	7020

Estimation of the annual budget (EBITDA)

The items of the annual budget of the system are shown in *Table 6.37* and they are estimated starting from the results of the energy and material flows already introduced in the energy analysis in *paragraph 6.2.2* for the full-electric configuration.

The contribution of the Operation & Maintenance costs for the three scenarios should be considered for the estimation of the EBITDA: they are 102 k€, 126 k€ and 171 k€ for the optimistic, realistic and pessimistic scenario respectively. In *Table 6.38* the final values of the EBITDA for the three different scenarios are represented.

Table 6.37 Expenditures composing the annual budget of the liquid CO₂ production plant for full-electric configuration

	Expenditure [k€]
Self-consumption of electricity	-443.8
“ex certificati verdi” (until 2028)	-407.9
Cooling water	-2.4
Water for solvent's refill	-7.6
MEA refill	-14.8

Table 6.38 EBITDA of the liquid CO₂ production plant for the three scenarios for full-electric configuration

	Optimistic	Realistic	Pessimistic
EBITDA (until 2028) [k€]	-979	-1003	-1047
EBITDA (after 2028) [k€]	-571	-595	-639

Cash flow and levelized cost of the CO₂ produced

Figure 6.14 shows the cumulative free cash flow of the system during the lifetime of the plant. Moreover, from equation [5-29] it is possible to evaluate the levelized cost of the liquid CO₂ produced; the results are introduced in Table 6.39 for the three scenarios.

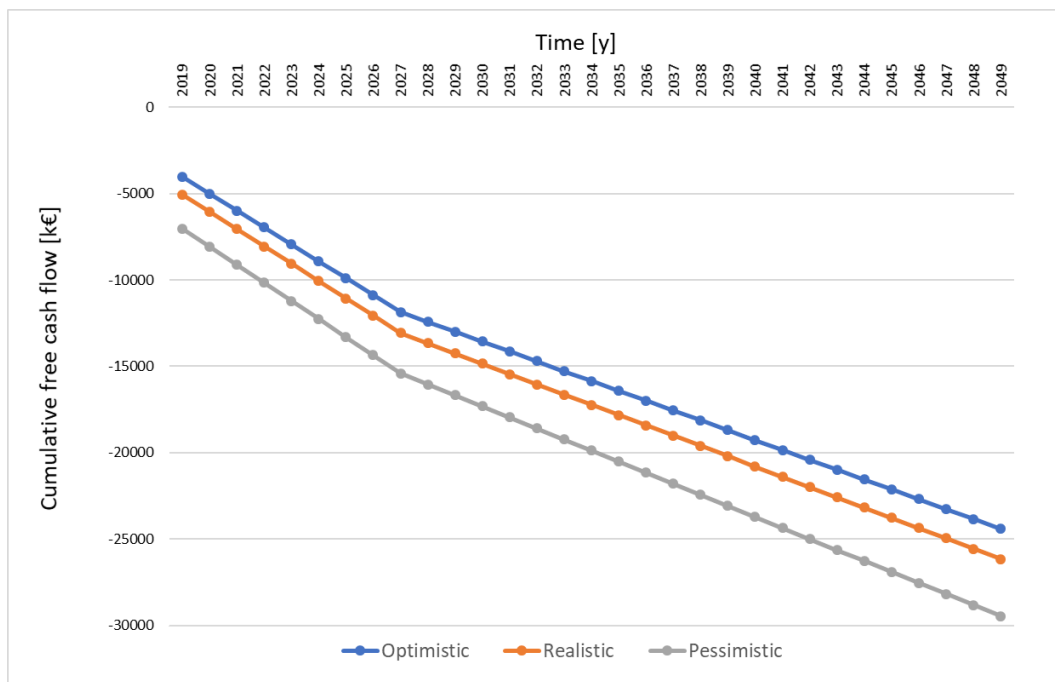

 Figure 6.14 CFCF for the liquid CO₂ production plant in the three scenarios for full-electric configuration

 Table 6.39 Levelized cost of liquid CO₂ for the three scenarios (full-electric configuration)

	Optimistic	Realistic	Pessimistic
Levelized cost of liquid CO ₂ [€/tco ₂]	105.1	112.61	126.9

6.5.3 Comparison between CHP and full-electric configuration

From the results introduced in *paragraph 6.5.1* and *6.5.2*, it is possible to make a comparison between the two configurations of the waste-to-energy plant to decide what the better choice from an economic point of view could be.

Table 6.40 shows the economic results for both the CHP and full-electric configuration only for the realistic scenario (the same comments could be made for the other two scenarios). Firstly, the results show that the initial investment cost is lower in the full-electric configuration by more than 1 million euros compared to the CHP case. On the contrary, the annual operating costs are much lower for the CHP configuration both before and after 2028. Therefore, although there is a saving in the initial investment in the full-electric case, the higher annual operating costs are disadvantageous for this configuration as can also be seen from *Figure 6.15* that represents the CFCF during the entire lifetime of the plant for both the configurations. The graph displays that from 2021 onwards the CFCF of the CHP configuration is always lower than in the full-electric case and this affects the final value of the levelized cost of the liquid CO₂ that is considerably lower in the CHP case. In conclusion, for all these reasons, the CHP configuration of the waste-to-energy plant would be preferable to the full-electric case.

Table 6.40 Comparison of the main economic results of the liquid CO₂ production plant between CHP and full-electric configuration in the realistic scenario

		CHP	Full-electric
CAPEX [k€]		6243	5049
OPEX [k€]	Ante 2028	528	1003
	Post 2028	408	595
Levelized cost liquid CO₂ [€/tco₂]		83.77	112.61

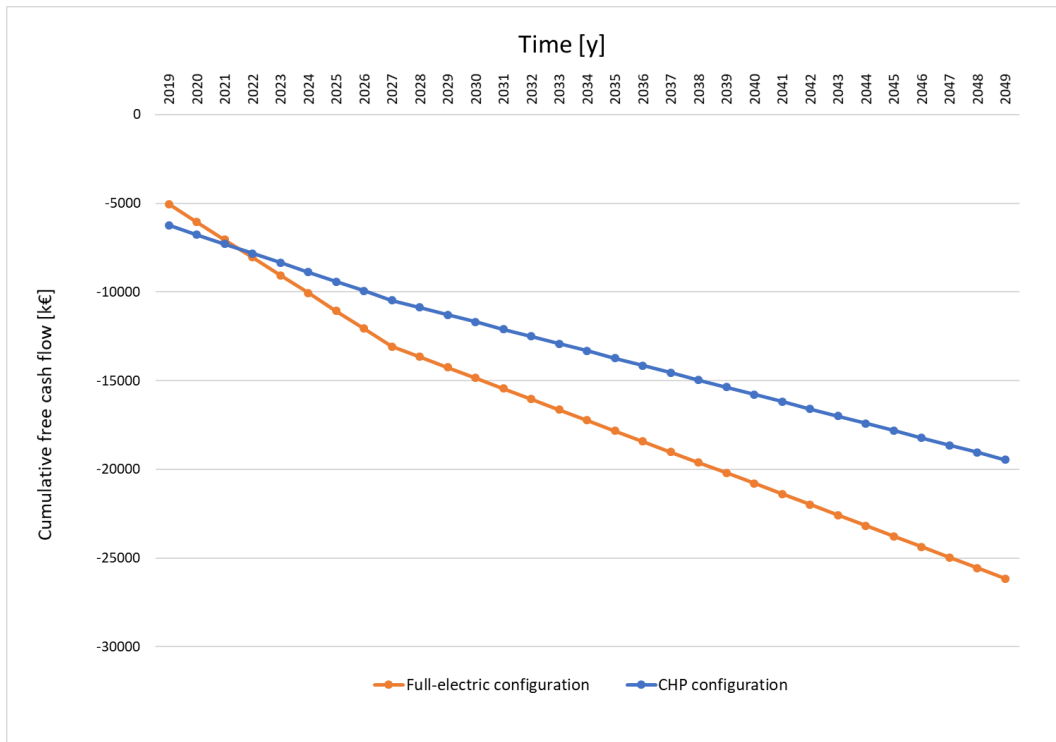


Figure 6.15 CFCF for the CHP and full-electric configuration for the realistic scenario

6.5.4 Final considerations on the levelized cost of liquid CO₂

Considering the realistic scenario and the CHP configuration of the waste-to-energy plant, the final levelized cost of the liquid CO₂ produced is 83.77 €/tCO₂.

Firstly, this value can be compared to that obtained for the CO₂ capture section in the power-to-gas system; in that case, the levelized cost of CO₂ (in gaseous form) was about 48 €/tCO₂, a much lower value than that of liquid CO₂. This is mainly due to the greater compression work for the liquefaction of CO₂ but, above all, to the cost of the steam produced by the waste-to-energy plant in CHP configuration for the regeneration of the solvent.

What is more interesting, however, is to compare the value of the levelized cost obtained with the current market values of liquid CO₂ to verify the competitiveness of the entire system studied. In particular, the liquid CO₂ market is very large: for example, in the food & beverage sector, it is mostly used for the carbonation of water and soft drinks or cryogenic rapid freezing. Furthermore, it can also be used for the treatment and purification of water or even in more niche sectors as a technical laboratory gas.

The cost of liquid CO₂ depends on several factors such as the distance between the manufacturer and the buyer or the annual quantity requested by the customer from the manufacturer. For instance, if it is used as technical laboratory gas inside special cylinders, prices can range from 1.3 €/kg up to even more than 2 €/kg. On the other hand, for large

volumes (bulk supplies) such as quantities between 200000 and 3 million kg of liquid CO₂ per year, the price falls within a range of between 150 €/t and 250 €/t (the greater the quantity requested, the lower the cost). In the study analyzed, the production of liquid CO₂ stands at over 7.7 million kg per year with a levelized cost of about 84 €/t.

In conclusion, from the comparison with the market prices for higher annual volumes, it can be stated that the liquid CO₂ production plant studied can lead to a potential annual profit (given by the difference between the market price of about 150÷250 €/t and LC_{CO₂} of 84 €/t) and that, therefore, the solution can be considered competitive from an economic point of view.

Table 6.41 Comparison between levelized cost of liquid CO₂ (CHP configuration and realistic scenario) and market values

	Value [€/t]
Levelized cost of liquid CO₂	83.77
Liquid CO₂ price as technical laboratory gas	1300 ÷ 2000
Liquid CO₂ market price (bulk conditions)	150 ÷ 250

7 Conclusions

This thesis aimed to study the technical and economic feasibility of two different solutions for the conversion of CO₂ present inside the exhausts of a waste-to-energy plant, into two reusable products, i.e. synthetic natural gas and liquid CO₂. The topic examined in this study is related to the long-term strategy developed by the European Union in 2018 with the aim of building an economy with net-zero greenhouse gas emissions by 2050.

The estimated annual energy consumption and the economic analysis of the two plants did not highlight any particular issue concerning their feasibility. However, the two solutions present some critical points that may be investigated in future studies.

In particular, the power-to-gas plant allows the production of fewer than 4 million Nm³/y of SNG starting from the removal of 7740 t/y of CO₂ from the exhausts coming from the waste-to-energy plant and from the production of about 1400 t/y of H₂ by a 10 MW alkaline electrolyzer. The electrolysis section is the one with the greatest impact on the entire system from both energy and economic standpoints: in fact, this contributed to the annual electricity consumption of 82.69 GWh_{el}, most of which covered by the waste-to-energy plant. This means that the overall efficiency of the entire power-to-gas system was found to be 0.52 (on an HHV basis). A possible solution that would lead to an increase of efficiency could be to use a different technology from that considered in this study: as a matter of fact, replacing the alkaline electrolyzer with a solid oxide one (SOEC) could also lead to efficiencies close to 80%; however, this option can increase investment and operating costs. The electrolysis section is also the one that occupies the largest surface among the three sections of the power-to-gas system; while the CO₂ capture and methanation sections result in a land occupation of respectively 213 m² and 286 m², the electrolyzer system can occupy an area of 1200 m². Furthermore, from the economic analysis carried out on the entire power-to-gas system, it was found that the largest cost is the one related to the electrolysis section both in terms of investment costs and of the consumption of electricity. If the electrolyzer is fed with electricity produced by the waste-to-energy plant, the final levelized cost of the SNG is approximately 1.77 €/Nm³, a value that is higher than the national prices of natural gas or biomethane. In order to reduce this value and bring it back to a threshold that can allow a profit during the useful life of the plant, the surplus of electricity coming from renewable energy sources must be used as much as possible. For this purpose, a zero cost for the electricity consumed by the electrolyzer has also been assumed, thus obtaining a levelized SNG cost of around 0.42 €/Nm³, a much more competitive value than the previous one.

For what concerns the second solution examined, it allowed the production of 7740 t/y of CO₂ in liquid form. In this system, the reboiler is the most energy-intensive component which results in a thermal consumption of 7519 MWh_{th}/y. As a matter of fact, since there was no heat source available inside the plant for the regeneration of the solvent, two alternative operating settings were considered for the waste-to-energy plant: CHP or full-electric with the

replacement of the reboiler with an electric heater. In both cases, the SPECCA exceeded 1 MWh/t_{CO₂}, hence higher than the 0.0428 MWh/t_{CO₂} for the power-to-gas plant because in this configuration the heat necessary for the regeneration of the solvent was recovered from the methanation section. From the economic analysis, however, more encouraging results were obtained. The CHP setup was found to be the most interesting option with a levelized cost of the liquid CO₂ produced around 84 €/t_{CO₂} (compared to 112 €/t_{CO₂} for the full-electric configuration). The value obtained is very competitive when compared with the current market prices of liquid CO₂, which fluctuates around 150÷250 €/t, thus allowing a possible gain over the lifetime of the plant.

In conclusion, this thesis can represent the starting point for future studies related to the decarbonization of existing plants. In particular, the liquid CO₂ production plant was found to be the most promising option from an economic point of view. The section related to the regeneration of the solvent could be developed to reduce the energy consumption of the plant, for instance by experiencing another type of solvent or by recovering the heat from an external source, thus making the process even more efficient and allowing an even higher economic return.

References

- [1] Global CCS Institute, “Global Status of CCS 2019,” 2019.
- [2] International Energy Agency (IEA), “World Energy Outlook 2019 – Analysis - IEA,” *World Energy Outlook 2019*. 2019.
- [3] J. Gibbins and H. Chalmers, “Carbon capture and storage,” *Energy Policy*, vol. 36, no. 12, pp. 4317–4322, 2008, doi: 10.1016/j.enpol.2008.09.058.
- [4] F. Lecomte, “Post-Combustion CO₂ Capture - Knovel,” pp. 37–62, 2010.
- [5] A. Brunetti, F. Scura, G. Barbieri, and E. Drioli, “Membrane technologies for CO₂ separation,” *J. Memb. Sci.*, vol. 359, no. 1–2, pp. 115–125, 2010, doi: 10.1016/j.memsci.2009.11.040.
- [6] M. J. Tuinier, M. van Sint Annaland, G. J. Kramer, and J. A. M. Kuipers, “Cryogenic CO₂ capture using dynamically operated packed beds,” *Chem. Eng. Sci.*, vol. 65, no. 1, pp. 114–119, 2010, doi: 10.1016/j.ces.2009.01.055.
- [7] G. Puxty and M. Maeder, “The fundamentals of post-combustion capture,” in *Absorption-Based Post-Combustion Capture of Carbon Dioxide*, 2016.
- [8] A. Godula-Jopek, *Hydrogen Production: By Electrolysis*. 2015.
- [9] S. Rönsch *et al.*, “Review on methanation - From fundamentals to current projects,” *Fuel*, vol. 166, pp. 276–296, 2016, doi: 10.1016/j.fuel.2015.10.111.
- [10] J. Gao, Q. Liu, F. Gu, B. Liu, Z. Zhong, and F. Su, “Recent advances in methanation catalysts for the production of synthetic natural gas,” *RSC Advances*. 2015, doi: 10.1039/c4ra16114a.
- [11] S. Sahebdehfar and M. Takht Ravanchi, “Carbon dioxide utilization for methane production: A thermodynamic analysis,” *J. Pet. Sci. Eng.*, 2015, doi: 10.1016/j.petrol.2015.07.015.
- [12] M. Götz *et al.*, “Renewable Power-to-Gas: A technological and economic review,” *Renewable Energy*. 2016, doi: 10.1016/j.renene.2015.07.066.
- [13] European Commission, “2030 Climate & Energy Framework,” 2014.
- [14] Renewables 2020 Global Status Report, “Renewables Global Status Report,” *REN21 Secretariat*, 2020. .
- [15] G. Buffo, P. Marocco, D. Ferrero, A. Lanzini, and M. Santarelli, “Power-to-X and power-to-power routes,” in *Solar Hydrogen Production*, 2019.
- [16] G. Centi and S. Perathoner, “Opportunities and prospects in the chemical recycling of carbon dioxide to fuels,” *Catal. Today*, 2009, doi: 10.1016/j.cattod.2009.07.075.
- [17] E. Giglio, A. Lanzini, M. Santarelli, and P. Leone, “Synthetic natural gas via integrated high-temperature electrolysis and methanation: Part I-Energy performance,” *J. Energy Storage*, vol. 1, no. 1, pp. 22–37, 2015, doi: 10.1016/j.est.2015.04.002.
- [18] R. Tichler and S. Bauer, “Power-to-Gas,” pp. 373–389, 2016.

- [19] J. E. O'Brien, M. G. McKellar, E. A. Harvego, and C. M. Stoots, "High-temperature electrolysis for large-scale hydrogen and syngas production from nuclear energy - summary of system simulation and economic analyses," *Int. J. Hydrogen Energy*, 2010, doi: 10.1016/j.ijhydene.2009.09.009.
- [20] W. L. Becker, R. J. Braun, M. Penev, and M. Melaina, "Production of Fischer-Tropsch liquid fuels from high temperature solid oxide co-electrolysis units," *Energy*, 2012, doi: 10.1016/j.energy.2012.08.047.
- [21] W. L. Becker, M. Penev, and R. J. Braun, "Production of synthetic natural gas from carbon dioxide and renewably generated hydrogen: A techno-economic analysis of a power-to-gas strategy," *J. Energy Resour. Technol. Trans. ASME*, 2019, doi: 10.1115/1.4041381.
- [22] M. Bailera, P. Lisbona, L. M. Romeo, and S. Espatolero, "Power to Gas projects review: Lab, pilot and demo plants for storing renewable energy and CO₂," *Renewable and Sustainable Energy Reviews*. 2017, doi: 10.1016/j.rser.2016.11.130.
- [23] G. Gahleitner, "Hydrogen from renewable electricity: An international review of power-to-gas pilot plants for stationary applications," *International Journal of Hydrogen Energy*. 2013, doi: 10.1016/j.ijhydene.2012.12.010.
- [24] R. Notz, H. P. Mangalapally, and H. Hasse, "Post combustion CO₂ capture by reactive absorption: Pilot plant description and results of systematic studies with MEA," *Int. J. Greenh. Gas Control*, vol. 6, pp. 84–112, 2012, doi: 10.1016/j.ijggc.2011.11.004.
- [25] H. Ahn, M. Luberti, Z. Liu, and S. Brandani, "Process configuration studies of the amine capture process for coal-fired power plants," *Int. J. Greenh. Gas Control*, vol. 16, pp. 29–40, 2013, doi: 10.1016/j.ijggc.2013.03.002.
- [26] E. Tractebel, Engie, and Hinicio, "Study on Early Business Cases for H₂ in Energy Storage and More Broadly Power To H₂ Applications," *EU Comm.*, 2017.
- [27] A. Pilenga, G. Tsotridis, P. Millet, and et al., "EU Harmonised Terminology for Low Temperature Water Electrolysis for Energy Storage Applications," *Publ. Off. Eur. Union*, 2018.
- [28] Snam Rete Gas, "Codice Di Rete - Revisione Lxix," 2000.
- [29] E. Giglio *et al.*, "Power-to-Gas through High Temperature Electrolysis and Carbon Dioxide Methanation: Reactor Design and Process Modeling," *Ind. Eng. Chem. Res.*, vol. 57, no. 11, pp. 4007–4018, 2018, doi: 10.1021/acs.iecr.8b00477.
- [30] F. Salomone, E. Giglio, D. Ferrero, M. Santarelli, R. Pirone, and S. Bensaid, "Techno-economic modelling of a Power-to-Gas system based on SOEC electrolysis and CO₂ methanation in a RES-based electric grid," *Chem. Eng. J.*, 2019, doi: 10.1016/j.cej.2018.10.170.
- [31] "50 kW Electric Heater Rentals | Portable and Electric Heating Rentals | Aggreko | Aggreko." [Online]. Available: <https://www.aggreko.com/en-us/products/heating-and-cooling/heater-rental/electric-heaters/electric-heater-50-kw>. [Accessed: 16-Nov-2020].
- [32] H. Deng, S. Roussanaly, and G. Skaugen, "Techno-economic analyses of CO₂ liquefaction: Impact of product pressure and impurities," *Int. J. Refrig.*, vol. 103, pp. 301–315, 2019, doi: 10.1016/j.ijrefrig.2019.04.011.

- [33] K. Gerdes, W. M. Summers, and J. Wimer, "Quality Guidelines for Energy System Studies: Cost Estimation Methodology for NETL Assessments of Power Plant Performance," no. September, p. 26, 2019.
- [34] R. Turton, *Analysis, Synthesis, and Design of Chemical Processes Fourth Edition*. 2013.
- [35] Remers D.S. and L.H. Chai, "Design cost factors for scaling-up engineering equipment," *Chem. Eng. Prog.*, 1990.
- [36] K. Jordal *et al.*, "CEMCAP - Making CO₂ Capture Retrofittable to Cement Plants," in *Energy Procedia*, 2017, doi: 10.1016/j.egypro.2017.03.1755.
- [37] "APPLICAZIONE DELLA DELIBERAZIONE ARERA N. 665/2017/R/IDR DEL 28/09/2017 (TICSI) - ARTICOLAZIONE TARIFFARIA PER IL SERVIZIO IDRICO INTEGRATO ANNO 2018." [Online]. Available: http://www.at03torinese.it/site2015/utenti/tariffe/004_tariffe-TICSI-2018_del-704.pdf. [Accessed: 16-Nov-2020].
- [38] T. E. Akinola, E. Oko, and M. Wang, "Study of CO₂ removal in natural gas process using mixture of ionic liquid and MEA through process simulation," *Fuel*, 2019, doi: 10.1016/j.fuel.2018.08.152.
- [39] J. Proost, "State-of-the art CAPEX data for water electrolyzers, and their impact on renewable hydrogen price settings," *Int. J. Hydrogen Energy*, 2019, doi: 10.1016/j.ijhydene.2018.07.164.
- [40] M. F. Shehzad, M. B. Abdelghany, D. Liuzza, V. Mariani, and L. Glielmo, "Mixed logic dynamic models for MPC control of wind farm hydrogen-based storage systems," *Inventions*, 2019, doi: 10.3390/inventions4040057.
- [41] Aguas de Portugal Serviços, "Establishment of cost functions for construction of various types of public water services assets in Portugal," pp. 1–19, 2010.
- [42] John G Wimer (NETL); Wm Morgan Summers (NETL), "Cost Estimation Methodology for NETL Assessments of Power Plant Performance Quality Guidelines for Energy Systems Studies," 2011.
- [43] G. D. Ulrich and P. T. Vasudevan, "How to estimate utility costs," *Chem. Eng.*, 2006.
- [44] S. J. Olson, B. Nguyen-Phuoc, and K. Ibsen, "Gas cleanup technologies suitable for biomass gasification to liquid fuels," in *AIChE Annual Meeting, Conference Proceedings*, 2006.
- [45] "Energy Transition calls for 100% renewable energy systems with Renewable Hydrogen, without fossil fuels. RENEWABLE HYDROGEN: THE GAME-CHANGING vector of a low-carbon energy system." [Online]. Available: <http://www.hydrogenics.com/wp-content/uploads/Renewable-Hydrogen-Brochure.pdf>. [Accessed: 16-Nov-2020].
- [46] "Elektrolyseanlagen für Multi-MW Anwendungen." [Online]. Available: https://windenergietage.de/2019/wp-content/uploads/sites/4/2019/11/28WT05_F23_1805_McPhy_20191104.pdf. [Accessed: 16-Nov-2020].
- [47] Zep Zero emissions platform, "The Costs of CO₂ Capture , Transport and Storage," p. 50, 2019.

- [48] B. Lee, H. Lee, H. S. Cho, W. C. Cho, C. H. Kim, and H. Lim, “Projected economic outlook and scenario analysis for H₂ production by alkaline water electrolysis on the basis of the unit electricity price, the learning rate, and the automation level,” *Sustain. Energy Fuels*, vol. 3, no. 7, pp. 1799–1807, 2019, doi: 10.1039/c9se00148d.
- [49] S. B. Presidente, G. Castelli, A. Guerrini, C. Poletti, and S. Saglia, “Autorità di Regolazione per Energia Reti e Ambiente.” [Online]. Available: https://www.arera.it/allegati/relaz_ann/20/RA20_volume1.pdf. [Accessed: 16-Nov-2020].
- [50] “DECRETO 2 marzo 2018 Promozione dell’uso del biometano e degli altri biocarburanti avanzati nel settore dei trasporti.” [Online]. Available: <https://www.gazzettaufficiale.it/eli/id/2018/03/19/18A01821/SG>. [Accessed: 16-Nov-2020].
- [51] “Procedure applicative DM 2 marzo 2018.” [Online]. Available: https://www.gse.it/documenti_site/Documenti_GSE/Servizi_per_te/BIOMETANO/Procedure_applicative_DM_2_marzo_2018_18062018.pdf. [Accessed: 16-Nov-2020].